Investigating the use of drone-acquired thermal imagery as an effective new tool to inform the management and conservation of flying-fox colonies

Submitted by

Eliane McCarthy

BSc (Biology)

A thesis submitted in requirement

for the degree of Master of Research

Hawkesbury Institute for the Environment

Western Sydney University

August 2020

Supervisory panel:

Associate Professor Justin Welbergen, Hawkesbury Institute for the Environment, Western Sydney University (Principal Supervisor)

Doctor John Martin, Taronga Institute for Science and Learning, Taronga Conservation Society Australia (Co-supervisor)

Associate Professor Matthias Boer, Hawkesbury Institute for the Environment, Western Sydney University (Co-supervisor)

Acknowledgements

The work undertaken in this thesis would not have been possible without the help of many people and organisations. First and foremost, thank you for the support of my supervisors, Associate Professor Justin Welbergen, Doctor John Martin, and Associate Professor Matthias Boer. Thank you for your assistance with getting this project up and running, helping to organise drone pilot training, your help in the field, especially when I was still learning to use equipment, and of course your data analysis and writing support.

I would not have been able to put the time and effort into this thesis without financial support from Western Sydney University (WSU) in the form of the Master of Research scholarship. There is a number of people at Western Sydney University whose help was invaluable throughout this thesis. This work would not have been possible without the help of Doctor Sebastian Pfautsch, who assisted with organising drone pilot training, and allowed me to use his drone for my research for extended periods of time. Thank you also to Doctor Russell Thompson, who was always happy to answer my statistics-related questions. Finally, for the support of Master of Research coordinators Doctor Alex Norman and Doctor Jack Tsonis, throughout this project. Through the Master of Research degree and the backing of Alex and Jack, I was able to go on a six-month exchange to Utrecht University in The Netherlands, where I gained highly valuable skills for my thesis. Thank you also to WSU for providing me with a travel grant for my exchange.

This thesis required me to work with several external organisations throughout Sydney and beyond. I am very grateful for the help I received from the staff at Camellia Gardens, Bec

Williams and Jaynia Sladek of Sutherland Shire Council, Andrew Jennings of Northern Beaches Council, Michael Ellison and Mitchell Clark of Campbelltown City Council, Amara Glynn of Centennial Parklands and Matthew Mo at NSW Department of Planning, Industry and Environment. These people shared their colony population estimates with me, and where necessary, were more than happy to grant me access to flying-fox colonies.

Thank you to the participants who very kindly agreed to count thousands upon thousands of flying-foxes in thermal imagery for me and contributed to the findings of Chapter 2. Thanks also to my partner Roy, for always making the time to assist me with fieldwork, answer my questions, and reassure me I was on the right track. To my grandfather, Laurence, who instilled in me a love of wildlife, and flying, and was a very good, and special man. Finally, thank you to my mum, Anne, for her patience and unending support, for reading so much of my writing throughout my schooling and instilling in me the curiosity to investigate everything thoroughly.

This research was funded by Western Sydney University, Hawkesbury Institute for the Environment, and a Paddy Pallin Foundation-sponsored Australasian Bat Society Grant, awarded in 2019.

This research has been conducted under Animal Research Authority no. A12217, issued by Western Sydney University, approved 11/04/19.

Statement of authentication

The work presented in this thesis is, to the best of my knowledge and belief, original except as acknowledged in the text. I hereby declare that I have not submitted this material, either in full or in part, for a degree at this or any other institution.

(Eliane McCarthy)

Table of contents

List of Tables

List of Figures

List of Appendices

List of Abbreviations

ACEC	Animal Care and Ethics Committee
AGL	Above ground level
ANOVA	Analysis of Variance
BIC	Bayesian information criterion
CI	Confidence interval
CSIRO	Commonwealth Scientific and Industrial Research Organisation
GCP	Ground control point
GLMM	Generalised linear mixed model
GLAMA	Gap Light Analysis Mobile App
MVS	Multi-view stereo
NFFMP	National Flying-Fox Monitoring Program
OBIA	Object-based image analysis
R-JPEG	Radiometric JPEG
ROI	Region of interest
RPAS	Remotely piloted aircraft system
RSE	Relative standard error
SE	Standard error
SfM	Structure from motion
3D	Three-dimensional

Summary

Population estimates are fundamentally important for sound wildlife conservation and management, and yet, are well known to be subject to biases and inaccuracies. Flying-foxes (*Pteropus* spp.) roost in the canopies of trees and form colonies of tens to thousands of individuals. They are difficult to survey accurately, due to inaccessibility, lack of visibility within colonies, and between-counter variability.

This study aims to develop more accurate, precise and less-biased methods for quantifying the number of individuals within flying-fox colonies, as well as monitoring changes in the number of individuals, area occupied, shape and animal density of flying-fox colonies. A method for quantifying the number of flying-foxes in roosts was developed, whereby a drone-acquired thermal orthomosaic of a colony is generated. In an orthomosaic, flying-foxes appear as bright circular objects against a darker background. Flying-foxes may be counted manually, or a Computer Vision workflow can be used to generate semi-automatic counts of flying-foxes with relatively high accuracy.

I validated the accuracy of the thermal orthomosaic counting method by comparing direct counts of small groups of flying-foxes to counts derived from drone-acquired thermal imagery. Then I compared whole colony ground counts to counts derived from drone-acquired thermal orthomosaics. Counts derived from thermal orthomosaics tended to be approximately twice as high as those from ground counting methods conducted by both the experimenter and National Flying-Fox Monitoring Program. This suggests that ground count estimates underestimate the true number of individuals within flying-fox colonies, and that densely roosting flying-foxes may be more drastically undercounted. Finally, I demonstrated the utility of drone-acquired thermal imagery for mapping colony roosting density, roost area occupied and movement throughout the roost over time. This study highlights the utility of a new monitoring method for accurately estimating the flying-fox colony size, assessing roosting dynamics and assisting in the conservation and management of flying-foxes.

Chapter 1 - Introduction and Thesis Overview

1.1 Population monitoring and conservation

Monitoring animal populations is a fundamental activity in conservation biology (Gibbs, 2000; Marsh & Trenham, 2008). Population monitoring can provide baseline information about the abundance and distribution of a species (Fretwell et al., 2012). For species at risk of extinction, monitoring populations over time can provide insights into possible causes of decline by associating changes in population density with other measured factors (Marsh & Trenham, 2008). Monitoring data can also be used to determine the effectiveness of management strategies, such as the control of pest species (Reddiex et al., 2006), or to assess the effects of harvesting practices on population viability (McIntosh et al., 1995). Accurate monitoring also provides more precise predictions of species reactions to environmental and human impacts (Sutherland, 2006).

Species tend to be distributed in a non-random manner, governed by their respective habitat preferences (Lewis, 1970). Traditionally, population surveys are conducted through direct observation of the species of interest, by methods such as direct counts, or when the species is widespread and abundant, by strip transect sampling (Eberhardt, 1978), distance sampling (Buckland et al., 2015), or capture-mark-recapture modelling (Nichols, 1992). When the survey species is elusive because individuals have cryptic or solitary lifestyles, population estimation may be conducted indirectly, through observing the abundance of their tracks (Keeping & Pelletier, 2014), scats (Neff, 1968), and vocalisations (Reby et al., 1998). These methods are essential for determining the abundance and welfare of a species and informing conservation and management decisions.

Several factors may bias the reliability of traditional population survey methods, thereby generating inaccurate and unreliable population estimates (Seber, 1986). The accuracy of population surveys has been shown to decrease with increasing population size (Manning et al., 1995), and is subject to size biases, whereby larger animals or clusters of animals are more likely to be visible to the observer while smaller animals may be missed (Otto & Pollock, 1990). Population surveys may also be biased by accessibility, whereby sites that have a nearby road or are sparsely vegetated are more frequently sampled than sites that are less accessible (Reddy & Dávalos, 2003; Wagner, 1981). Moreover, some areas are subject to geographic bias in population survey intensity; where more affluent regions have the funding and resources to monitor population trends more closely (Archer et al., 2014). Survey methods are also influenced by between-observer variability (Erwin, 1982), with experienced observers more likely to locate species of interest than novice counters, as shown for example for koalas (*Phascolarctos cinereus*) (Hanger et al., 2017). Traditional methods may also require a long survey period to generate precise estimates (Silveira et al., 2003). Critically, bias in traditional animal survey methods may lead ecologists and conservationists to draw inaccurate conclusions about species population sizes.

Successful implementation of conservation and management plans relies on accurate monitoring practices. Numerous studies have focused on reducing bias, ensuring the accuracy of existing techniques and developing new methods (Eberhardt & Thomas, 1991; Pimm et al., 2015; Seber, 1986). Recent technological advances are enabling researchers to identify, track, count and assess the habitats of species faster, more cheaply and more reliably than before (Pimm et al., 2015). One rapidly evolving technology, remote sensing, is increasingly being used for generating more accurate population estimates for wildlife conservation and management.

1.2 Remote sensing for species population monitoring

Remote sensing is the acquisition of information from overhead imagery recording the reflection or emission of one or more regions of the electromagnetic spectrum; remote sensing instruments can be either spaceborne or airborne (Aplin, 2005; Cracknell, 2007; Thenkabail, 2016). The advent of aerial and satellite remote sensing has greatly improved the ability of environmental scientists to monitor and map land cover changes and other environmental phenomena (Horning et al., 2010). Improved sensor resolution permits monitoring of smaller and more complex objects of interest (Horning et al., 2010). The development of a wider range of remote sensors; including thermal-infrared, multispectral, hyperspectral and LiDAR, allows ecologists to ask novel and more complex questions about our environment (Wang et al., 2010). Remote sensing technologies will continue to become cheaper and more available, alongside continual technological advances, making them more suitable for use in the ecological sciences.

Recent technological advances have made remotely piloted aircraft systems (RPAS; hereafter ‘drones’), more affordable and available (Jiménez López & Mulero-Pázmány, 2019). Drones, being autonomously piloted from ground level and smaller and quieter than piloted vehicles, can collect higher resolution imagery closer to sites of interest (Anderson & Gaston, 2013). Drones are relatively easy to use and are highly customizable, allowing for pre-programmed flight and monitoring by multiple sensors (Carrivick et al., 2013). Drones, flying lower than larger piloted aircraft, generally provide the user with higher-resolution spatial data that is better suited to monitoring animals than imagery from piloted aircraft (Anderson & Gaston, 2013). Low-altitude aerial surveys are becoming increasingly common in ecological studies and have been used to observe many species such as mixed-species aggregations of

waterfowl (McEvoy et al., 2016); gentoo penguins (*Pygoscelis papua*) (Ratcliffe et al., 2015); blacktip reef sharks (*Carcharhinus melanopterus*) (Rieucau et al., 2018); American black bears (*Ursus americanus*) (Ditmer et al., 2015); Bornean orangutans (*Pongo pygmaeus*) and proboscis monkeys (*Nasalis larvatus*) (Burke et al., 2019b). Critically, ecologists comparing ground counts of artificial seabird colonies with automated counts of drone images, have found that counts obtained from low altitude aerial surveys are significantly less variable and up to 96% more accurate than ground counts (Hodgson et al., 2018). The increased accuracy and precision of remote sensing wildlife observation methods could allow for researchers to detect fine-scale population fluctuations for more informed conservation and management.

The miniaturization of thermal sensors has been an important technological advance enabling wildlife monitoring from drones. Thermal sensors form a thermal image of an animal by detecting radiation emitted by the animal in the thermal infrared region of the electromagnetic spectrum (Burke et al., 2019a). Thermal technology aboard piloted aircraft has been used for more than half a century to count animals, such as white-tailed deer (*Odocoileus virginianus*) (Croon et al., 1968) and red deer (*Cervus elaphus*) (Dunn et al., 2002). More recently, drones equipped with thermal sensors have been used to quantify aggregations of common hippopotami (*Hippopotamus amphibius*) (Lhoest et al., 2015) and discriminate between mixed-species aggregations of monkeys, including mantled howler monkeys (*Alouatta palliata*), black-handed spider monkeys (*Ateles geoffroyi*) and kinkajous (*Potos flavus*) (Kays et al., 2019). Thermal remote sensing has a very promising future as a conservation and monitoring tool for ecologists and conservationists who wish to identify, quantify and monitor animal populations.

1.2.1 Improvements in automation capabilities and processing for remote sensing

With drone-enabled remote sensing, an area of interest can be mapped out prior to flight so that the drone can complete an autonomous survey, automatically capturing photo or video (Wich & Koh, 2018). A geographically rectified photo composite of an area, called an orthomosaic, can be generated by stitching together images of a scene taken with high overlap, using photogrammetric techniques (Hung et al., 2019; Westoby et al., 2012). Until recently, any large-scale orthomosaic mapping required surveyors to place ground control points (GCPs) on the ground throughout the scene. Each GCP having precise known three-dimensional (3D) location and positioning in relation to the camera, in order to reconstruct a scene accurately (Westoby et al., 2012). When mapping complex and less accessible areas with dense vegetation or other obstacles the placement of GCPs may not be possible (Tomaštík et al., 2017). By contrast, the recently developed Structure from Motion (SfM) with Multi-View Stereo (MVS) workflow, which is most commonly used in orthomosaic construction software today, has stemmed from 3D Computer Vision algorithms as well as traditional photogrammetric principles and does not require GCP inputs (Smith et al., 2015). Following image acquisition, SfM-MVS identifies matching features between images and uses a bundle adjustment procedure to automatically determine camera position and create a 3D point cloud or a two-dimensional orthomosaic (Wich & Koh, 2018). These products are then scaled and georeferenced based on known positions and the internal measurement unit of the drone during image acquisition (Smith et al., 2015; Westoby et al., 2012). The SfM-MVS workflow enables the accurate mapping of areas with complex ground cover which may be difficult to access by foot.

Automated processes for analysing remotely sensed data, such as processes for generating exact counts of the number of animals in imagery, can save time and increase

efficiency for ecologists (Anderson & Gaston, 2013; Laliberte & Ripple, 2003). Moreover, automated processes may eliminate some of the bias associated with data collection from aerial imagery (Corcoran et al., 2019). Object-based image analysis (OBIA) is a relatively new classification technique in remote sensing, which expands upon traditional pixel-based classification approaches (Blaschke, 2010). In OBIA, an image is first segmented into groups of spatially and spectrally homogenous pixels, the user then creates training samples identifying their objects of interest (Horning et al., 2010); then a rule-based classifier can be applied to classify the image (Thenkabail, 2016). OBIA-based classification can be implemented alongside supervised machine learning algorithms such as Maximum Likelihood (Harris & Stocker, 1998); Support Vector Machines (Cortes & Vapnik, 1995); and Random Forest (Pal, 2005). This method optimises performance when working with complex, multi-layered and high-resolution data (Thenkabail, 2016). OBIA machine learning approaches have previously been used to count mixed-species ghost crab burrow openings (Bycroft et al., 2019); and count and speciate between mixed-species aggregations of birds (Francis et al., 2020) from visible spectrum imagery; using the Random Forest algorithm, to highest accuracies of 66% and 99% respectively (Bycroft et al., 2019).

Computer Vision is another branch of image analysis that allows the user to define rules and infer information about an image based on pixel and object-based characteristics such as intensity, shape and texture (Weinstein, 2018). Computer Vision can be used to extract information about an object of interest automatically and has applications in automated species identification, counting, tracking (Dell et al., 2014) and examination of morphological characteristics (Weinstein, 2018). In the biological sciences, Computer Vision-based image analysis workflows are used most commonly to identify, quantify and track organisms in small-

scale laboratory studies (Pennekamp & Schtickzelle, 2013). However, multistep Computer Vision-driven workflows have also been used to quantify aggregations of snow geese (*Chen caerulescens*), Canada geese (*Branta canadensis*), caribou (*Rangifer tarandus*), and grey seals (*Halichoerus grypus*), achieving a highest accuracy of 98% when compared to manual counts of aerial imagery (Seymour et al., 2017). The Computer Vision and OBIA machine learning classification workflows share some workflow similarities and can be used together or independently to enable semi-automated classification of an area of interest.

1.3 Monitoring flying-foxes for management and conservation

Flying-foxes (*Pteropus* spp.) are a group of species of key ecological significance (Fujita & Tuttle, 1991), despite this, the methods currently used to monitor and count species populations have been shown to be inaccurate and imprecise (Brooke, 2001; Forsyth et al., 2006; O'Shea & Bogan, 2003; Westcott et al., 2012; Westcott & McKeown, 2004). Remote sensing methods may enable researchers to more accurately and precisely manage and conserve this group of species. In this section, I will provide a brief overview of the distribution and conservation status of the family Pteropodidae, including the genus *Pteropus*, the history of *Pteropus* spp. population monitoring in Australia, and the new technologies that are beginning to be employed for monitoring bat populations for conservation and management.

1.3.1 Global flying-fox distribution and conservation status

The family Pteropodidae (or Old World fruit bats) is made up of 200 species spread across 45 genera (Taylor, 2019). This family occurs mostly in tropical regions, across Africa, south Asia and Australia (Figure 1.1). Bats of the family Pteropodidae feed mostly on fruit and nectar which they locate through sight and scent, unlike insectivorous bats (Courts, 1998). As such, these

species tend to be larger with longer wingspans, and longer noses, enabling long distance-flight and a heightened sense of smell to seek out food resources more effectively (Taylor, 2019). These species represent a major component of mammal diversity, where they fulfil important ecological roles as pollinators and seed dispersers (Florens et al., 2017; Fujita & Tuttle, 1991). However, according to the IUCN Red List, the population of 82 species of pteropodids are decreasing, while for a further 59 species, their population status is unknown (International Union for Conservation of Nature and Natural Resources, 2020).

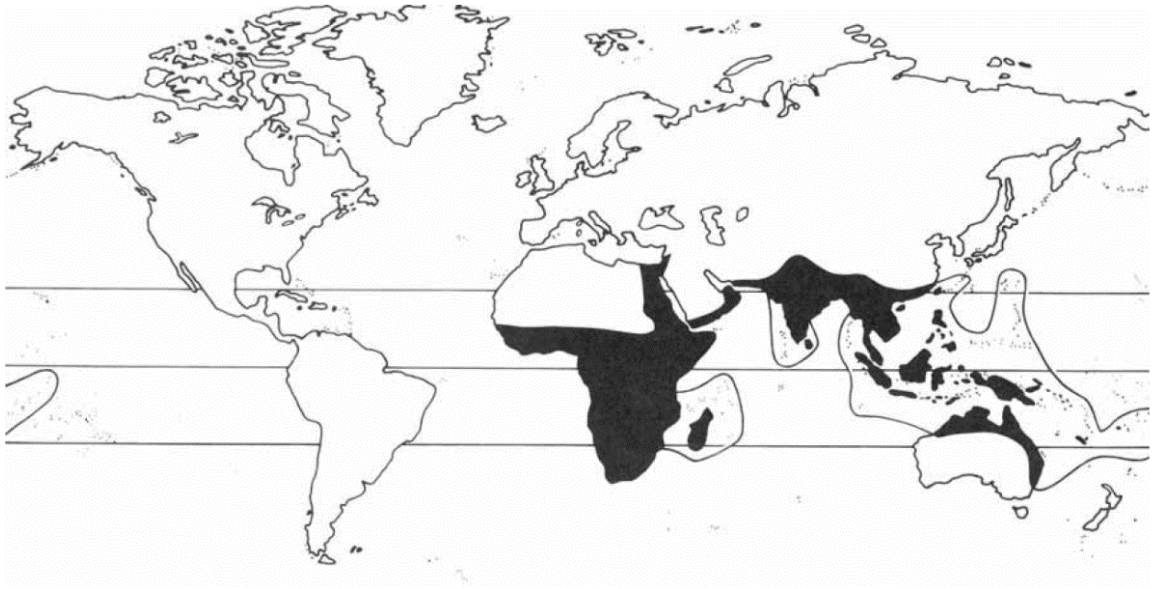

Figure 1.1. Global distribution of bats in the family Pteropodidae (Hill & Smith, 1984).

Flying-foxes are species of the largest genus of the Pteropodidae, *Pteropus*, and are distributed throughout sub-tropical Africa, the Asia-Pacific and Australia (Fujita & Tuttle, 1991). The *Pteropus* genus consists of 67 species, of which 33 species are in decline, while for 15 species the population status is unknown (International Union for Conservation of Nature and Natural Resources, 2020). Monitoring *Pteropus* species, as well as other species in the family

Pteropodidae, is vital for assessing their population statuses and for determining the factors that drive their declines.

1.3.2 Australian flying-fox biology and conservation status

In mainland Australia, there are four species of flying-fox; the grey-headed flying-fox (*Pteropus poliocephalus*), little red flying-fox (*P. scapulatus*), black flying-fox (*P. alecto*) and spectacled flying-fox (*P. conspicillatus*) (Van Dyck & Strahan, 2008). These four species have overlapping habitat ranges and can coexist in colonies where their ranges overlap (Figure 1.2) (Currey et al., 2018; Hall & Richards, 2000). During the day, flying-foxes reside in colonies comprising between a few hundred to thousands of individuals found in amongst the canopies of trees (Lewis, 1995; Parry-Jones & Augee, 2001). Between sunset and sunrise, they feed primarily on nectar, pollen, and fruit, travelling up to 270 km per night while foraging, and thousands of kilometres annually (Tidemann & Nelson, 2004; Welbergen et al., 2020). Australian flying-foxes are highly nomadic and have been shown to move between roosts frequently so that colonies have extremely high turnover rates (Welbergen et al., 2020). Across their range flying-foxes perform highly valuable ecosystem services as long-distance pollinators and seed dispersers between fragmented landscapes (Hall & Richards, 2000).

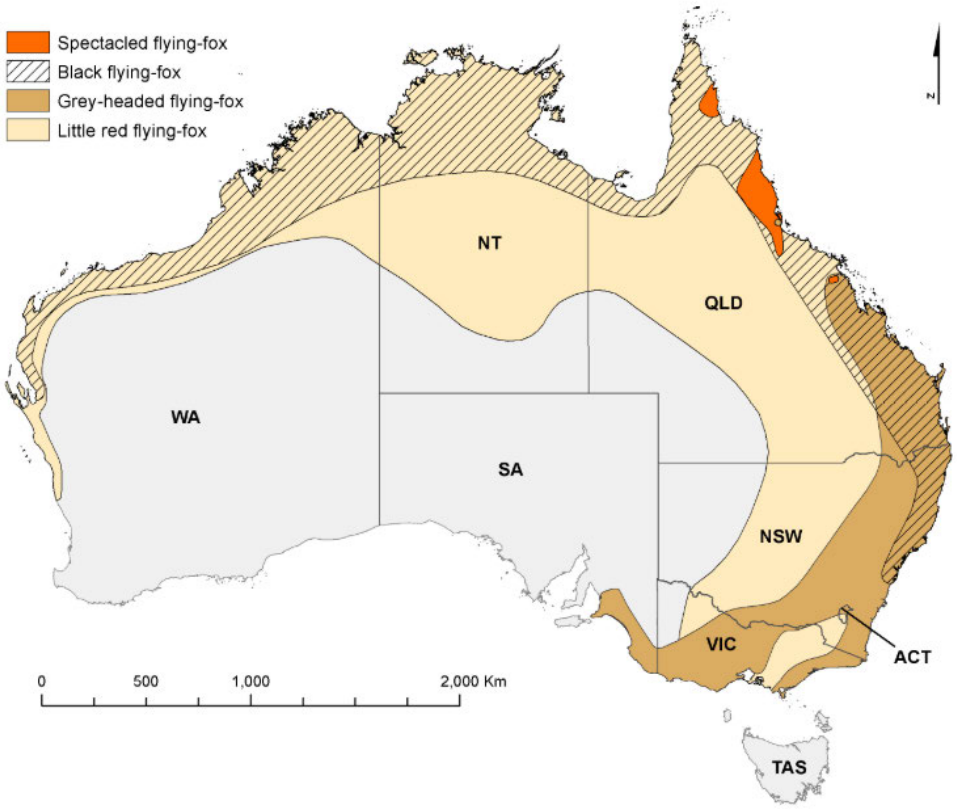

Figure 1.2. Distribution of flying-fox species across the Australian mainland (Currey et al., 2018).

The major threats to Australia's flying-foxes are thought to be habitat clearing (Westcott et al., 2015a) and extreme heat events (Welbergen et al., 2008), as well as electrocution by powerlines, entrapment on barbed wire, culling and colony disturbance (Fox et al., 2008). Flying-foxes were formerly thought to roost non-selectively in many habitat types such as large forests, as well as small patches of trees in urban environments, their migrations driven by mass flowering events (Eby et al., 1999). However, Australia's flying-foxes are becoming increasingly urbanised, possibly in response to habitat fragmentation and an increased abundance and temporal availability of foraging resources in urban environments (Williams et al., 2006). Flying-foxes roosting and foraging in urban environments may come into increased contact and

conflict with humans (Tait et al., 2014), and can face opposition from local communities and landowners due to the noise and smell associated with flying-fox colonies (Currey et al., 2018; Lentini & Welbergen, 2019). Flying-foxes are also the reservoir hosts for several zoonotic diseases including Hendra virus, Menangle virus and Australian Bat Lyssavirus (Halpin et al., 1999); therefore, their movement into urban and peri-urban environments may pose increased risks of these viral agents for humans and their livestock (Hassell et al., 2017; Plowright et al., 2011).

Grey-headed flying-foxes and spectacled flying-foxes have been listed respectively as 'vulnerable' and 'endangered' under the Australian *Environment Protection and Biodiversity Conservation Act 1999* (Commonwealth of Australia Department of Environment and Energy, 2019a) due to a decline in estimated population size in recent years (Westcott et al., 2015a). The most recent available estimates (May 2019) put the combined population of Australia's four mainland flying-fox species at 970,000, including approximately 586,000 grey-headed flying-foxes and 38,000 spectacled flying-foxes (Commonwealth Scientific and Industrial Research Organisation, 2019). The latter experienced an extreme heat event in November 2018 that killed ~23,000 individuals, representing approximately one-third of the species' population in Australia at the time (Mao, 2019).

1.3.3 The history of flying-fox population monitoring in Australia

The first review of Australia's flying-fox populations was completed in the early 20th century, in response to concerns over the damage done to fruit orchards by flying-foxes across the eastern coast (Ratcliffe, 1931). Ratcliffe (1931) writes of the difficulty associated with gaining accurate estimates of the number of individuals in a colony due to the view of the colony being partially

or almost entirely obstructed in most cases. They also comment on the tendency of observers to underestimate colony size while flying-foxes are roosting, and overestimate colony size if the observer is counting as they fly-out. Importantly, Ratcliffe (1931) estimates the total population of flying-foxes across Australia as “many millions”.

Since these initial attempts at monitoring Australian flying-foxes, several large-scale programs have aimed to establish flying-fox species population baselines (Eby et al., 1999; Garnett et al., 1999; Westcott et al., 2015a). Flying-foxes are a highly mobile group of species and are known to move nomadically between colonies, so colony size is not static (Augee & Ford, 1999; Welbergen et al., 2020). This renders flying-fox population censuses complex, and range-wide surveys must be conducted over a limited timeframe to avoid double counting animals that have moved between roosts (Westcott et al., 2015a).

Several publications have presented methods for quantifying the number of flying-foxes in a colony through counting the animals as they emerge from their roosts at sunset (Brooke et al., 2000; Eby et al., 1999; Garnett et al., 1999; Parry-Jones & Augee, 1992; Vardon & Tidemann, 1999) as well as while they roost during the day (Eby et al., 1999). These ‘fly-out counts’ and ‘ground’ or ‘static counts’ continue to be the most common methods for monitoring flying-fox numbers to date (Westcott et al., 2015a). Other methods include analysing the frequency and intensity of flying-fox calls during roosting as a predictor for the number of individuals in a colony (Parry-Jones & Augee, 1992). However, no unified method is used to monitor Australia’s flying-foxes nor other pteropodids globally.

In response to growing concerns over the long-term population status of Australia’s flying-foxes, particularly the grey-headed and spectacled flying-fox, the National Flying-Fox

Monitoring Program (NFFMP) was developed in collaboration with Australian federal and state governments, as well as the Commonwealth Scientific and Industrial Research Organisation (CSIRO) (Westcott et al., 2015b). The NFFMP aims to generate more up-to-date information on the status, distribution and trends of Australia's four mainland flying-fox species (Westcott et al., 2015b). The NFFMP aims to estimate the number of individuals in every known flying-fox roost across the species ranges by either ground or fly-out count every three months (Westcott et al., 2015a). The NFFMP uses ground counts of colonies as their primary method for estimating colony size as they can rapidly be implemented across large geographical scales; are said to have estimable biases (Westcott et al., 2012); and are relatively low cost compared to other monitoring methods (Westcott et al., 2015b). Between February 2018 and February 2020, 94% of the NFFMP colony size counts were conducted using the ground count method (A. Mckeown, personal communication, August 20, 2020).

Traditional ground counts of flying-foxes are conducted during the day when flying-foxes are roosting. If the roost comprises a colony of fewer than 1,000 individuals or is easily accessible, a direct count of every visible flying-fox is conducted. If the colony is larger or the roost is inaccessible, a colony size estimate can be derived from point or line transect-based distance sampling. Here, observers move through a roost or along its perimeter and stop at numerous points to count all visible flying-foxes and record the distance of each flying-fox from the researcher's standpoint. These data can then be used to estimate the probability of detecting a flying-fox, an estimate of flying-fox density and thus the number of animals in a given roost of known area (Westcott et al., 2011). Alternatively, surveyors can conduct a direct count of individuals in a section of known area to generate a value for colony density (Westcott et al., 2011). Critically, state-space modelling has shown that trends derived from spectacled flying-fox

colony size estimates from ground counts at all known roosts throughout their range, between 2006 and 2013, had a very high amount of variation (coefficient of variation = 67%) (Westcott et al., 2015a).

Fly-out counts are another colony size estimation method for pteropodids, used both in Australia and internationally (Brooke et al., 2000; Garnett et al., 1999; Parry-Jones & Augee, 2001). During a fly-out count, observers count individuals within streams of flying-foxes as they fly overhead and leave the colony to forage at dusk (Westcott & McKeown, 2004). Fly-out counts require more volunteers and are logistically complex compared to ground counts (Westcott et al., 2015a). Westcott and McKeown (2004) evaluated the accuracy of fly-out counts by comparing counts by observers in the field to counts of video-recorded footage of the same fly-out and found that observer counts, whilst significantly related to the true video count, underestimated the video count by 14.7%. Another study compared the accuracy and precision of human-conducted fly-out counts across three flying-fox colonies and compared it to counts from recorded video footage of each fly-out that has been slowed-down (Forsyth et al., 2006). They found that for two colonies, the number of individuals was underestimated by an average of 17%, but in the third it was overestimated by 96% (Forsyth et al., 2006). Furthermore, the accuracy and precision of counts decreased as the number of individuals in the flying-fox colony increased (Forsyth et al., 2006). Human error has also been shown to increase with increasing width of the fly-out stream (Westcott & McKeown, 2004). Similarly, nightly differences in emergence pattern and environmental conditions can contribute considerably to variations in fly-out counts of Pacific Island flying-foxes (*Pteropus* spp.) (O'Shea & Bogan, 2003).

Flying-foxes remain notoriously difficult to monitor (Forsyth et al., 2006; Westcott et al., 2012; Westcott & McKeown, 2004). Both ground counts and fly-out counts are costly, labour

intensive, and lack accuracy and precision; therefore, there is a great practical need for the development of alternative methods for estimating the number of individuals in flying-fox colonies. Remote sensing using drones equipped with thermal sensors may provide a viable alternative, allowing for more accurate and precise monitoring of these species.

1.3.4 Technological advances in monitoring bat populations

Several promising methods other than direct counts from human observers have been used to monitor bat populations. For example, thermal cameras have been used to film the cave emergence of Brazilian free-tailed bats (*T. brasiliensis*), and video analysis software has been used to track and count the true number of emerging bats (Betke et al., 2008). Critically, the true number of bats was found to be up to ten times lower than previous estimates derived from manual fly-out counts by observers (Betke et al., 2008). In Australia, colony size estimates from the cave emergence of the common bent-winged bat (*Miniopterus schreibersii*) obtained from infrared video footage have been found to be more accurate and precise than those obtained from visual census (Brown et al., 2008). A similar method, employing automatic counting techniques, based on missile tracking technology has also been used to monitor populations of the critically endangered southern bent-wing bat (*Miniopterus schreibersii bassanii*) (Lumsden & Jemison, 2015). For flying-fox monitoring, colony size estimates derived from weather radar data have proven useful in the long-term monitoring of a flying-fox colony, where estimates derived from radar correspond closely with those derived from traditional colony size estimation methods (Meade et al., 2019). To date there is no known published research on the use of drones equipped with thermal sensors to monitor flying-fox colony size, and through my MRes research I aimed to develop and test this as a method for monitoring flying-fox populations.

1.4 Thesis aims

The overarching aim of this thesis is to investigate the use of drone-acquired thermal imagery as an effective new tool to inform the management and conservation of flying-fox populations.

Specifically, I aim to:

1. Optimise methods for the collection of drone imagery and generation of thermal orthomosaics of a flying-fox colony (Chapter 2).

2. Generate machine learning and Computer Vision-driven methods for semi-automated counting of the number of flying-foxes in a roost and compare the accuracy of these methods (Chapter 2).

3. Evaluate the extent of between-counter and between-orthomosaic variability for flying-fox colony size estimates derived from thermal orthomosaics (Chapter 2).

4. Compare flying-fox colony size estimates from drone-acquired thermal orthomosaics to traditional ground counting methods (Chapter 3).

5. Monitor changes in the number and density of individuals present, and patterns in roost area occupancy, over time (Chapter 3).

1.5 Study area

The Greater Sydney region was chosen as it is known to contain approximately 20 permanently occupied flying-fox colonies (Commonwealth of Australia Department of Environment and Energy, 2019b). This region is within the Sydney Basin Bioregion and remnant vegetation in the region consists mainly of Eucalypt open forests and woodlands, with an understory of grass,

shrubs, ferns, or herbs (Geoscience Australia, 2001) as well as non-native species (Downey et al., 2010).

When selecting drone survey roosts, legislation pertaining to drone use in the study area must be considered. In Australia, drones are prohibited from flying within 5.5 km of an aerodrome or within restricted areas without special permission (Australian Goverment Civil Aviation Safety Authority, 2019); therefore, all flying-fox roosts located within these areas were excluded from this study.

Colonies were also selected based on their accessibility and ease of access for ground counting estimates to be made. For example, the colonies at Balgowlah (-33.7890°, 151,2600°) and Avalon (-33.6256°, 151.3251°) were excluded because they were too close to main roads and housing to allow for legal and safe drone operation.

Eight flying-fox roosts fit the criteria: including roosts located in Camellia Gardens, Campbelltown, Centennial Park, Emu Plains, Kareela, Macquarie Fields, Warriewood and Yarramundi, and were selected as study sites for this research (Figure 1.3).

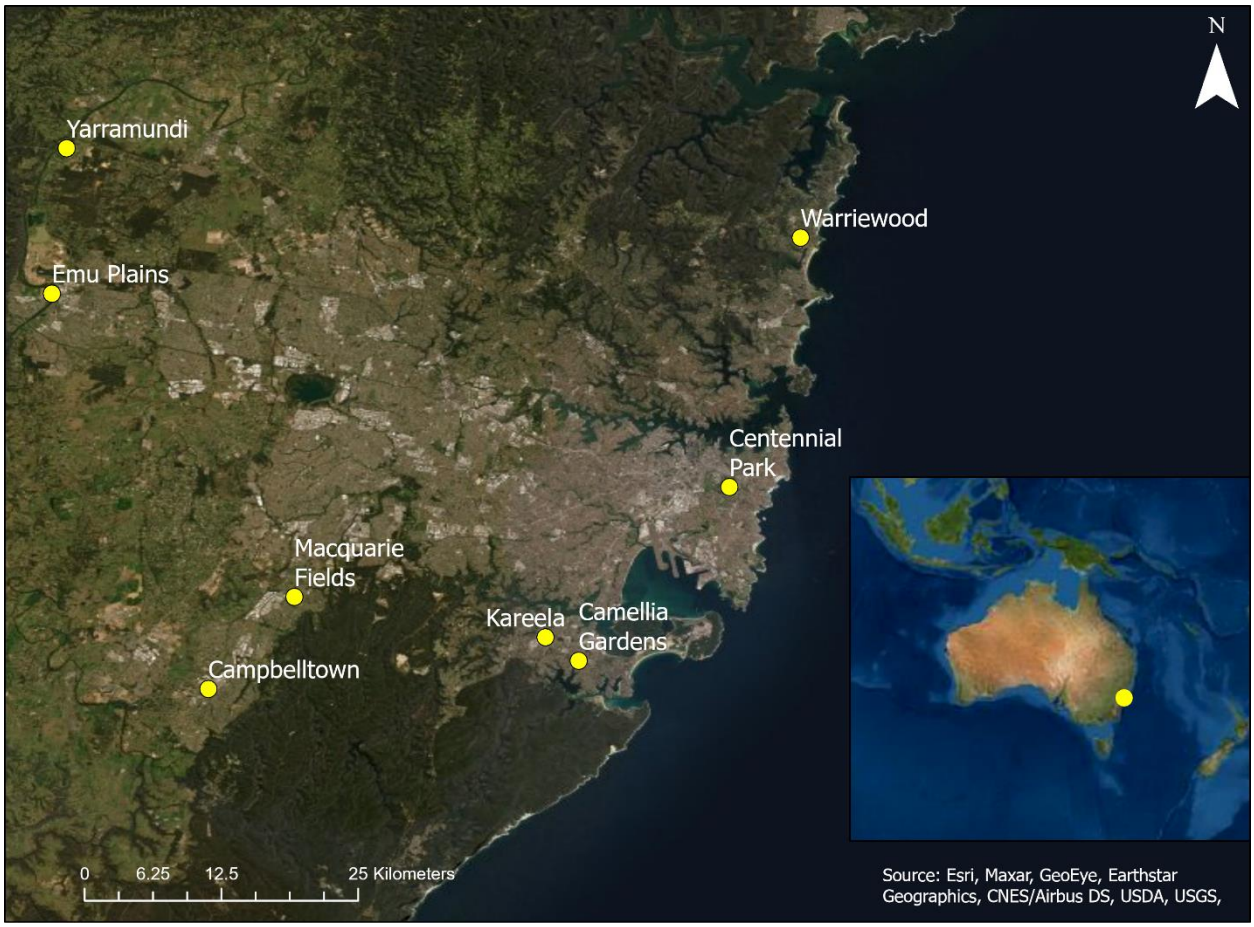

Figure 1.3. Locations of the eight flying-fox roosts across the Greater Sydney region which were selected as study sites for this research.

The geographic coordinates of these roosts are given below (Table 1.1).

Table 1.1. Geographic coordinates of the eight flying-fox colonies throughout the Greater Sydney region which were included in this study. Coordinates are accurate as of August 2020.

Location	Latitude (°)	Longitude (°)
Camellia Gardens	-34.0426	151.1128
Campbelltown	-34.0658	150.8088
Centennial Park	-33.8998	151.2365
Emu Plains	-33.7408	150.6803
Kareela	-34.0233	151.0855
Macquarie Fields	-33.9901	150.8794
Warriewood	-33.6948	151.2950
Yarramundi	-33.6189	150.6946

1.6 Thesis structure

This thesis consists of the current introductory chapter (Chapter 1), two data chapters (Chapter 2 & 3), and one concluding chapter (Chapter 4).

In Chapter 2, I develop a method for remotely surveying flying-fox colonies and generating colony size estimates using a drone equipped with a thermal camera. I then assess the performance of different automated counting techniques employing OBIA, machine learning and Computer Vision processes. Lastly, I evaluate the precision and user bias associated with colony size estimates derived from this new method by comparing results of visual point counts of flying-foxes between counters, and between repeated surveys on the same day.

In Chapter 3, I compare the results from exhaustive ground counts of the true number of individuals present in single trees with the corresponding counts from drone-acquired thermal imagery for the same single trees to determine the accuracy of monitoring colony size using drone-acquired thermal imagery. Here I also analyse the effect of air temperature and canopy

cover on drone-acquired thermal imagery count accuracy. Following this I compare whole colony estimates derived from ground counts collected during the NFFMP for October and November 2019, and February, June and August 2020, with counts from drone-acquired thermal imagery collected concurrently. I also demonstrate the utility of the new method to map colony roosting density, roost area occupied and colony movement throughout the roost over time.

In Chapter 4, I present a summary of my results and place my research in the broader context of population monitoring of flying-foxes in Australia. Here, I also consider directions for future research.

Chapters 2 and 3 have been prepared as stand-alone papers for submission to peer-reviewed journals – this means that there will inevitably be some overlap, including with Chapter 1.

All references in this thesis have been formatted in APA 7th edition style.

Chapter 2 - Using drone-based thermal remote sensing and computer vision for semi-automated counting of flying-foxes at their roosts

2.1 ABSTRACT

Accurate monitoring practices allow researchers to gather information about species abundance and distribution, which is essential for determining population trends and species responses to environmental change. However, traditional population survey methods can be inaccurate and unreliable. Flying-foxes are large species of bat that roost in the canopies of trees in groups of a few hundred to many thousands of individuals, where they are difficult to census accurately by human observers. This is problematic for the effective conservation and management of these species. I developed and tested a new method for censusing flying-fox colonies, using drone-acquired thermal orthomosaics. I tested this method at eight grey-headed flying-fox roosts across the Greater Sydney region, Australia. I assessed the accuracy of four semi-automated methods for counting flying-foxes in orthomosaics, including machine learning and Computer Vision approaches. I also evaluated the precision and user bias associated with this new method by comparing results of visual point counts of flying-foxes between counters, and between repeated surveys on the same day. I found that the Computer Vision semi-automated counting method delivered counts most consistently similar to visual point counts ($\rho c = 0.83$). Additionally, I found that visual counts of the number of flying-foxes in orthomosaics from repeated surveys were highly precise (RSE 0.93-6.91%) and did not vary between counters ($F_{4,9} = 1.055$, $p = 0.433$). Thus, the method presented here is valuable for accurately and precisely estimating the number of individuals in a flying-fox colony, with limited user bias, and will aid in the

conservation and management of these species as well as other warm-blooded colonial tree roosting species.

2.2 INTRODUCTION

Monitoring and quantifying animal populations is a fundamental activity in conservation biology (Marsh & Trenham, 2008). Population censuses can provide baseline information about the welfare of a species, while monitoring populations over time can elucidate population trends including declines (Woinarski, 2018), and determine the effectiveness of management practices (Reddiex et al., 2006). For this, it is essential that population censuses produce reliable, accurate and reproducible estimates of the target population so that researchers and policy makers can make well-informed decisions regarding species conservation and management (Goldsmith, 1991).

The validity of population survey methods may be biased by several factors that can generate inaccurate and imprecise, and therefore unreliable, population estimates (Seber, 1986). The accuracy and precision of population surveys has been shown to decrease with increasing population size (Manning et al., 1995). Population surveys are also subject to accessibility biases, where areas which are further away from roads or densely vegetated are less frequently surveyed than those which are more accessible (Reddy & Dávalos, 2003; Wagner, 1981). Additionally, surveys are also subject to between-observer variability in resulting population estimates (Erwin, 1982). Critically, inaccurate and imprecise population survey methods may lead researchers and policy makers to draw incorrect conclusions about species status and abundance (Guschanski et al., 2009; Margalida et al., 2011). Ultra-high-resolution remote

sensing is an emerging technology being used to generate more reliable population estimates for flora and fauna globally (Wang et al., 2010).

Recent technological advances have made remotely piloted aircraft systems (RPAS), hereafter drones, more affordable and available for remote sensing (Jiménez López & Mulero-Pázmány, 2019). Drones are used increasingly as tools for wildlife surveillance (Christie et al., 2016) and tend to be quieter, more manoeuvrable and to cause less disturbance to wildlife than traditional piloted aircraft (Christie et al., 2016). Advancements in drone technology are paralleled by improvements in sensor resolution and a reduction in the cost of commercially available thermal imaging devices (Wich & Koh, 2018).

Thermal sensors detect and quantify thermal radiation emitted from an object or living thing (Burke et al., 2019a). Thermal imaging has long been used for the detection, quantification, and tracking of animal populations (Croon et al., 1968; Graves et al., 1972) and has applications in the study of reproductive processes, thermoregulation, and animal behaviour (Cilulko et al., 2013). Previously, thermal sensors aboard piloted aircraft have successfully detected and estimated the density of mixed-species aggregations in complex environments (Garner et al., 1995; Naugle et al., 1996), located radio-collared Florida panthers (*Puma concolor coryi*) (Havens & Sharp, 1996), and quantified the population of Pacific walruses (*Odobenus rosmarus divergens*) in remote locations (Burn et al., 2006). More recently, drones equipped with thermal sensors have been used to semi-automatically identify and age populations of breeding colonies of grey seals (*Halichoerus grypus*) (Seymour et al., 2017); to detect and quantify arboreal primates, such as mantled howler monkeys (*Alouatta palliata*), black-handed spider monkeys (*Ateles geoffroyi*) and kinkajous (*Potos flavus*) (Kays et al., 2019; Spaan et al., 2019); common

hippopotami (*Hippopotamus amphibius*) (Lhoest et al., 2015); and koalas (*Phascolarctos cinereus*) (Corcoran et al., 2019).

Maps derived from Structure from Motion (SfM) photogrammetry have allowed researchers to create hyper-resolution photomaps or orthomosaics and quantify individuals of a diverse range of species spread over large areas (Bycroft et al., 2019; Francis et al., 2020; Old et al., 2019). However, manually counting animals in remotely sensed imagery is time consuming and can be subject to human error (Erwin, 1982; Harris & Lloyd, 1977). Furthermore, as the volume and availability of aerial imagery increases, automated methods are required for image analysis (Terletzky & Ramsey, 2016). Two such systems that can be used for automated image classification are object-based image analysis (OBIA) enabled machine learning and Computer Vision.

Machine learning-based classification techniques have a wide range of applications in ecology and species population monitoring (Chen & Liu, 2017; Corcoran et al., 2019; Dell et al., 2014; Francis et al., 2020; Tabak et al., 2019; Terletzky & Ramsey, 2016; Valletta et al., 2017; Yang et al., 2015). OBIA segments an image into groups of spatially and spectrally connected pixels, or image objects. These objects can then be classified more accurately based on their attributes and multiscale variation (Kelly et al., 2011). OBIA can be used alongside supervised classification and machine learning workflows, where the user defines objects or training samples in a scene that are used to classify the entire segmented image through a machine learning algorithm (Kotsiantis et al., 2007). Some commonly used machine learning algorithms include: Support Vector Machines (Vapnik, 1999); Maximum Likelihood (Harris & Stocker, 1998); and Random Forest (Breiman, 2001). OBIA-supervised classification workflows are commonly used to classify land use and land cover (Weih & Riggan, 2010). However, they have

also been used in ecological studies to identify, classify, and quantify populations of coral (Phinn et al., 2012); vegetation (Dronova et al., 2012); to differentiate between 16 species of marine birds (Groom et al., 2013); and to detect mixed-species ghost crab burrows (Bycroft et al., 2019).

Computer Vision-based classification is a branch of computer science where classification is user driven. Computer Vision allows the user to define rules and infer information about an image based on pixel characteristics such as intensity, shape and texture (Weinstein, 2018). Computer Vision has applications in automated species identification; counting; tracking (Dell et al., 2014); and examination of morphological characteristics (Weinstein, 2018). However, in the biological sciences, Computer Vision-based image analysis workflows are most commonly used to identify, quantify and track organisms in small-scale laboratory studies (Pennekamp & Schtickzelle, 2013).

Old World fruit bats, of the family Pteropodidae, are largely understudied (International Union for Conservation of Nature and Natural Resources, 2020) and difficult to monitor due to their expansive distribution and the inaccessibility of roosting sites (Westcott et al., 2012). They are distributed throughout Africa, southeast Asia, Australia, and the Pacific Islands, where they perform key roles in pollination and seed dispersal (Fujita & Tuttle, 1991). This family is threatened throughout its range by habitat loss (Mohd-Azlan et al., 2001); the effects of climate change (e.g. Welbergen et al., 2008); and overhunting (Brooke & Tschapka, 2002). According to the IUCN Red List, the populations of 82 of the 200 species of pteropodids are decreasing, while for a further 59 species, their population status is unknown (International Union for Conservation of Nature and Natural Resources, 2020). There is thus a great need for more reliable monitoring practices for pteropodids.

In mainland Australia, there are four species of flying-fox of the genus *Pteropus* within Pteropodidae. Of these species, the grey-headed flying-fox (*Pteropus poliocephalus*) is listed as Vulnerable and the spectacled flying-fox (*P. conspicillatus*) is listed as Endangered under national environmental legislation (Commonwealth of Australia Department of Environment and Energy, 2019a). During the day, these species are found in roost sites (or 'camps') where they form colonies of a few hundred to many thousands of individuals in the canopies of trees, in natural, rural and urban bushland areas (Eby et al., 1999; Garnett et al., 1999; Palmer & Woinarski, 1999; Parry-Jones & Augee, 2001; Tait et al., 2014). They are often the subject of human-wildlife conflict (Kung et al., 2015; West, 2002) especially when colonies are located in close proximity to housing and public areas (Currey et al., 2018; Mo et al., 2020). Conflicts can be exacerbated by perceptions of the risk of wildlife diseases (Halpin et al., 1999; Hassell et al., 2017). Presently in Australia, the number of individuals that comprise a colony at a roost (defined here as 'colony size') is estimated by ground counts (also known as 'static counts'), where counters survey the number of individuals present during the day, and fly-out counts, where counters count flying-foxes as they fly-out of the colony in streams for nightly foraging (Westcott et al., 2011). Accurate ground counts require counters to walk through a flying-fox colony, which can be impractical with dense vegetation and also cause a high degree of disturbance (Westcott et al., 2011), while fly-out counts have been shown to be inaccurate and imprecise (Forsyth et al., 2006; Westcott & McKeown, 2004). The development of more accurate monitoring practices for assessing colony sizes of flying-foxes would enhance the evidence base for effective conservation and management of these species.

Herein, I describe a methodology for producing drone-acquired thermal orthomosaics of flying-fox roosts and quantifying the number of flying-foxes in orthomosaics. To begin, I discuss

ethical considerations for drone operation over a flying-fox colony, then ideal environmental conditions and optimal drone settings for orthomosaic construction. Then, four semi-automated approaches are used to quantify flying-foxes in a series of orthomosaics of flying-fox roosts throughout the Greater Sydney region, to determine the best-performing approach for semi-automated colony counting. I examine the capabilities of Maximum Likelihood; Random Forest; and Support Vector Machine algorithms using OBIA; as well as a Computer Vision approach, for detecting flying-foxes in thermal imagery. Lastly, I examine the variability of flying-fox colony size estimates derived from repeated orthomosaics at the same roosts.

2.3 METHODS

2.3.1 Ethical considerations

The ethical considerations and risks associated with the use of drone technology near wildlife must be considered, as drones, when used improperly, have the potential to cause immediate harm and large-scale disruption to an ecological community (Grémillet et al., 2012; van Wynsberghe & Donhauser, 2018). Drone disturbance on most species remains largely understudied; however, disturbance is thought to depend on speed, angle and height at which the drone approaches (Mulero-Pázmány et al., 2017). Smaller, quieter, slower-moving and horizontally flying drones are thought to minimise disturbance to wildlife (Mulero-Pázmány et al., 2017).

Drones are a newly-emerging ecological survey tool, as such, it is important to develop and observe best practices when using them, utilising the institutional animal ethics process, adhering to equipment maintenance schedules, exercising practices that minimise disturbance to wildlife and ceasing operations if they are deemed excessively disruptive (Hodgson & Koh,

2016). The experimental procedures conducted throughout this study align with these recommendations.

At the time of writing, to the best of my knowledge, this was the first research to use drones near to and above flying-fox colonies. So, for this study it was crucial to develop clear guidelines for preventing and identifying flying-fox disturbance or distress. Prior to experimentation, a trial flight was performed in the presence of members of the Animal Care and Ethics Committee (ACEC) at Western Sydney University so that they could observe flying-fox behaviour whilst the drone was overhead. Observers did not perceive any noticeable effects of disturbance to the colony. For all subsequent flights, several procedures were set up to avoid causing disturbance to flying-fox colonies. I took care to ensure that the drone and I remained greater than 15 m from a flying-fox during drone surveys. In addition, a disturbance threshold was adhered to, whereby if more than 20 flying-foxes took flight for more than one minute during a survey, the survey would be terminated, albeit the disturbance threshold was never reached. Moreover, all surveys were conducted when the air temperature was less than 30°C, in order to avoid adding to heat stress in the flying-foxes that are known to experience mass mortality when ambient air temperatures exceed 42°C (Welbergen et al., 2008).

Occasionally, white-bellied sea eagles (*Haliaeetus leucogaster*), powerful owls (*Ninox strenua*) or nesting white ibis (*Threskiornis molucca*) are also present in flying-fox colonies (J. Welbergen, personal communication, May 13, 2019). In this study, to avoid any potential impacts on other wildlife, a visual survey of each roost was conducted prior to each aerial survey to determine the presence of non-target wildlife. If such other non-target wildlife were present, a drone survey would not be conducted.

2.3.2 Temperature requirements for detecting flying-foxes in thermal imagery

Collecting reliable imagery for this study relied on flying-fox external body temperature being different to the ambient temperature. As expected, preliminary observations suggested that as ambient temperature increased, and approached flying-fox external body temperature, flying-foxes became more difficult to distinguish from the background (Figure 2.1). To account for this, all drone surveys were conducted in the early morning (commencing 66 to 130 mins after sunrise) when flying-foxes would be warm, having recently returned from foraging, and ambient temperature would be comparatively low (similar to Brunton et al. (2020) for eastern grey kangaroos (*Macropus giganteus*), and Kays et al. (2019) for arboreal primates). Thermal surveys were also trialled immediately after first light in the morning, when air temperature was likely to be lowest in the day; however, imagery from these surveys could not be stitched to form an orthomosaic. While reasons for this were not tested empirically in this study, colder, moist, and often foggy morning air closer to vegetation may have adversely affected image quality, as described in Burke et al. (2019a). For all formal surveys in this study, air temperature ranged from 5.0-22.6°C, with a mean air temperature of 18.3°C.

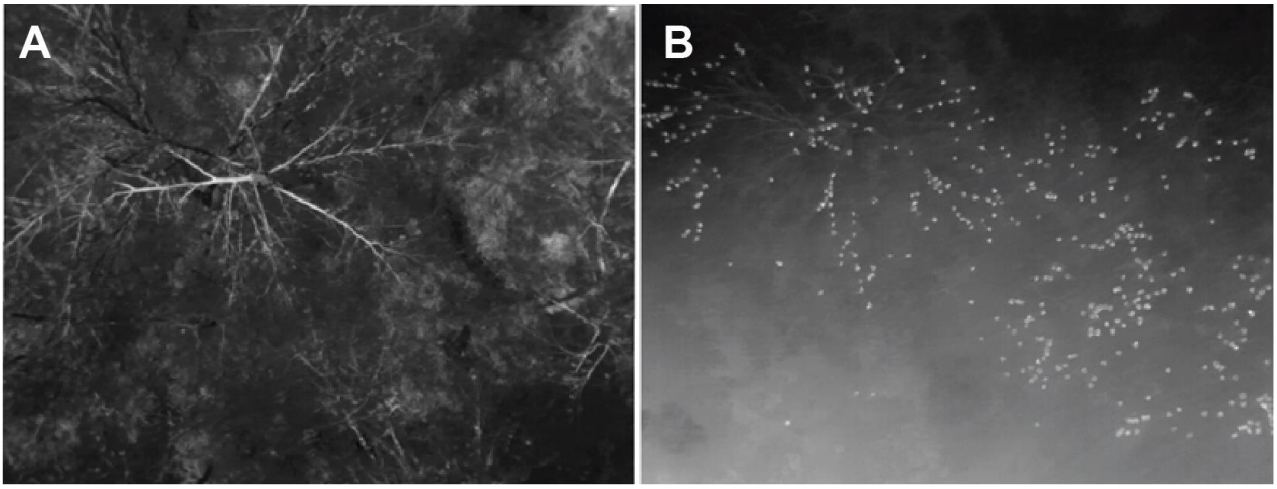

Figure 2.1. Preliminary drone-acquired thermal images taken at 50 m above ground level at the same point in the Emu Plains flying-fox colony (-33.7408°, 150.6803°). Aerial image (A) was taken when air temperature was 29°C, while image (B) was taken when air temperature was 10°C. Flying-foxes in (B) are bright and easily distinguishable from dark (cooler) background, while in (A), there is markedly less spectral contrast between the flying-foxes and the vegetation.

2.3.3 Thermal orthomosaic construction using drones

When conducting aerial surveys of flying-foxes, surveyors must balance collecting high resolution imagery, where individuals are best resolvable, with the need to minimise disturbance to focal animals and cover large land areas in a limited amount time (Burke et al., 2019a). Therefore, it was crucial to determine the ideal flight height of the drone, to ensure flying-foxes were depicted in drone-acquired thermal imagery whilst balancing against the other considerations. Flying-foxes roost upside down in the canopy during the day, and so will appear as circular objects in drone-acquired thermal imagery. The diameter of a roosting flying-fox from an aerial perspective, as given by the widest cross section through an individual, is approximately 0.10 m (Meade et al., 2019).

The Drone Observing tool (Burke et al., 2019a) was used to calculate the height above the canopy that the drone should be flown in nadir direction, in order to achieve an approximate flying-fox resolution of 5 x 5 pure pixels or 2 cm^2 per pixel in thermal imagery for the average flying-fox. Accounting for the technical specifications of the Zenmuse XT radiometric thermal camera (FLIR, Wilsonville, USA) that was used in this study (resolution: 640 x 512, angular resolution: 32° x 26°), the required flight height was found to be 23 m above roosting flying-foxes. Previously, the mean vegetation height of grey-headed flying-fox roost areas has been shown to be 27 ± 0.6 m (Timmiss, 2017). Therefore, the drone was flown at 50 m above ground level (AGL), approximately 23 m above flying-foxes for all surveys, to achieve a maximum approximate resolution of 2 cm^2 per pixel for roosting flying-foxes.

To determine the optimal overlap between successive thermal images for orthomosaic construction, a DJI Inspire 1 v. 2.0 quadcopter (DJI, Shenzhen, China) and Zenmuse XT radiometric thermal camera (640 x 512 resolution, 19 mm focal length), were used to complete a series of autonomously controlled flights over Yarramundi Reserve flying-fox colony (-33.6189°, 150.6946°), capturing images with front and side overlap between successive images of 75, 80, 85 and 90%, at height 50 m AGL, using the flight planning application Pix4Dcapture 4.9.0 (Pix4D, 2017).

All images were taken while the drone was in motion, or cruising mode, flying at 2 m/s, which allowed for significantly reduced survey time and more stable image orientation compared to the stationary drone for image acquisition (Eisenbeiss & Sauerbier, 2011). An example flight path for the Yarramundi roost (-33.6213°, 150.6924°) is shown below (Figure 2.2).

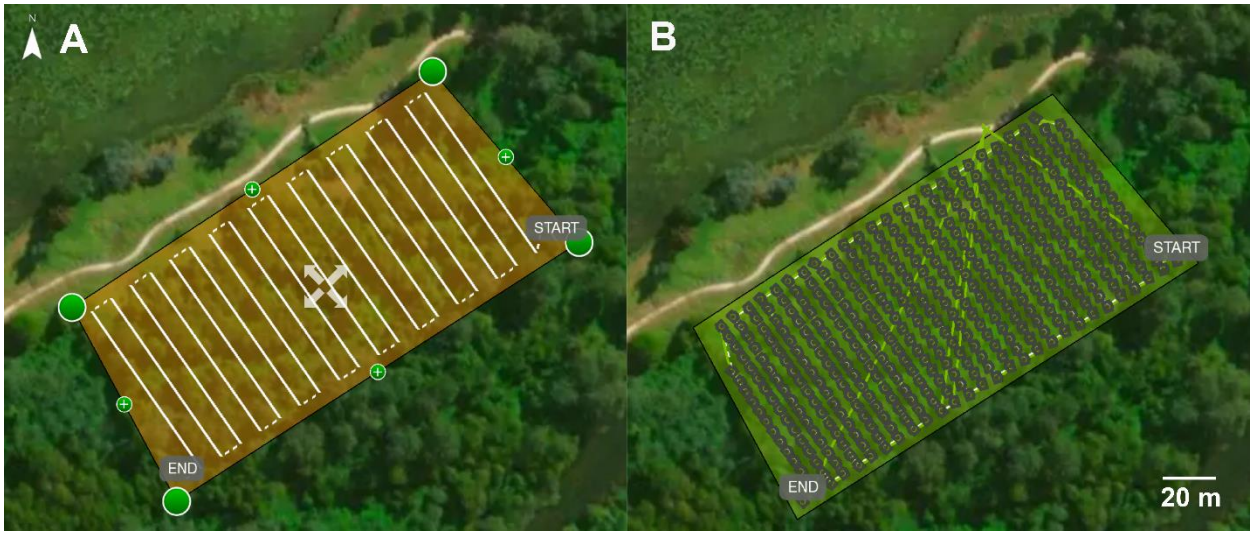

Figure 2.2. Flight path over the Yarramundi Reserve flying-fox roost: (A) shows the planned drone flight path; (B) shows the post-flight path, indicating where images were captured (black symbols; Pix4D, 2017) (background image source: Maxar).

All drone flights were conducted when wind speed was below 10 km/hr (measured from the nearest weather station), as wind has been shown to affect the positional accuracy of a drone (Hung et al., 2019) and cause vegetation movement that can impede feature-matching between images for orthomosaic construction (Duffy et al., 2018).

All survey images were saved as radiometric JPEG files, with embedded EXIF data providing latitude, longitude, and altitude. Images were visually inspected, and blurry images were manually deleted prior to orthomosaic construction, as they may prevent the software from generating tie points between images (Fonstad et al., 2013; Grenzdörffer et al., 2008; Thiele et al., 2017).

Agisoft Metashape Professional Version 1.5 (LLC Agisoft, 2019) was used for orthomosaic generation. The settings used for orthomosaic construction in Agisoft Metashape Professional Version 1.5 are given in Appendix 1 (LLC Agisoft, 2019). Resulting orthomosaic

resolution varied depending on the quality of contributing images. Average orthomosaic resolution for all orthomosaics was recorded. Through repeated trials, I determined that the overlap between thermal images should be no less than 90%, to generate an orthomosaic. Due to reduced resolution and low contrast in thermal images, images collected with less than 90% overlap could not be aligned in photogrammetry software (see Ribeiro-Gomes et al., 2017).

2.3.4 Developing and testing semi-automated counting methods

To test semi-automated counting methods on thermal orthomosaics from a range of colonies, thirteen thermal orthomosaics were generated for eight flying-fox colonies throughout the Greater Sydney region. For all surveys, drone-acquired thermal images contributing to orthomosaics were collected with 90% overlap at a height of 50 m AGL. Two orthomosaics were generated for each of the colonies located at Campbelltown (-34.0658°, 150.8088°); Camellia Gardens (-34.0426°, 151.1128°); Emu Plains (one capturing approximately 50% of the colony extent; -33.7408°, 150.6803°); Kareela (-34.0233°, 151.0855°); and Yarramundi (-33.6213°, 150.6924°). One orthomosaic was generated for colonies located at Centennial Park (-33.8998°, 151.2365°); Macquarie Fields (-33.9901°, 150.8794°); and Warriewood (-33.6948°, 151.2950°). For all orthomosaics, the median air temperature recorded at the nearest weather station during drone operation was recorded (Bureau of Meteorology, 2020).

The number of flying-foxes in each orthomosaic was manually counted by exporting each orthomosaic as a TIFF file from Agisoft Metashape Professional Version 1.5 (LLC Agisoft, 2019) and importing into Fiji 1.8.0_172 (Schindelin et al., 2012) using the Bio-Formats plugin (Linkert et al., 2010). The ‘Enhance Contrast’ command was applied with 0.3% saturated pixels. Then, the multi-point tool was used by the operator to mark every visible flying-fox in the

orthomosaic until the counter was confident that no individuals had been missed and the resulting 'visual point count' was recorded (example shown in Appendix 2). Following this, the number of flying-foxes in each orthomosaic was semi-automatically counted using the OBIA enabled machine learning and Computer Vision analysis workflows.

2.3.4.1 Computer Vision method

For the Computer Vision analysis workflow, each orthomosaic was clipped to the spatial extent of the flying-fox colony in ArcGIS Pro 2.5.0 (Environmental Systems Research Institute, 2020). The cropped image was then opened in Fiji 1.8.0_172 (Schindelin et al., 2012) using the Bio-Formats plugin (Linkert et al., 2010).

The Computer Vision image analysis workflow was adapted from cell counting methods (DeGroote & Rodewald, 2008; Drury et al., 2011; Grishagin, 2015), and implemented in Fiji 1.8.0_172 (Schindelin et al., 2012). The optimum functions and parameters for this process were identified through visual inspection, by systematically adding one function or varying one parameter at a time while fixing all other functions and parameters. To begin, the image was smoothed, to reduce noise, using the 'Smooth' function. Then the background was subtracted using 'Subtract Background' with a rolling ball radius of 50. Then, the 'Find Edges' function was used to discriminate between brighter flying-foxes and the more homogenous background. Following this, the image was manually thresholded using the 'Threshold' function, until it appeared that flying-foxes were represented in the thresholded image and background was excluded, from visual examination of the thresholded image. The 'Despeckle' function was used to remove smaller spectrally intense fragments that did not represent a flying-fox. Following this, the 'Watershed' function was used to separate multiple flying-foxes roosting close together that

appeared as a large spectrally intense clump in the orthomosaic. Then, the ‘Analyse Particles’ function was used to count the number of particles representing flying-foxes in the image, with the size range to be detected set to 10-300 pixels and the circularity to 0.3-100, with ‘Include Holes’ enabled. A region of interest (ROI) was generated for each segment of pixels representing a flying-fox. Then, each orthomosaic was magnified to visually confirm that flying-fox segments were accurately represented as ROIs in each image. The total number of ROIs in each orthomosaic was then recorded. This process is illustrated below (Figure 2.3), and a macro written to run this process automatically in Fiji 1.8.0_172 is provided in Appendix 3.

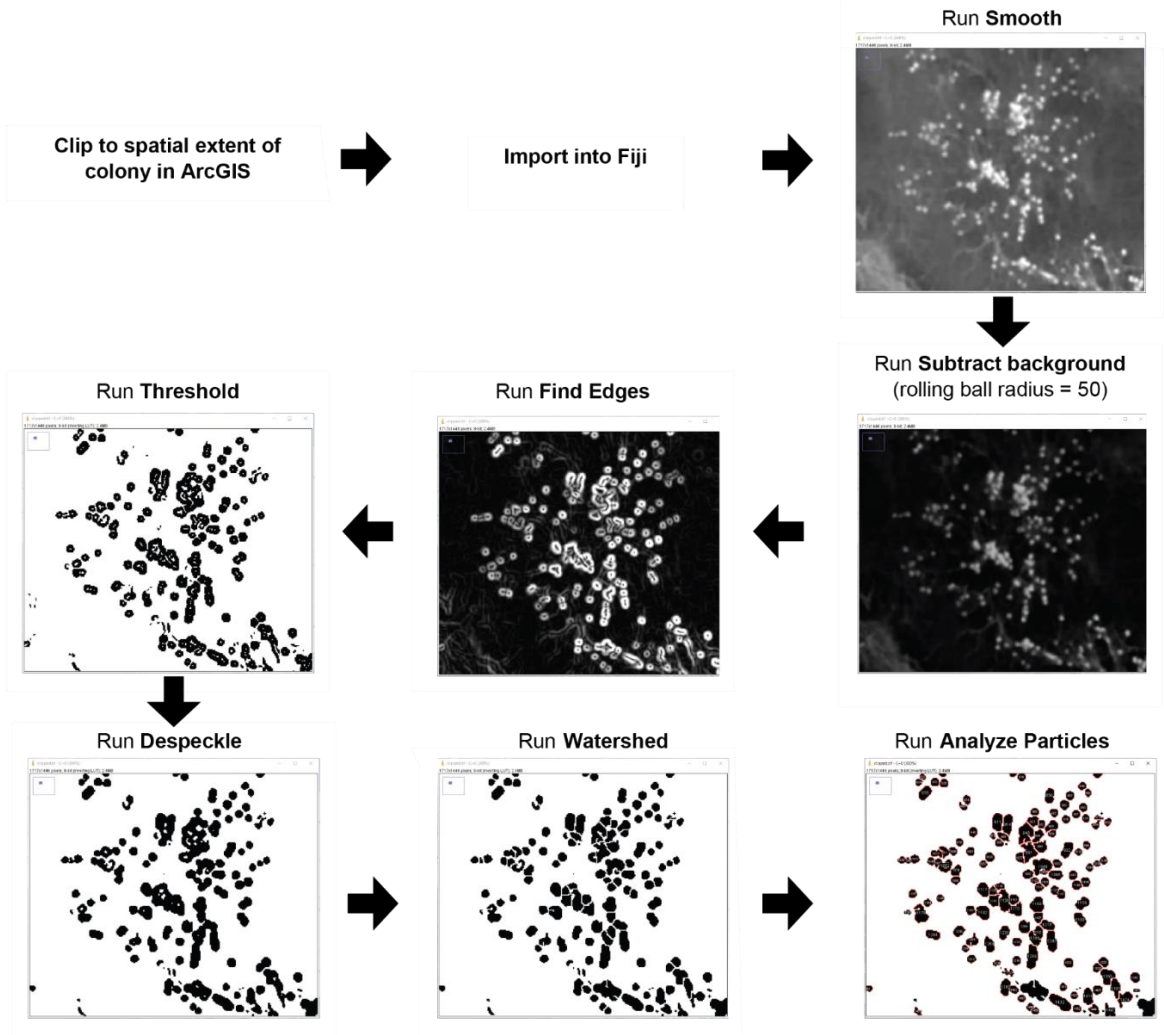

Figure 2.3. Flowchart outlining the steps taken to generate a semi-automated colony size estimate of the Yarramundi flying-fox colony through Computer Vision – implemented in Fiji 1.8.0_172 (Schindelin et al., 2012). Images depict the classification process for a small area of the colony.

2.3.4.2 Object-based image analysis method

Flying-fox and background classes were semi-automatically classified in each orthomosaic using ArcGIS Pro 2.5.0 (Environmental Systems Research Institute, 2020) through an OBIA supervised classification machine learning approach. Each orthomosaic was clipped to the spatial extent of the flying-fox colony and a 5% clip stretch was applied to increase the contrast between flying-foxes and background. Each orthomosaic was then segmented through a 'segment mean shift' approach (Comaniciu & Meer, 2002) where areas with homogenous intensity were grouped together (spectral detail = 15, spatial detail = 15.5). The minimum segment size was set to three pixels (pix), to ensure smaller or partially covered flying-foxes were represented in the segmented product.

Then, training samples were generated throughout the orthomosaic, for the classification scheme that was made up of two classes: (1) flying-fox and (2) background, using the segment picker and free hand selection tools. For each orthomosaic, 100 training samples were generated for each class.

Following training sample generation, histograms displaying the pixel brightness (thermal intensity) were generated for each pixel in a training sample. Histograms generated for background training samples displayed a bell-shaped curve with a single peak, with low numbers of pixels at higher and lower intensities (Appendix 4A). Histograms for the pixel intensity of flying-fox training samples were left-skewed and tended to have higher pixel intensity when compared with background training samples (Appendix 4B).

Each orthomosaic was then classified using the Random Forest, Maximum Likelihood, and Support Vector Machines classifiers (parameters provided in Appendix 5). Each classified

raster image was imported into Fiji 1.8.0_172 (Schindelin et al., 2012) and the ‘Watershed’ function was applied to separate individuals roosting close together, which may have been classified as a single larger flying-fox. Then, the ‘Analyse Particles’ tool was used to quantify the number of pixel groups classified as flying-foxes. The classification process is illustrated below (Figure 2.4). In addition, the colony area (m^2) of each orthomosaic was measured by tracing around the spatial extent of visually observable flying-foxes in the original thermal orthomosaic in ArcGIS Pro.

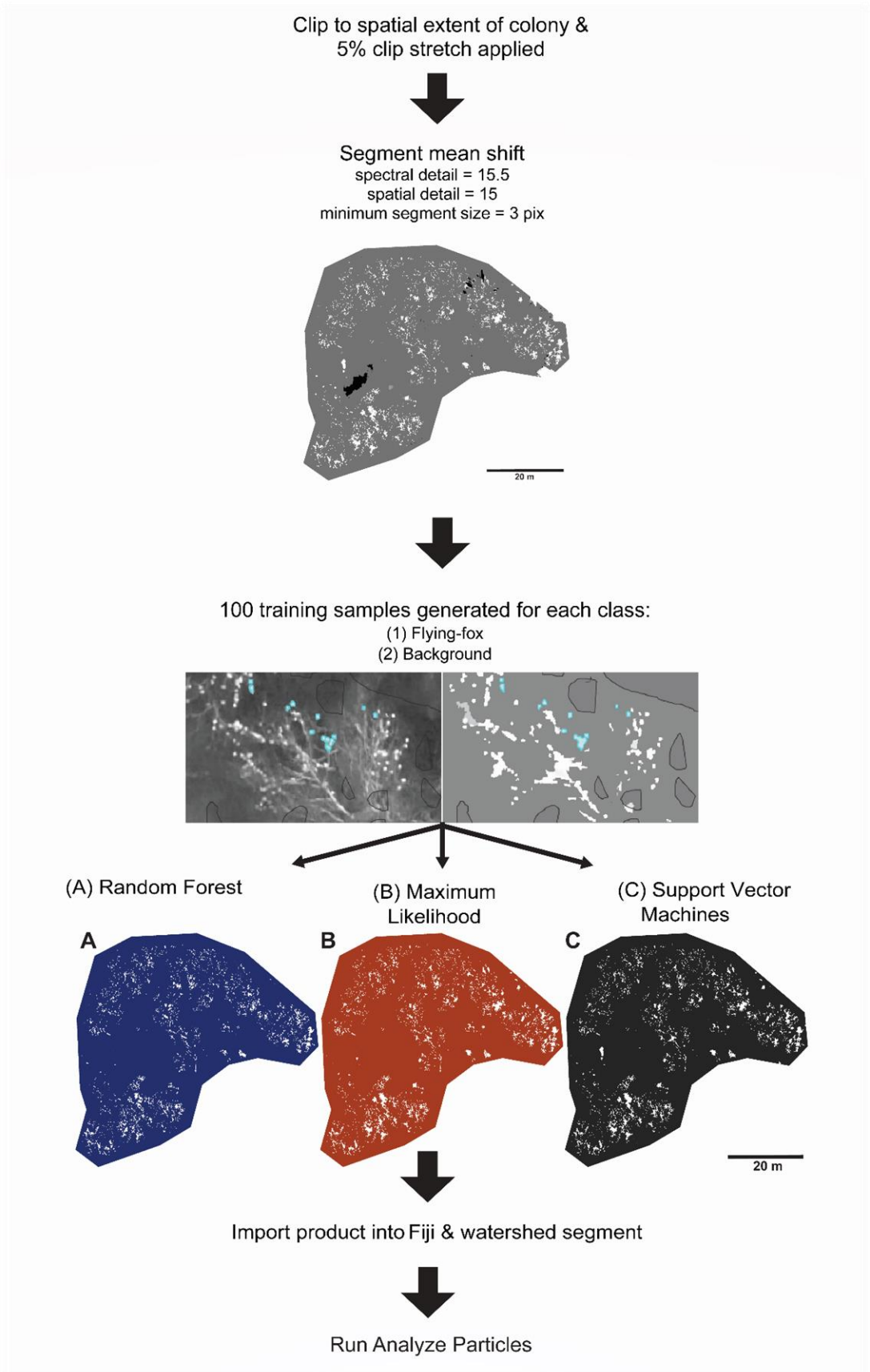
Clip to spatial extent of colony &
5% clip stretch applied
Segment mean shift
spectral detail = 15.5
spatial detail = 15
minimum segment size = 3 pix
20 m
100 training samples generated for each class:
(1) Flying-fox
(2) Background
(A) Random Forest
(B) Maximum Likelihood
(C) Support Vector Machines
A
B
C
20 m
Import product into Fiji & watershed segment
Run Analyze Particles

Figure 2.4. Flowchart outlining the steps taken to generate a semi-automated colony size estimate of the Yarramundi flying-fox colony through OBIA and machine learning - implemented in ArcGIS Pro 2.5.0 (Environmental Systems Research Institute, 2020) and Fiji 1.8.0_172 (Schindelin et al., 2012). To begin, the thermal orthomosaic is clipped to the spatial extent of the colony, then segmented through a segment mean shift approach, then 100 training samples are generated for flying-fox and background classes and the orthomosaic is classified through Random Forest (blue), Maximum Likelihood (orange) and Support Vector Machines (black) machine learning algorithms. The classified product is then watershed segmented, and the number of flying-foxes is counted automatically.

2.3.4.3 Accuracy assessment

Computer Vision-classified outputs were imported into ArcGIS Pro and georeferenced. Then, 200 equalised stratified random points of one-hundred pixels classified as flying-fox, and one-hundred pixels classified as background, were generated for each of the four classified products for each orthomosaic. The classification accuracy of each pixel point was determined by visual comparison with the original orthomosaic. Results were used to generate a confusion matrix for each orthomosaic (Appendix 6). From this, predicted overall classification accuracy (%) was calculated for each orthomosaic.

2.3.5 Determining precision of flying-fox colony size estimates derived from manual counts

To determine the precision of manual counts derived from drone-acquired orthomosaics, I compared counts of orthomosaics generated from repeated surveys on the same day. I completed three thermal drone surveys on one day, at flying-fox roosts located at Campbelltown, Kareela and Yarramundi, as well as two repeated surveys at Macquarie Fields. For all orthomosaics generated, resolution was constant to within ±0.12 cm^2/pixel (Table 2.3), with the exception of orthomosaics generated for the Kareela colony, where resolution was approximately 1.8 cm^2/pixel lower for the third orthomosaic compared to the other two Kareela orthomosaics. All orthomosaics were randomised before I manually counted the number of flying-foxes in each orthomosaic in Fiji 1.8.0_172 (Schindelin et al., 2012).

To determine the extent of between-counter variability in manual counts, the set of three orthomosaics for the Kareela colony were then manually counted by four additional human counters. Counters were selected on the basis that they had previously visited a flying-fox colony

and were familiar with their appearance from the ground. Each counter was sent an email outlining the purpose of the task, the three orthomosaics, and a set of instructions for completing the task (Appendices 7 and 8). Counters worked independently to count the flying-foxes and did not share their results.

2.3.6 Statistical analyses

All statistical analyses were two-tailed, employed an α value of 0.05 and were conducted in RStudio Desktop 1.2.5042 (R Core Team, 2018). To determine the relationship between flying-fox colony size estimates generated using the semi-automated counting methods and visual point counts, four generalised linear mixed models (GLMMs) were fitted using package *nlme* (Pinheiro et al., 2016). GLMMs had visual point counts as the response variable. For each GLMM, counts obtained through each of the semi-automated methods, including Computer Vision, Support Vector Machines, Maximum Likelihood, and Random Forest were fitted as a fixed effect. To account for scale issues in model fit, all manual orthomosaic and semi-automated count results were divided by one thousand. Bayesian Information Criterion (BIC) values for each of the four GLMMs were compared, and where possible, the p-value for the predictive power of the fixed effect was recorded. For all semi-automated counting methods, accounting for the effect of roost ID as a random effect in the model failed to improve fit, based on BIC, and was excluded from the final models.

To compute the concordance between the counts obtained from each of the semi-automated counting methods and visual point counts, Lin's concordance correlation coefficient (ρc) (Lawrence & Lin, 1989) was calculated for each semi-automated method using the package *DescTools* (Signorell, 2016).

A GLMM was constructed to determine the relationship between the predicted overall accuracy of each classified orthomosaic (obtained from confusion matrices generated in 2.3.4.3) and the difference between counts generated using the semi-automated methods and visual point counts. The model was fitted with predicted overall accuracy as the response variable; absolute value percent difference between the semi-automated and visual point count (%) and semi-automated method type as the fixed effects; and roost ID as a random effect. For this GLMM, the effects of the independent variables were tested through likelihood ratio tests (ANOVAs), and Tukey's test was used to test for between level effects post-hoc. The significance of the random effect was tested through parametric bootstrapping with one thousand iterations. In this analysis, the Maximum Likelihood classified product for Campbelltown orthomosaic was excluded as an outlier as the visual point count differed 268.13% from the Maximum Likelihood classified count.

For each semi-automated method, a GLMM was constructed to evaluate the relationship between absolute value percent difference between semi-automated and visual point count (%) versus air temperature, orthomosaic resolution, colony area, and number of flying-foxes - independent variables that were expected to affect classification accuracy. For these GLMMs, the response variable was absolute value percent difference between visual point count and semi-automated counts. Median air temperature during survey (°C), colony area (m^2), orthomosaic resolution (cm^2/pixel), and visual point count, were included as fixed effects, and roost ID as included as a random effect. The effects of the independent variables were tested through likelihood ratio tests (ANOVAs). The significance of the random effect was tested through parametric bootstrapping with one thousand iterations.

To determine the extent of variability between manual visual point counts of flying-foxes from repeated surveys of colonies on the same day, and thus the precision of manual counts, the standard error (SE) and relative standard error (RSE) were calculated for all repeated orthomosaics, grouped by colony ID. For the three Kareela orthomosaics, to determine whether there was a significant difference between counts derived from each orthomosaic, and each counter, a two-way ANOVA was run, and Tukey's test was used to test between level effects post-hoc. To test for homogeneity of variance between the counts grouped by counter and by image, two Levene's tests were run using the package *car* (Fox & Weisberg, 2018).

2.4 RESULTS

2.4.1 Performance of semi-automated methods

For the 13 drone-acquired thermal orthomosaics collected from eight flying-fox colonies, average orthomosaic resolution varied from 2.53 cm^2/pix to 8.24 cm^2/pix, according to Agisoft Metashape Professional Version 1.5 metrics, with an average orthomosaic resolution of 4.24 cm^2/pix. Colony area varied between 1,451 m^2 at Camellia Gardens to 21,112 m^2 at Centennial Park. The number of flying-foxes manually counted in a thermal orthomosaic varied from 1,126 individuals for the Camellia Gardens colony on the 22nd of October 2019, to 12,131 individuals, for a partial area of the Emu Plains colony on the 19th of October 2019 (Appendix 9).

Counts derived from semi-automated methods all increased linearly with increasing visual point counts (Figure 2.5). The semi-automated method with the strongest relationship between visual point counts and semi-automated count results was Random Forest classification (GLM: $F_{4,7} = 34.80$, $p = 0.004$, marginal $R^2 = 0.75$; Table 2.1), followed by Computer Vision,

Support Vector Machines and Maximum Likelihood. Results of likelihood ratio testing could only be obtained for the effect of the fixed effect in the Random Forest model, as all other models had a singular fit.

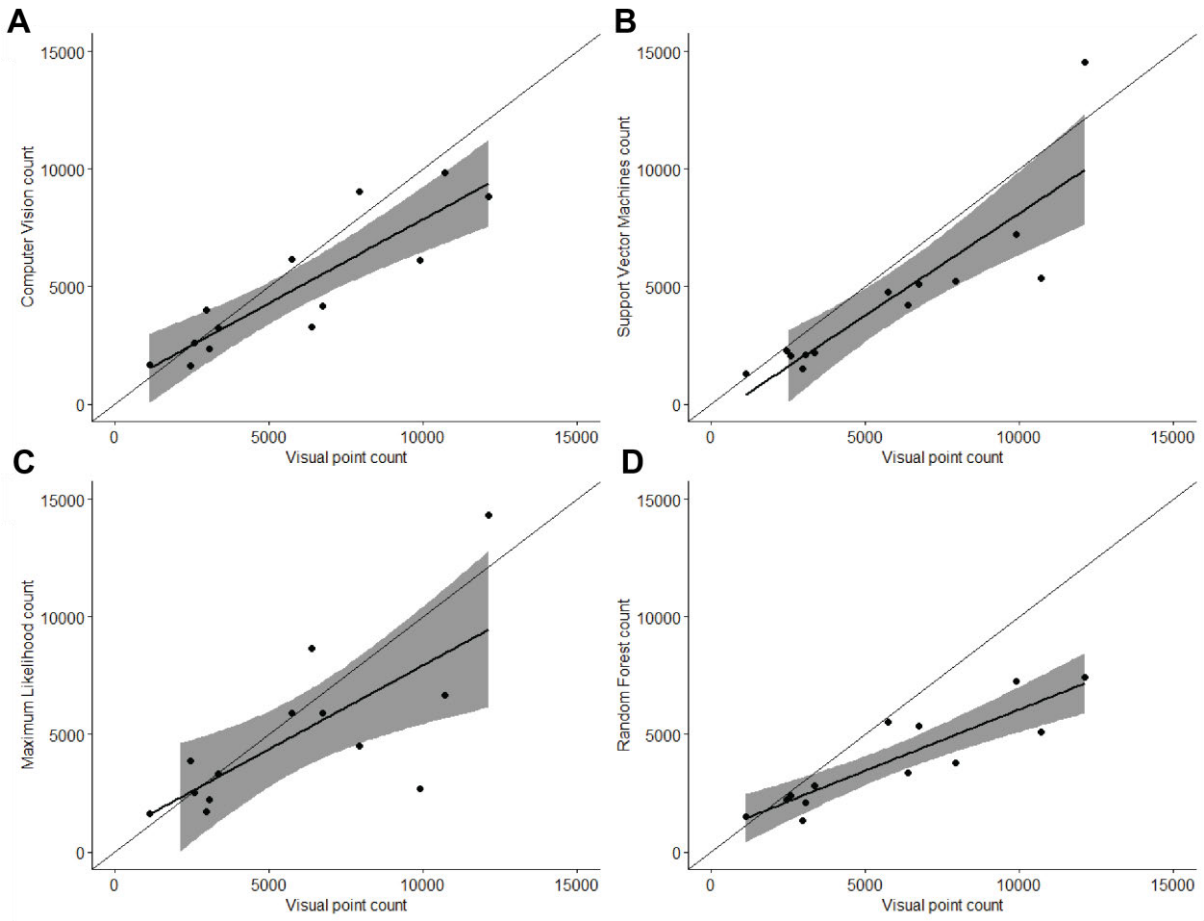

Figure 2.5. Relationship between manual visual point counts and counts obtained through each of the semi-automated counting methods: (A) Computer Vision, (B) Support Vector Machines, (C) Maximum Likelihood, and (D) Random Forest. Grey shaded area indicates ± 95 CI (confidence interval).

Table 2.1. GLM results evaluating the relationship between manual visual point counts and semi-automated Computer Vision, Support Vector Machines, Maximum Likelihood and Random Forest classification techniques for thirteen orthomosaics of eight flying-fox colonies.

Semi-automated method	**BIC with fixed effect**	**BIC without fixed effect**	**Equation**
Computer Vision	57.12	70.78	y = 0.7136x + 734.28
Support Vector Machines	58.06		y = 0.8682x – 555.13
Maximum Likelihood	67.15		y = 0.7133x + 814.51
Random Forest	56.09		y = 0.51213x + 855.79

Semi-automated count results obtained from the Computer Vision method had the highest concordance with visual point counts (ρc = 0.83, 95% CI 0.57-0.94; Figure 2.6), followed by Support Vector Machines (ρc = 0.81, 95% CI = 0.53-0.93), Maximum Likelihood (ρc = 0.70, 95% CI = 0.28-0.89) and Random Forest (ρc = 0.70, 95% CI = 0.28-0.89). All classified orthomosaic products are viewable through the link provided in Appendix 8.

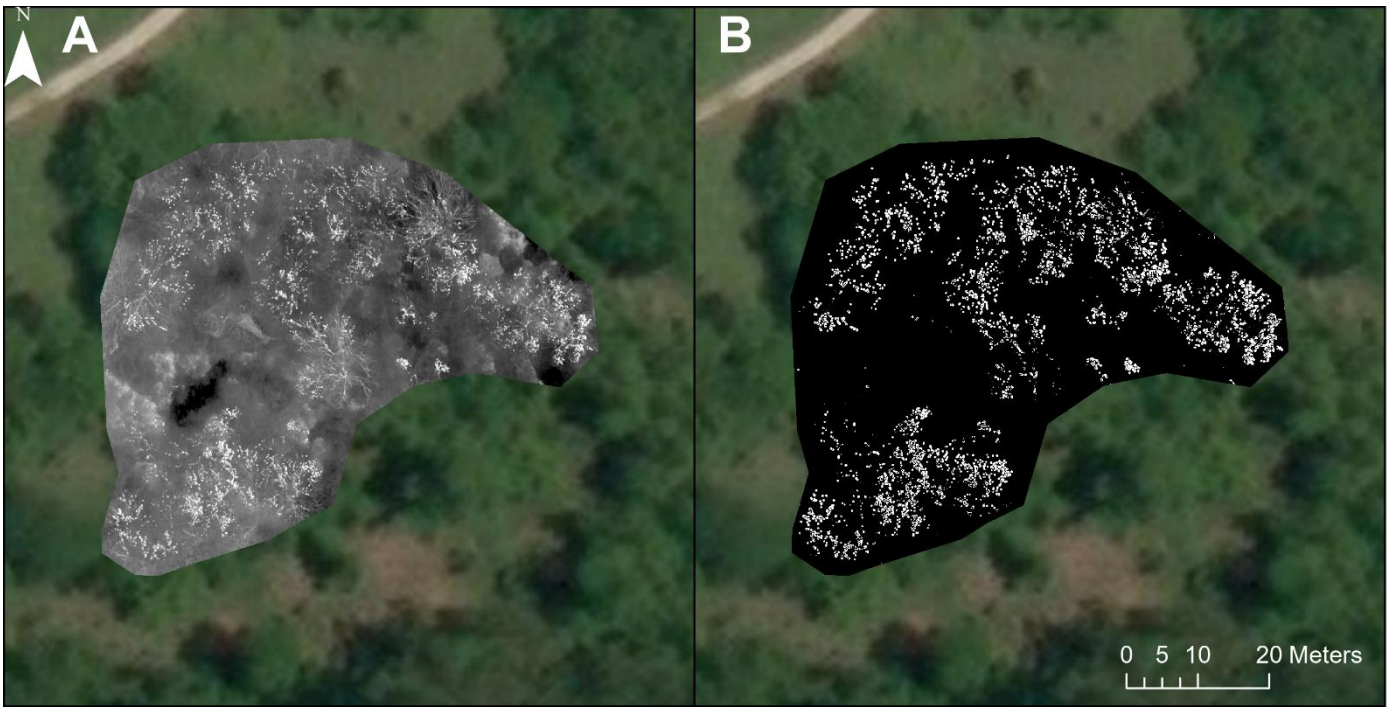

Figure 2.6. (A) Thermal orthomosaic depicting the Yarramundi flying-fox colony, and (B) Computer Vision classified product (Background image source: Maxar).

2.4.1.1 Relationship between predicted overall accuracy and percentage difference between semi-automated and visual point counts

Overall accuracy of classified orthomosaics for all four classification methods, obtained through accuracy assessments (example shown in Figure 2.7), ranged from 66.5-97.5%, with a mean overall accuracy of 84.0%. There was no significant relationship between predicted overall accuracy and the absolute value percent difference between the count obtained through each semi-automated method and visual point count (GLMM: $F_{1,40} = 0.15$, $p = 0.705$; Figure 2.8).

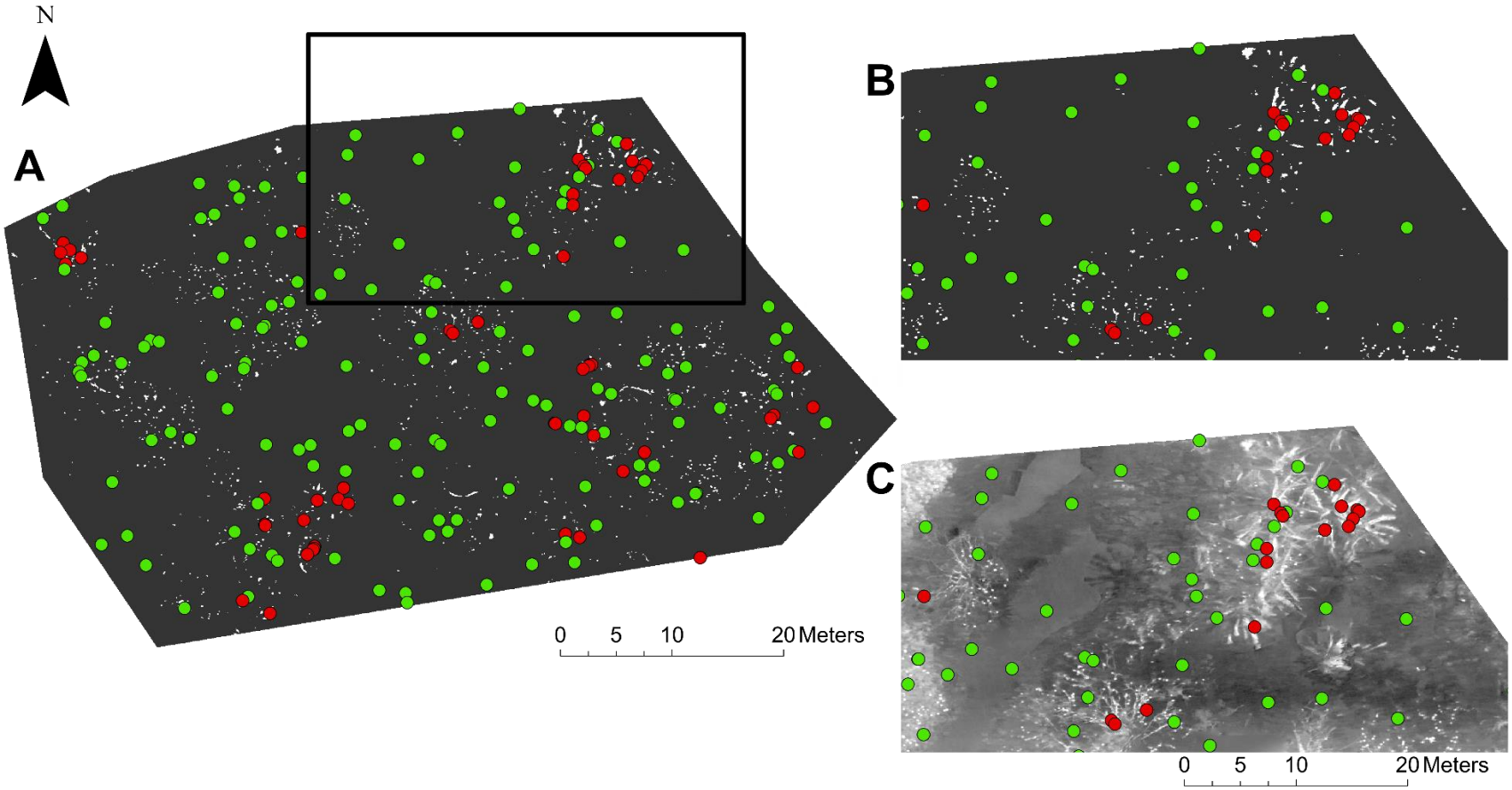

Figure 2.7. Completed accuracy assessment for the Random Forest classified product of the Camellia Gardens colony on the 22nd of October 2019, red points show pixels that were incorrectly classified using the Random Forest method, green points show correctly classified pixels. Classification accuracy of each pixel was determined through visual comparison with the original orthomosaic. (A) Shows the entire classified orthomosaic; (B) shows a close up of the classified product with accuracy assessment points overlaid; (C) shows the original thermal orthomosaic for the same area, with accuracy assessment points overlaid.

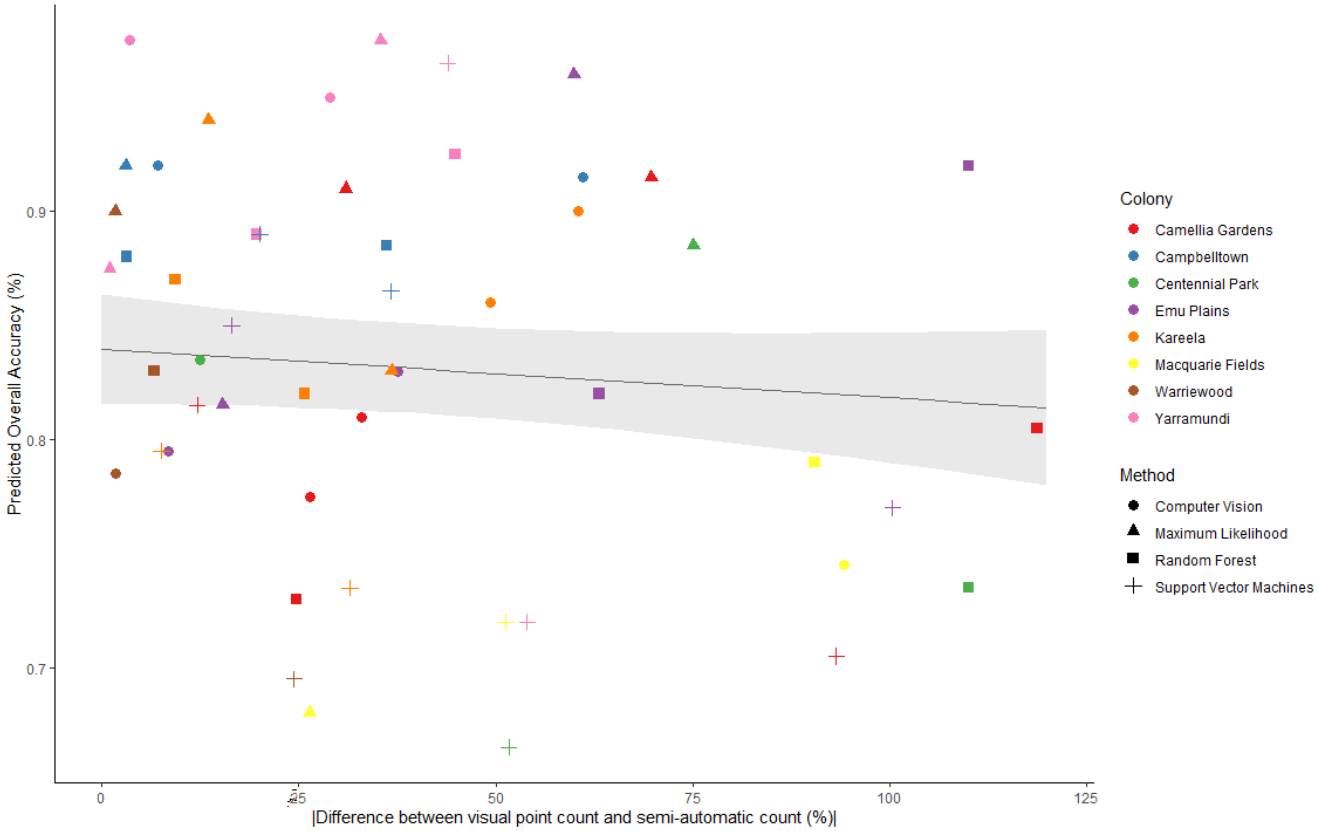

Figure 2.8. There was no significant relationship between the absolute value percent difference between counts obtained through semi-automated methods and visual point counts and predicted overall accuracy, obtained through an accuracy assessment. Grey shaded area indicates ± SE (standard error).

Predicted overall accuracy differed significantly between the semi-automated methods (GLMM: $F_{3,40} = 6.66$, $p < 0.001$). There was a significant difference between predicted overall accuracy for the Maximum Likelihood and Support Vector Machines classified orthomosaics

(p = 0.008; Figure 2.9). The random effect, roost ID, was significant for all semi-automated counting methods (|p| < 0.001).

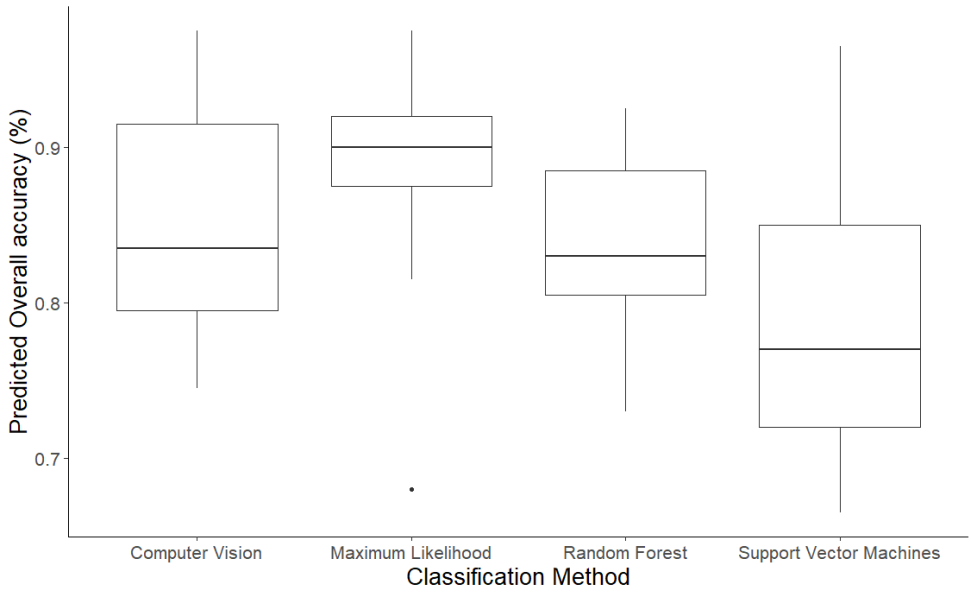

Figure 2.9. Overall accuracies obtained through accuracy assessments of each orthomosaic were significantly lower for the Support Vector Machines classified products, compared with Computer Vision, Maximum Likelihood, and Random Forest classified products.

2.4.1.2 Conditions that affect the accuracy of semi-automated methods

There was no significant relationship between median air temperature at time of survey (°C), visual point count, colony area (m^2) and resolution (cm^2/pixel), and the percent difference between visual point counts and semi-automated counts for all classification methods (Table 2.2). The random effect, roost ID, was significant for all semi-automated counting methods (|p| < 0.001).

Table 2.2. There were no significant relationships between absolute value percent difference between visual point counts and semi-automated counts and the variables theorised to affect the performance and accuracy of Computer Vision, Support Vector Machines, Maximum Likelihood, and Random Forest classification of orthomosaics.

	Classification method			
Effect	Computer Vision	Support Vector Machines	Maximum Likelihood	Random Forest
Median air temperature at time of survey (°C)	$F_{1,7}$ = 40.94, p = 0.099	$F_{1,7}$ = 0.01, p = 0.954	$F_{1,7}$ = 3.49, p = 0.312	$F_{1,7}$ = 0.42, p = 0.634
Visual point count	$F_{1,7}$ = 59.99, p = 0.082	$F_{1,7}$ = 0.03, p = 0.900	$F_{1,7}$ = 5.94, p = 0.248	$F_{1,7}$ = 0.32, p = 0.672
Colony area (m^2)	$F_{1,7}$ = 31.84, p = 0.112	$F_{1,7}$ = 0.12, p = 0.788	$F_{1,7}$ = 2.20, p = 0.377	$F_{1,7}$ = 0.86, p = 0.524
Resolution (cm^2/pixel)	$F_{1,7}$ < 0.01, p = 0.964	$F_{1,7}$ = 0.01, p = 0.949	$F_{1,7}$ = 3.63, p = 0.308	$F_{1,7}$ = 0.02, p = 0.908

2.4.2 Precision of visual point counts between repeated orthomosaics

To determine the precision of colony size estimates derived from manual counts of drone-acquired thermal orthomosaics, I assessed the variability between visual point counts of repeated orthomosaics. The RSE between visual point counts of flying-foxes visible in orthomosaics for the three repeated surveys at the Campbelltown, Kareela, Yarramundi, and Macquarie Fields colonies varied from 0.93% for the three Campbelltown orthomosaics, to 6.91% for the three Kareela orthomosaics, with an average of 3.63% (Table 2.3).

Table 2.3. Manual point count results for orthomosaics generated from repeated surveys at the Campbelltown, Kareela, Yarramundi, and Macquarie Fields colonies. The exact number of flying-foxes in each orthomosaic was counted manually by a single observer. Standard error and relative standard error were calculated for each colonies' counts. Resolution (cm^2/pixel) was obtained from Agisoft Metashape Professional 1.5 (LLC Agisoft, 2019).

Survey	Resolution (cm^2/pixel)	My visual point count	Standard error	Relative standard error (%)
Campbelltown 1	4.9	9888		
Campbelltown 2	4.8	9614		
Campbelltown 3	4.9	9883	90.51	0.92
Kareela 1	3.6	2138		
Kareela 2	3.5	2247		
Kareela 3	5.4	1777	142.03	6.91
Yarramundi 1	2.5	2003		
Yarramundi 2	2.6	2246		
Yarramundi 3	2.5	2255	79.64	4.33
Macquarie Fields 1	4.7	6384		
Macquarie Fields 2	4.6	6166	109.00	1.74

For the three Kareela orthomosaics manually counted by four additional counters and me, the four additional counters reported that counting flying-foxes in each orthomosaic took 45 minutes to 1 hour. There was no significant effect of counter ID on the resulting counts (GLMM: $F_{4,9} = 1.06$, $p = 0.433$; Figure 2.10A). However, counts varied significantly between the three orthomosaics (GLMM: $F_{1,9} = 23.53$, $p < 0.001$). I found that there was no significant difference between the counts for orthomosaics 'Kareela 1' and 'Kareela 2' (Tukey's test: $p = 0.747$), which had a similarly high resolution (Table 2.3). However, the counts for orthomosaics 'Kareela 2' and 'Kareela 3' and orthomosaics 'Kareela 1' and 'Kareela 3' were significantly different (Tukey's test: $p = 0.001$ and $p < 0.001$, respectively), with 'Kareela 3' having a lower

resolution than ‘Kareela 1’ and ‘Kareela 2’ (Table 2.3, Figure 2.10B). All orthomosaics are viewable through the link provided in Appendix 8.

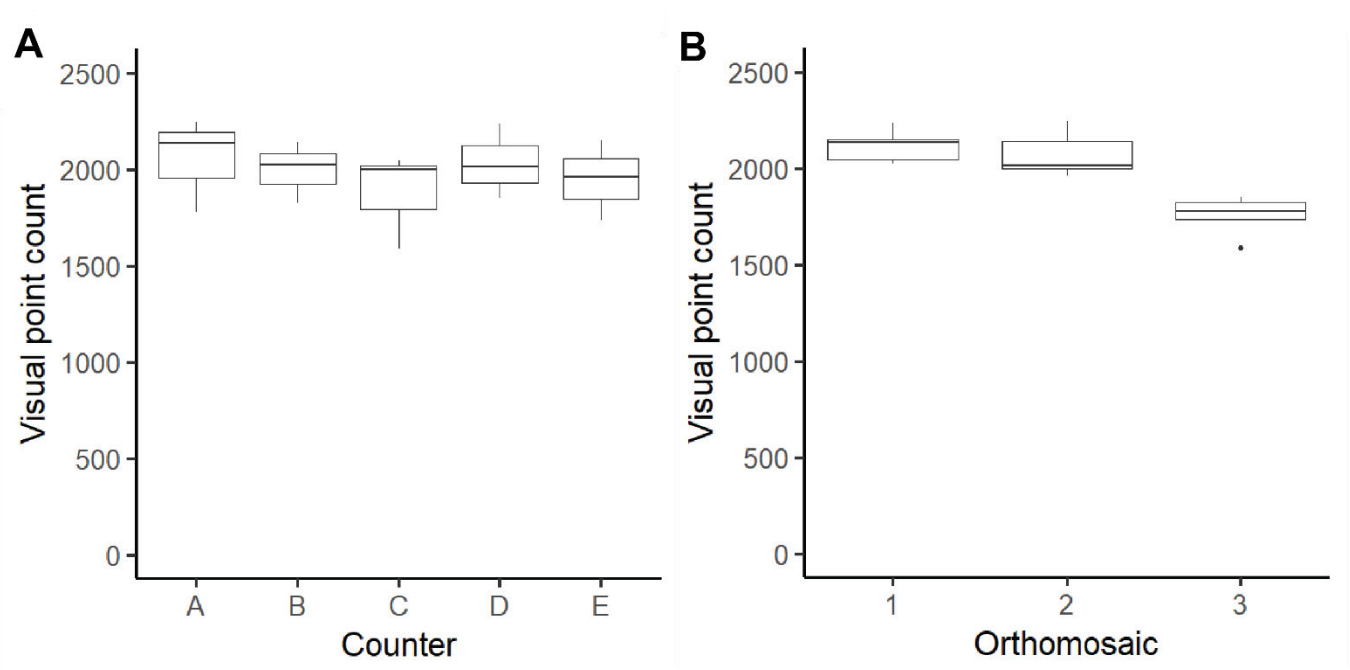

Figure 2.10. (A) There was no significant effect of counter ID on visual point counts of flying-foxes in three thermal orthomosaics of the Kareela flying-fox colony. (B) Counts of the Kareela colony varied significantly between orthomosaics ‘Kareela 1’ and ‘Kareela 2’ and orthomosaic ‘Kareela 3’, where counts were lower for orthomosaic ‘Kareela 3’. Levene’s tests showed that the variance between counts was homogenous for both counters ($F_{4,10} = 0.05$, $p = 0.994$) and orthomosaics ($F_{2,12} = 0.11$, $p = 0.897$).

2.5 DISCUSSION

This study demonstrated that drone-acquired thermal imagery can be used to generate thermal orthomosaics of flying-foxes roosting in temperate forests, and that from these thermal orthomosaics the number of flying-foxes can be quantified reliably semi-automatically using OBIA and Computer Vision analysis workflows. Drones equipped with thermal cameras have

previously been recommended as a powerful tool for the remote detection of animals (Burke et al., 2019a) and have been used to help determine population sizes of several species (Burke et al., 2019b; Kays et al., 2019; Lhoest et al., 2015; Seymour et al., 2017; Spaan et al., 2019). However, this was the first study to use drone-based thermal imaging to detect and count roosting flying-foxes, and to demonstrate that thermal remote sensing using drones can be used for objectively quantifying flying-fox colony size and hence is a promising tool for monitoring flying-fox populations.

2.5.1 Performance of semi-automated methods

I found that flying-fox colony size estimates derived from Random Forest classified orthomosaics were most strongly related to counts derived from visual point counts. However, Random Forest classified counts tended to be lower than visual point counts. Random Forest classifiers have previously been shown to be more robust to overfitting compared with other classifiers for landcover classification (Pal, 2005). They have also performed best alongside six other machine learning classifiers for mapping coastal ecological zones (Guilherme et al., 2018), and performed better than Support Vector Machines for quantifying aquatic bird colonies (Díaz-Delgado et al., 2017). As Random Forest classified counts are most strongly related to visual point counts, to account for underfitting of the classifier, in future studies, the equation describing the relationship between Random Forest classified counts of flying-foxes and visual point counts (Table 2.1) may be used to calibrate the count derived from Random Forest classification.

Flying-fox colony size estimates derived from the Computer Vision workflow had the highest concordance with visual point counts ($\rho c = 0.83$). Therefore, this semi-automated method

may be used to estimate flying-fox colony size from drone-acquired thermal orthomosaics without the need for calibration. Computer Vision techniques are commonly used in the life sciences to characterise and quantify microorganisms under a microscope (Grishagin, 2015; Papadopulos et al., 2007) but also have many applications in animal ecology (Weinstein, 2018), and have previously been used successfully to quantify grey seals (*H. grypus*) in thermal orthomosaics with 95-98% accuracy compared with visual point counts (Seymour et al., 2017). In the aforementioned examples, target organisms are highly distinguishable against a homogenous background; however, in this study, the background was often heterogenous and three-dimensional, and the user was required to subtract the background and manually threshold the image. When thresholding the image, the user needs to take care to ensure that the majority of flying-foxes are conserved when defining the threshold point, as some less distinguishable flying-foxes (i.e. those surrounded by warmer vegetation) may be excluded, and this is a potential source of error in the workflow (also discussed in Gonzalez et al., 2016). Despite this, the software used to develop and implement the Computer Vision classification workflow in this study is open source and more user friendly than its command line Computer Vision counterparts, while providing very similar levels of functionality (Pennekamp & Schtickzelle, 2013). Thus, the Computer Vision Workflow presented here is easily implementable and can provide semi-automated colony size estimates for thermal orthomosaics depicting flying-fox colonies.

All four classification methods tended to predict fewer flying-foxes in orthomosaics compared to visual point counts (Figure 2.5). Further, this study was unable to detect a significant relationship between the percent difference between visual point counts and semi-automated counts and variables theorised to affect this, including air temperature, visual point

count, colony area and resolution (Table 2.2). The discrepancy between visual point counts and semi-automated counts may have been due to misclassification of multiple close together flying-foxes as a single flying-fox, or failure to detect flying-foxes in warmer vegetation. Pixels are often misclassified if they lie on the boundary between two different land cover classes where pixels are a mix of reflected energy, in this case heat, from both flying-foxes and background (Burke et al., 2019a; Congalton, 1988; Townshend et al., 2000). This makes definition of discrete boundaries between land classes difficult, as in Figure 2.7, where bright vegetation (Bangalow palm trees; *Archontophoenix cunninghamiana*) was misclassified as flying-foxes in the top right corner of the orthomosaic. This issue is also described for discriminating glossy ibis (*Plegadis falcinellus*) from background in visual spectrum imagery using the Random Forest classifier (Afán et al., 2018). Therefore, areas of bright vegetation may be misclassified by semi-automated classification methods, so results from these semi-automated methods should be compared with the original orthomosaic to ensure their accuracy.

The predicted overall accuracy obtained from the accuracy assessments in this study was not related to the percentage difference between the counts of the thermal orthomosaics from the semi-automated and visual point count methods. From pixel-based accuracy assessments (section 2.3.4.3), orthomosaics classified using the semi-automated classification methods were shown to have relatively high accuracies (average 84%; Figure 2.8). This further suggests that the classification error lay in accurately quantifying and discriminating between groups of flying-foxes, the accuracy of which was not measured in this study. However, using an object-based accuracy assessment method may have more accurately represented this issue and the count accuracy of each classified product (Terletzky & Ramsey, 2016). Nevertheless, in future studies,

continual improvements in sensor resolution will allow for improved discrimination between individual flying-foxes by semi-automated classification methods.

The resolution of the orthomosaics generated in this study ranged from 2.5-8.2 cm^2/pixel. Lower orthomosaic resolutions resulted because some thermal images were omitted from the final orthomosaic as photogrammetry software was unable to align them into the orthomosaic successfully (resolutions listed in Appendix 9). It has been established that thermal images, generally having lower resolution and a single thermal band, can be more difficult to stitch together to form an orthomosaic, compared to visual spectrum imagery (Yang & Lee, 2019). This is evidenced in some of the orthomosaic images presented in Appendix 8, where blank spaces in the orthomosaic show where images could not be aligned. For the Centennial Park colony, the visual point count of flying-foxes was markedly lower than expected, given the large area of the colony (Appendix 9), and considering that the roost appeared densely populated throughout this entire area from on-the-ground observations. As discussed in section 2.5.2, though not tested empirically, lower resolution orthomosaics may lead to underestimations of flying-fox colony size, as not all flying-foxes will be represented in the orthomosaic. This may be true of Centennial Park, and more flying-foxes may have been present than are visible in the orthomosaic. The orthomosaic from the Warriewood colony had a similarly low resolution, and the colony size estimate generated for this colony may therefore be inaccurate. Further, the lower resolution of the Kareela 3 orthomosaic may have resulted in lower manually counts of flying-foxes in this orthomosaic, compared with Kareela 1 and Kareela 2 (discussed in detail below). For future applications of this method, users should ensure orthomosaics are of a sufficiently high resolution (ideally 2-3 cm^2/pixel). This ensures each flying-fox is represented by 3-5 pixels

(Meade et al., 2019), and all animals are captured so that the colony size is accurately represented.

2.5.2 Evaluating sources of variability in visual point counts

Through counting the exact number of visible flying-foxes in repeated drone-acquired thermal orthomosaics of entire flying-fox colonies, the proposed method was found to have a low average RSE (3.63%) for repeated surveys at the same colonies, indicating that the method is precise. The RSE between counts of flying-foxes in repeated orthomosaics was highest for the Kareela colony at 6.91%, where orthomosaic 'Kareela 3' had a resolution of 5.4 cm^2/pixel that was substantially lower than the 3.6 cm^2/pixel resolution of 'Kareela 1' and the 3.5 cm^2/pixel resolution of 'Kareela 2'. This likely explains why 'Kareela 3' also had a lower estimated colony size than 'Kareela 1' and 'Kareela 2', for the same reason as presented above in 2.5.1. Future formal assessments of the effects of orthomosaic resolution on flying-fox colony size estimates would help still further increase the precision and accuracy of this method.

No significant effect of human counter was found on counts of flying-fox colonies derived from drone-acquired thermal orthomosaics, suggesting that manually counting flying-foxes in drone-acquired thermal orthomosaics does not require specialised skills. Between-observer variability is often cited as a source of error in animal population surveys that employ both ground-based and aerial surveillance techniques (Bowler et al., 2020; Short & Bayliss, 1985; Stapleton et al., 2014). Results from ground-based animal detection surveys have been shown to depend on observer experience, when spotting koalas (*Phascolarctos cinereus*) (Hanger et al., 2017) as well as for estimating flying-fox colony size from fly-out counts (Forsyth et al., 2006). Contrastingly, counts of rafting canvasbacks (*Aythya valisiner*) from black

and white aerial photographs did not vary significantly between counters with different levels of training and experience (Erwin, 1982). However, fewer flying-foxes were counted in 'Kareela 3' compared to 'Kareela 1' and 'Kareela 2' orthomosaics by all counters. Two counters noted that 'Kareela 3' was more difficult to count due to a high amount of bright vegetation in the orthomosaic because of solar glare, which made flying-foxes less distinguishable from background, something that has been noted previously for sighting riverine rabbits (*Bunolagus monticularis*) in thermal imagery (Burke et al., 2019a). Despite this, point counts of thermal orthomosaics of flying-fox colonies may be conducted by any interested individual, provided they are familiar with the counting software and the appearance of flying-foxes in drone-acquired thermal imagery. Furthermore, the training material provided in Appendix 8 may be used to train counters in future studies involving counting flying-foxes in drone-acquired thermal imagery.

2.5.3 Conservation and management implications

More accurate monitoring of flying-fox colony size enhances the evidence base for their conservation and management. With the drone-based thermal remote sensing method demonstrated in this study, researchers can more accurately monitor species status changes over time using a unified method, subject to fewer biases than ground-based counting methods (Forsyth et al., 2006; Westcott & McKeown, 2004). On a local scale, researchers and land managers may use more precisely measured changes in flying-fox abundance to identify environmental and other factors which influence flying-fox abundance in particular colonies, aiding in evidence-based human-wildlife conflict mitigation (Kung et al., 2015). More accurate flying-fox colony size estimates may also improve modelling of the local potential for zoonotic disease spillover risks (Edson et al., 2015; Walsh et al., 2017). If the method were implemented

more widely across whole species ranges over time, it would enable a more precise understanding of the drivers behind flying-fox temporal redistribution, and the impacts of extreme weather events, such as cyclones and extreme heat events (Shilton et al., 2008; Welbergen et al., 2008; Westcott et al., 2018; Westcott et al., 2012), as well as the magnitude of flying-fox ecosystem services in a given location (van Toor et al., 2019). Understanding the drivers of flying-fox abundance and redistribution will in turn enable researchers to develop predictive models for proactive flying-fox management.

2.5.4 Future directions

Drones can be equipped with multiple sensors, capturing information that may be difficult to detect or measure for researchers on the ground (Grémillet et al., 2012; Wich & Koh, 2018). Vegetation in densely populated flying-fox colonies is often damaged by defoliation (visible in Figure 2.11; Mo et al., 2020; Westcott et al., 2015b), causing tree mortality (Dobbertin & Brang, 2001; Lowman & Heatwole, 1992) and has been linked to complaints from nearby residents (Westcott et al., 2015b). In future work involving drone monitoring of flying-fox colonies, aerial imagery from a commercially available dual spectrum camera, capturing thermal and visual spectrum imagery synchronously (as in Figure 2.11), would enable researchers to gather information on vegetation morphology and health (see Baena et al., 2017), and may also allow for more successful thermal orthomosaic construction (through four band mosaicking, as described in Yang & Lee, 2019). Additionally, drones equipped with LiDAR sensors may also be used to characterise three-dimensional forest structure (Moorthy et al., 2019), while hyperspectral sensors can capture highly complex information pertaining to many aspects of ecosystem health (Adão et al., 2017). Drones can thus enable complex analysis of many factors contributing to flying-fox colony health and abundance.

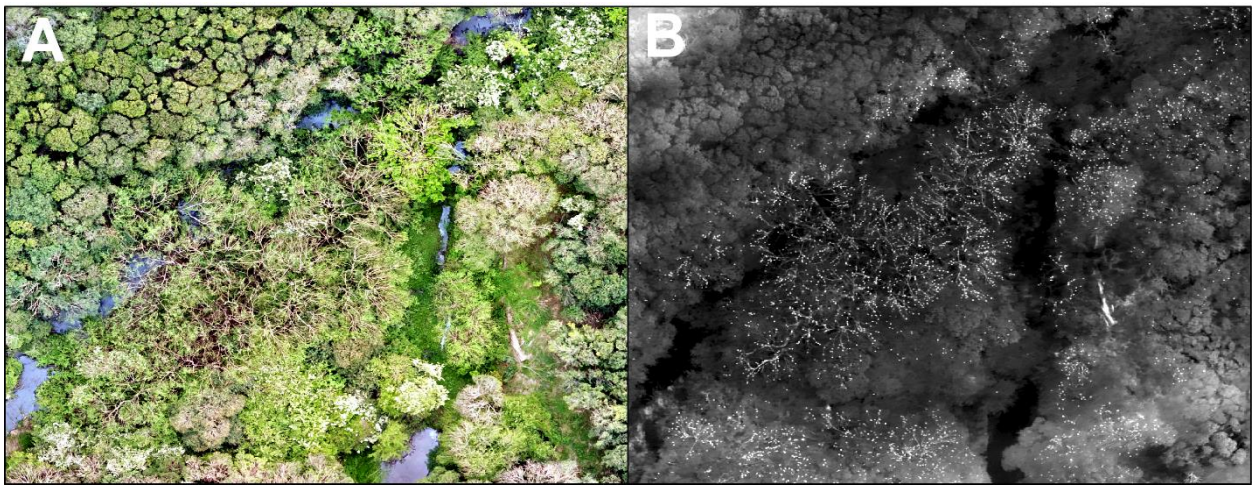

Figure 2.11. (A) Drone-acquired image depicting the Campbelltown roost. (B) Drone-acquired thermal image depicting the same area. Flying-foxes are more conspicuous in (B) due to high thermal contrast between flying-foxes and vegetation. However, (A) may be used to obtain information on vegetation density and health.

Another promising classification method that may assist in accurately monitoring colonies in drone-acquired thermal imagery is deep learning. Deep learning is a sophisticated machine learning method that enables complex classification of remotely sensed imagery through multiple processing layers (LeCun et al., 2015). Recently, it has been used for cell detection and counting (Höfener et al., 2018; Xue & Ray, 2017), as well as weed mapping and burrow detection, where it has been shown to outperform shallow machine learning methods, including OBIA Random Forest classification (Bycroft et al., 2019; Huang et al., 2020). Specialised programs have been written for the automated detection of cell aggregations through Deep Learning frameworks, such as U-net (Falk et al., 2019), as well as for finding and delineating regions of interests from drone-acquired aerial imagery, such as oyster reefs, with OysterNet (Ridge et al., 2019). Deep Learning has already been successfully used to analyse ground-based thermal imagery of multiple Pantanal Animal species (de Arruda et al., 2018) and

drone-acquired imagery of cattle (Barbedo et al., 2019). Given a sufficiently large dataset, a pre-existing deep learning model may be adopted for flying-foxes, or a new model developed to detect and quantify flying-fox colony size. This would enable researchers to generate automated estimates of flying-fox colony size from thermal imagery that may be more accurate than results from shallow machine learning methods presented here.

Finally, future research into the animal welfare effects of drones flying close to flying-fox colonies, and the ethical implications of this new survey method, as well as its potential to cause harm, must continue to be considered. For all drone surveys conducted in this study, little or no behavioural change was observed in flying-foxes. However, we should not rely purely on visual assessments of animal disturbance to determine the effects of drones on wildlife, as it may have unobservable effects (Vas et al., 2015). For example, biologgers have been used to measure the physiological response of American black bears (*Ursus americanus*) to a drone flying overhead, and found that the bears exhibited increased heart rate, a stress response, whilst not visibly reacting to the drone (Ditmer et al., 2015). Researchers should also compare the effects and disturbance of traditional survey methods to remote methods like drone surveys, as it is well understood that traditional methods also disturb species populations (Wich & Koh, 2018). If it is found that drone surveys cause less disturbance comparatively, then they may be adapted as the preferred method to survey select species. However, there is a need to conduct more extensive research into the long-term effects of drones on flying-fox behaviour and physiology.

2.5.5 Conclusion

Drones can conduct large-scale cost-effective surveys of difficult to monitor animal populations in short periods of time (Linchant et al., 2015). This study demonstrated that drones equipped

with thermal cameras can capture imagery for generating orthomosaics, which can be used to estimate flying-fox colony size with accuracy and precision. Ongoing developments in sensor resolution and semi-automated classification algorithms will only see the reliability of this method improve. As such, counts from drone-acquired thermal imagery represent a viable, effective and increasingly reliable new tool for the conservation and management of colonially roosting flying-foxes.

In developing a new monitoring method for flying-foxes, it was important to determine the accuracy and utility of the new method, using drone-acquired thermal imagery, compared with traditional ground based counting methods. In the next chapter I will determine the accuracy of counts derived from drone-acquired thermal imagery by comparing counts from imagery to direct ground counts of flying-foxes. Next, I will assess the accuracy of colony size estimates derived from drone-acquired thermal orthomosaics compared with ground count methods presently used by government for monitoring flying foxes and demonstrate the utility of the method for monitoring spatiotemporal changes in flying-fox colonies.

Chapter 3 - Drone-based thermal remote sensing of flying-fox colonies outperforms traditional counting methods

3.1 ABSTRACT

Accurate and unbiased monitoring practices are essential for gaining insight into species abundance, distribution, and responses to environmental change. Flying-foxes are a large species of bat that roost in groups of a few hundred to many thousands of individuals in the canopies of trees, where they are difficult to census accurately by human observers. In this study, I assessed the accuracy and utility of drone-acquired thermal orthomosaics for monitoring flying-fox colonies, as compared to traditional ground-based methods. I compared counts from drone-acquired thermal imagery to direct ground counts of flying-foxes in fifteen single trees, to assess 'small-scale count accuracy'. In addition, I compared flying-fox colony size estimates derived from counts of individuals in twenty-three drone-acquired thermal orthomosaics across seven colonies, to ground counts conducted by me and counters from Australia's National Flying-fox Monitoring Program (NFFMP). Finally, I examined the effectiveness of using drone-acquired thermal orthomosaics for monitoring changes in flying-fox colony size, density, and area of occupancy over time. Overall, there was a high concordance between ground counts and counts derived from thermal imagery for single trees ($\rho c = 0.89$). For whole colonies, I found that colony size estimates from drone-acquired thermal orthomosaics were positively related to ground counts conducted by me (GLMM: $F_{1,17} = 50.51$, $p < 0.001$, marginal $R^2 = 0.83$) and NFFMP counters (GLMM: $F_{1,9} = 14.41$, $p = 0.004$, marginal $R^2 = 0.50$). However, colony size estimates derived from drone-acquired thermal orthomosaics averaged 105% higher than ground counts conducted by me, and 92% higher than ground counts conducted by NFFMP counters.

For three colonies monitored over an 11-month period, I found that temporal changes in colony size and density were not consistent between colonies, and that both roosting density and the area of roost occupancy increased with increasing flying-fox colony size. More accurate colony size estimates derived from drone-acquired thermal orthomosaics may be used in place of, or to benchmark and periodically assess, the accuracy of ground-based flying-fox colony size assessment methods. The monitoring methods presented here will be valuable for informing evidence-based conservation and management of flying-foxes.

3.2 INTRODUCTION

Knowledge of the distribution, abundance and density of populations is key for conservation and management (Marsh & Trenham, 2008). Critically, monitoring species over time can elucidate trends and alert researchers and policy makers to species declines, so that conservation action can be taken (Goldsmith, 1991; Sutherland, 2006; Westcott et al., 2012; Woinarski, 2018). Traditional ground-based survey methods may be biased by several factors, including site accessibility (Reddy & Dávalos, 2003; Wagner, 1981); animal detectability (Otto & Pollock, 1990); and between-observer variability (Erwin, 1982). The use of inconsistent and inaccurate counting methods can prevent changes in species population status from being detected, with detrimental implications for species conservation and management (McKelvey et al., 2008).

With populations of known size, researchers have previously been able to test the accuracy and precision of traditional observer methods (Elphick, 2008). For example, using a physical model of a wading bird colony it was found that observer counts were 29% lower than true counts on average, and undercounting occurred for 81% of estimates, with high variation between and within individual counters, irrespective of experience (Frederick et al., 2003).

Conversely, distance sampling methods have been shown to produce large positive biases in predicted density, due to counting errors (Alldredge et al., 2008). Due to the biases inherent in existing survey methods, emerging technologies are increasingly being employed for more accurate and less biased wildlife monitoring and surveillance (Cilulko et al., 2013; Fretwell et al., 2012; Wich & Koh, 2018).

Thermal cameras detect radiation emitted by animals in the thermal infrared region of the electromagnetic spectrum to form a thermal image of that animal (Burke et al., 2019a). Infrared technology has been used for remotely censusing animals for more than half a century (Croon et al., 1968). Advances in infrared technology and improvements in the resolution and portability of thermal cameras allow for surveillance of increasingly smaller animals and allow surveys to be conducted further from target species, to minimise disturbance (Blackwell et al., 2006). Infrared population surveys have been conducted for many species, such as elk (*Cervus elaphus*) (Dunn et al., 2002), Brazilian free-tailed bats (*Tadarida brasiliensis*) (Betke et al., 2008), grey seals (*Halichoerus grypus*) (Seymour et al., 2017), common hippopotami (*Hippopotamus amphibius L.*) (Lhoest et al., 2015), mantled howler monkeys (*Alouatta palliata*), black-handed spider monkeys (*Ateles geoffroyi*), kinkajous (*Potos flavus*) (Kays et al., 2019), and greater gliders (*Petauroides volans*) (Vinson et al., 2020). Using a closed mark-recapture design, it was found that traditional animal survey techniques using spotlighting failed to detect 50.6% of white-tailed deer (*Odocoileus virginianus*) groupings compared with thermal imagers (Collier et al., 2007). Thermal imaging has been shown to be a non-invasive monitoring technique that allows detection of conspicuous animals, and with advances in sensor resolution, thermal imagers are expected to have increasing applicability in wildlife studies (Chabot & Bird, 2015; Cilulko et al., 2013).

Remotely piloted aircraft systems (RPAS; hereafter ‘drones’), are powerful tools for remote detection of animals, enabling researchers to collect imagery closer to target animals than is possible by piloted aircraft (Anderson & Gaston, 2013). Species population counts conducted from drone-acquired imagery in the visible spectrum have already been shown to be more accurate and precise than ground counts of target species (Hodgson et al., 2018). Results from imagery in the thermal spectrum are mixed. Recently, counts of spider monkeys (*A. geoffroyi*) obtained by a drone fitted with a thermal infrared camera have been compared to ground counts (Spaan et al., 2019). Researchers found that for smaller subgroups of monkeys, drone and ground surveys produced similar counts, while for larger subgroups, the number of monkeys observed by the drone was mostly higher than that observed by the ground counter (Spaan et al., 2019). Conversely, in drone-acquired thermal imagery, New Zealand fur seals (*Arctocephalus forsteri*) have been shown to have a detectability of 16-67% of in low density forest, compared with ground counts, while in high density coastal shrubland, they are undetectable (Gooday et al., 2018). These examples demonstrate that in suitable conditions, drone surveys can allow for the detection and quantification of less conspicuous and inaccessible animal populations.

The family Pteropodidae comprises nearly 200 species of Old-world fruit bat, distributed throughout Africa, southeast Asia, Australia, and the Pacific Islands (Simmons, 2005). Within these regions, species in this family perform key roles as pollinators and plant propagators (Fujita & Tuttle, 1991). This group of species has been shown to be highly nomadic, regularly travelling long distances in response to local changes in food availability. More than half of the species in Pteropodidae are threatened (International Union for Conservation of Nature and Natural Resources, 2020). Threats to these species are wide-ranging and include overhunting

(Brooke & Tschapka, 2002), climate change (Welbergen et al., 2008), and habitat loss (Mohd-Azlan et al., 2001).

Flying-foxes of the genus *Pteropus* forage for floral resources at night and during the day they roost independently or in groups comprised of up to many thousands of individuals (Hall & Richards, 2000). There are four flying-fox species on mainland Australia (Hall & Richards, 2000). Of these species, the grey-headed flying-fox (*Pteropus poliocephalus*) is listed as Vulnerable, and the spectacled flying-fox (*P. conspicillatus*) is listed as Endangered under national environment legislation; the spectacled flying-fox was recently reclassified following a significant mortality event, due to extreme heat, in November 2018 (Commonwealth of Australia Department of Environment and Energy, 2019a). Australia's mainland flying-foxes are increasingly found in urban and peri-urban bush and parkland (Tait et al., 2014), possibly due to large-scale natural habitat loss (Hall & Richards, 2000; Tait et al., 2014) or due to recent increases in the abundance and temporal stability of urban food resources (Parry-Jones & Augee, 2001; Williams et al., 2006), or a combination of these 'push' and 'pull' factors. Across their geographic range, they are often the subject of human-wildlife conflict (Aziz et al., 2017; Brooke & Tschapka, 2002; Florens et al., 2017; Kung et al., 2015). Conflicts arise due to the encroachment of flying-fox colonies on property or vice-versa (West, 2002), flying-foxes feeding in orchards (Aziz et al., 2017), and defoliation of roost tree vegetation (Mo et al., 2020; Westcott et al., 2015b), and smell, noise and amenity concerns (Kung et al., 2015; Lentini & Welbergen, 2019). There is also a perceived threat of zoonotic disease, where flying-foxes are known reservoirs of Hendra virus and Australian Bat Lyssavirus (Halpin et al., 1999). For these reasons, the development of accurate flying-fox population monitoring practises is valuable for conservationists and land managers alike.

Since 2012, the National Flying-fox Monitoring Program (NFFMP) has aimed to survey all known flying-fox colonies quarterly to generate population estimates for Australian flying-fox species, primarily the listed grey-headed flying-fox and spectacled flying-fox, by either ground or fly-out count (Westcott et al., 2015a). During a fly-out count, observers count streams of individuals as they leave the roost to forage at dusk (Westcott & McKeown, 2004), whereas a ground count (aka static count) is conducted during the day while flying-foxes roost in colonies (Westcott et al., 2011). For smaller colonies, every visible individual is counted using the ground count method; whereas for larger colonies, colony size estimates are derived from point-based distance sampling or from counts performed while traversing colonies (Westcott et al., 2011). Alternatively, surveyors may count a proportion of flying-foxes and estimate the corresponding area of the colony surveyed, then extrapolate the colony size by scaling up to the total area of the colony (Westcott et al., 2011). It is well established that the various flying-fox colony size count methods have their limitations (Forsyth et al., 2006; Westcott & McKeown, 2004; Westcott et al., 2011). Fly-out counts have been shown to be both inaccurate and imprecise (Forsyth et al., 2006; Westcott & McKeown, 2004); while ground counts can be impractical if the colony is inaccessible or situated in dense vegetation and, if accessible, counters passing through the colony can cause a high degree of disturbance to flying-foxes, affecting the count accuracy (Westcott et al., 2011). Despite this, ground counts are recognised as the most efficient method for conducting landscape scale population censuses of flying-fox colonies and are recommended for use in NFFMP surveys (Westcott et al., 2011).

In this study, I assessed the effectiveness of using drones equipped with a thermal camera to survey colonies of Australian flying-foxes, as compared to traditional ground count methods. To assess the accuracy of counts derived from drone-acquired thermal imagery, I compared the

number of flying-foxes detected by exhaustive ground counts to counts from drone-acquired thermal imagery in fifteen single trees across three colonies throughout the Greater Sydney region. In addition, I examined the effect of canopy cover on the detectability of flying-foxes in thermal imagery for single trees. Moreover, I compared colony size estimates obtained from drone-acquired thermal orthomosaics to colony size estimates obtained from ground counts for the same period, conducted by me as well as by NFFMP counters, for October and November 2019 and February, June and August 2020. Furthermore, I examined the abiotic factors that may contribute to the difference between ground counts and counts derived from drone-acquired thermal orthomosaics. Finally, I examined the effectiveness of using colony size surveys derived from drone-acquired thermal orthomosaics for monitoring flying-fox colony size, density and roost area occupied over time.

3.3 METHODS

3.3.1 Drone survey conditions

3.3.1.1 Study area

This study was conducted within the Greater Sydney Region in south-eastern Australia. This region is within the Sydney Basin Bioregion and remnant vegetation in the region consists mainly of Eucalypt open forests and woodlands, with an understory of grass, shrubs, ferns, and herbs (Geoscience Australia, 2001).

The Greater Sydney region comprises approximately 20 flying-fox roosts (Commonwealth of Australia Department of Environment and Energy, 2019b) that are continually or periodically occupied by the grey-headed flying-fox, little-red flying-fox (*P.*

scapulatus), and black flying-fox (*P. alecto*) (Currey et al., 2018). In the study area, by far the most common species is the grey-headed flying-fox (Commonwealth of Australia Department of Environment and Energy, 2019b).

For this study, flying-fox colonies were selected based on the airspace regulations for flying drones, their accessibility for safe drone flight, and access for ground counting (see also 3.3.4). Drone surveys were conducted across seven flying-fox colonies throughout the Greater Sydney region, including: Camellia Gardens (-34.0426°, 151.1128°), Campbelltown (-34.0658°, 150.8088°), Emu Plains (-33.7408°, 150.6803°), Kareela (-34.0233°, 151.0855°), Macquarie Fields (-33.9901°, 150.8794°), Warriewood (-33.6948°, 151.2950°), and Yarramundi (-33.6213°, 150.6924°).

3.3.1.2 Platform specifications, take off and retrieval

A DJI Inspire 1 Version 2.0 drone (DJI, Shenzhen, China) equipped with Zenmuse XT 19 mm radiometric thermal camera (FLIR, Wilsonville, USA) and fitted with one lithium polymer battery (TB48, 129.96 Wh), with a combined weight of 3.21 kg, was used for all methods described in this study. The battery life of the drone was approximately 15 minutes. The FLIR longwave infrared thermal sensor in the Zenmuse XT has a sensitivity of 50 mK @nf/1.0 at a resolution of 640 x 520 pixels at 30 fps. No specialised launching or landing equipment was required. The drone was launched from a cleared area, a minimum of 20 m from the colony, to minimise potential disturbance to the flying-foxes.

3.3.1.3 Environmental conditions for all flights

All drone flights were conducted in low wind conditions (< 10 km/hr; measured from the nearest weather station), as wind speed has been shown to affect the positional accuracy of a drone (Hung et al., 2019), and cause vegetation movement that can impede feature matching between images for orthomosaic construction (Duffy et al., 2018).

3.3.2 Comparing drone and ground counts for a single tree

To determine the accuracy of counting flying-foxes in drone-acquired thermal imagery, I assessed the concordance between small countable groups of flying-foxes and counts obtained by drone-acquired thermal imagery. In February 2020, counts of flying-foxes roosting in a single tree were conducted at Centennial Park at 2.5-3 hours after sunrise, in air temperature of 23.9°C, Camellia Gardens at 1.5-2 hours after sunrise, in air temperature of 19.0°C and Macquarie Fields at 7.5-8 hours after sunrise, in air temperature of 24.4°C. For each of these colonies, five trees were identified that allowed an observer to walk directly underneath without disturbing the roosting flying-foxes. For each tree, the drone was manually flown to hover above the tree and then lowered to an altitude of 50 m above ground level (AGL), so that flying-foxes were represented by a maximum of approximately 5 x 5 pure pixels (Chapter 2). Following this, I walked around and underneath the tree and counted the exact number of flying-foxes present. When I was confident that I had counted every flying-fox present, I captured a thermal image of the tree from above with the camera in nadir direction, before manually flying it back to the launch site.

To measure canopy cover for each tree, following each flight, five hemispherical photographs were taken from different points below the canopy of each tree using an Oppo A57

mobile phone, with 16 MP forward-facing camera equipped with a Black Eye Pro Fisheye Mobile lens attached. Canopy cover was then calculated using the 'Gap Light Analysis Mobile App' 3.0 (GLAMA) for each photo, following the procedure outlined in Tichý (2014). Estimates for canopy cover have previously been shown to be highly comparable for photos taken with mobile phones compared to higher resolution cameras (Tichý, 2016). From these five hemispherical photos, the average canopy closure for each tree was calculated. For air temperature (°C) I used observations from the nearest weather station recorded during acquisition of the drone imagery (Bureau of Meteorology, 2020). Following image capture, images were retrieved from the Zenmuse XT and the exact number of individuals in each target tree was manually counted with the aid of the multi-point tool in Fiji 1.8.0_172, generating a 'point count' for each image (Schindelin et al., 2012), as shown in Figure 3.1.

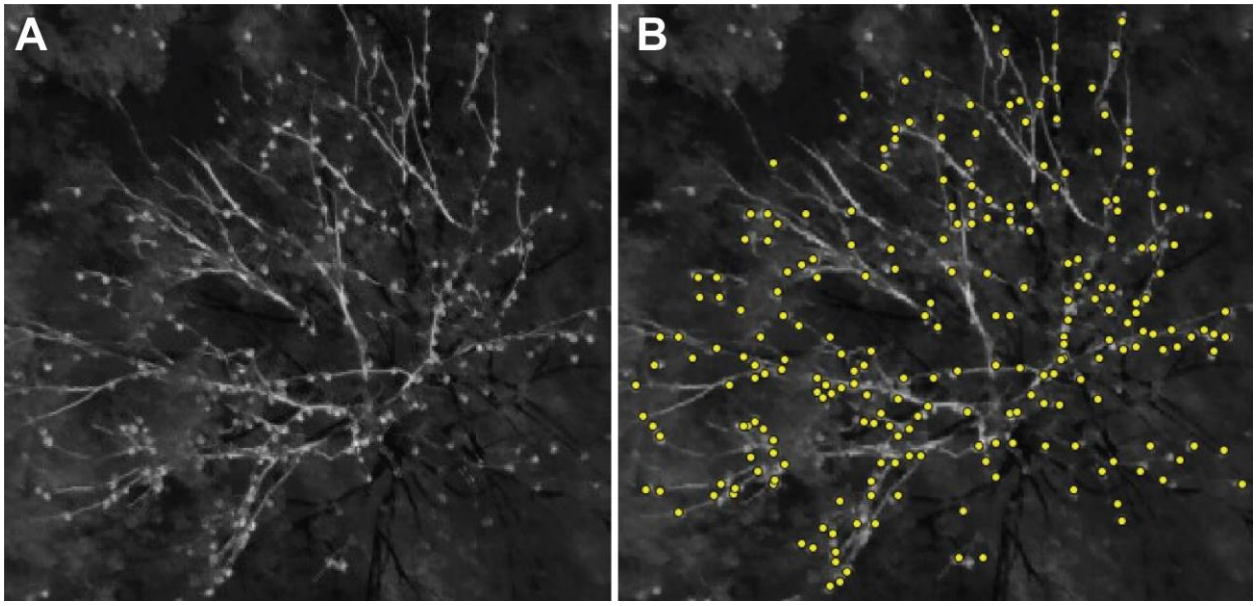

Figure 3.1. (A) Thermal image of flying-foxes roosting in a Eucalyptus sp. at the Centennial Park roost (B) Image with yellow markers depicting counts of every flying-fox in the tree using Fiji 1.8.0_172 (Schindelin et al., 2012).

3.3.3 Comparing colony size estimates from ground counts and counts derived from thermal orthomosaics

3.3.3.1 Whole colony drone survey and image processing method

Colony-wide drone surveys were conducted between October 2019 and August 2020 at the Campbelltown (n = 5), Camellia Gardens (n = 3), Emu Plains (n = 2), Kareela (n = 5), Macquarie Fields (n = 2), Warriewood (n = 1) and Yarramundi (n = 7) roosts.

All flights were mapped in the Pix4D Capture iOS application (Pix4D, 2017) prior to flight. Flight plan mapping was conducted on location, after a visual inspection of the extent of the flying-fox colony. When the colony was only partially accessible, this area was mapped, as well as the surrounding areas, where flying-foxes were known to have roosted previously.

Surveys commenced in the early morning, between 0-158 minutes after sunrise (mean commencement time = 94 minutes after sunrise), with air temperature ranging between 10.3-24.3°C (mean air temperature = 18.3°C; data sourced from nearest weather station). During flight, the drone flew at a speed of 2 m/s, and captured images with a forward and lateral overlap of 90% in a lawnmower pattern. Where possible, depending on battery life, the survey was repeated 1-2 times to ensure imagery of sufficient quality for orthomosaic construction was collected. For larger colonies where the battery life of the drone was not sufficient to complete the entire survey using one battery, the drone had to be returned to base and the batteries changed midway through the survey (up to five battery changes were required for large colonies). Following battery change (~5 minutes), the drone resumed the survey from the point at which the last picture was taken. Median air temperature recorded at the nearest weather station during the period of drone operation was recorded (Bureau of Meteorology, 2020).

All images were saved as radiometric JPEG files, with embedded EXIF data giving latitude, longitude and altitude at the precise time of each image capture. All images were visually inspected, and blurry images were deleted prior to orthomosaic construction as they may prevent photogrammetry software from generating tie points between images (Fonstad et al., 2013; Grenzdörffer et al., 2008; Thiele et al., 2017).

For each survey, orthomosaics were constructed in Agisoft Metashape Professional Version 1.5 (LLC Agisoft, 2019) according to the parameters set out in Appendix 1, this process is illustrated in Figure 3.2. Resulting orthomosaic resolution (cm^2/pixel) was recorded for all orthomosaics.

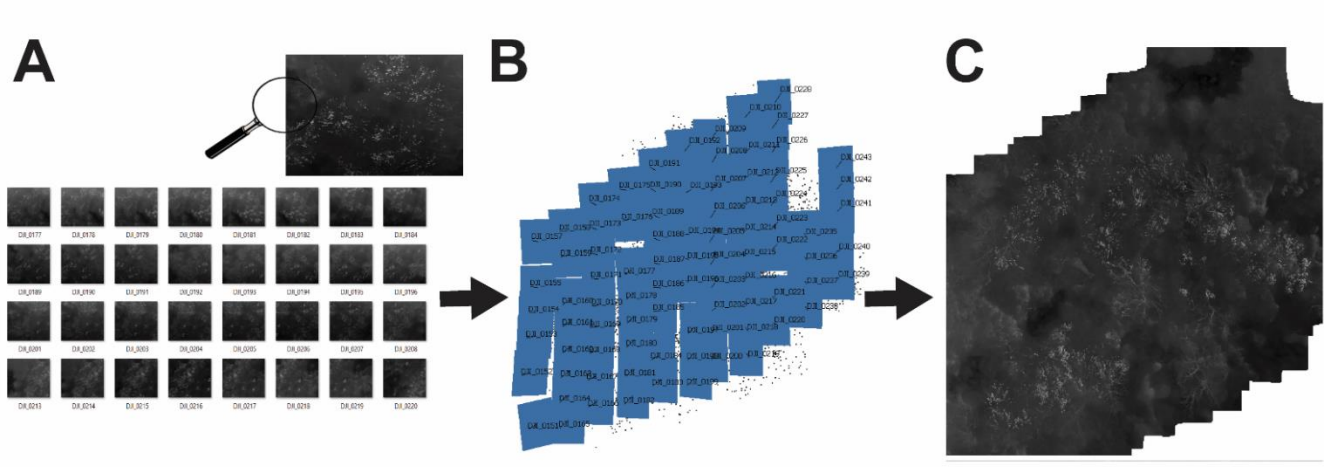

Figure 3.2. (A) Radiometric-JPEG files (R-JPEGs) were downloaded from the Zenmuse XT thermal camera following a drone survey. (B) Embedded EXIF data in R-JPEGs was used to align thermal photos in Agisoft Metashape Professional Version 1.5 (LLC Agisoft, 2019). (C) A thermal orthomosaic was then generated using structure from motion photogrammetric techniques in Agisoft Metashape Professional Version 1.5 (LLC Agisoft, 2019).

The number of flying-foxes in each orthomosaic was then counted. Orthomosaics were exported as .tiff files and opened in Fiji 1.8.0_172 (Schindelin et al., 2012) using the Bio-

Formats plugin (Linkert et al., 2010). The enhance contrast command was applied with 0.3% saturated pixels. The point tool was then used to mark every visible flying-fox in each orthomosaic until the counter was confident that they had not missed any individuals, generating a 'point count' for each orthomosaic.

Each orthomosaic was imported into ArcGIS Pro 2.5.0 (Environmental Systems Research Institute, 2020) and their colony area (m^2) was measured by manually digitising the perimeter of the colony. All orthomosaics are viewable through the link provided in Appendix 8.

3.3.3.2 Ground counting procedure

I conducted a ground count of each colony on the same day as each drone survey. For the Camellia Gardens colony, where flying-foxes exhibited a high tolerance to disturbance, I slowly passed through the accessible areas of the colony. During the walk through, I counted all visible individuals, with aid of a clicker counter, which was used to record groups of 10 sighted individuals.

All other roosts were either difficult to access fully or a walk through would have caused a high degree of disturbance to the local colony of flying-foxes. Therefore, for these roosts, whole or part of the colony boundary was traversed, and counts were performed from positions where many animals were visible. Following this, the proportion of the colony area surveyed was estimated, and a figure for the total number of flying-foxes in the roost extrapolated based on the partial count for the colony and the area which was not visible. This was the case for very large and inaccessible roosts such as Emu Plains. This counting method is also common practice for NFFMP counters (Westcott et al., 2011).

Within seven days of each aerial survey, another ground count of each colony was conducted by a flying-fox surveyor contributing to NFFMP quarterly counts. The methodology for flying-fox colony ground counts contributing to the NFFMP is set out by the Commonwealth Scientific and Industrial Research Organisation (CSIRO) (Westcott et al., 2015b). Five different NFFMP counters contributed to the counts used in this study.

3.3.3.3 Assessing spatiotemporal changes in flying-fox distribution within roosts

To investigate the utility of using drones for assessing the spatiotemporal changes in flying-fox distribution within roosts, I assessed changes in flying-fox roosting density, colony size, colony area and geometric centre for the Campbelltown (n = 5), Kareela (n = 5), and Yarramundi (n = 11) roosts, between September 2019 and August 2020.

Coordinates of all marked flying-foxes in drone-acquired thermal orthomosaics were extracted using Fiji 1.8.0_172 (Schindelin et al., 2012) and imported into ArcGIS Pro 2.5.0 (Environmental Systems Research Institute, 2020) and georeferenced by aligning the points with the original georeferenced orthomosaic. Then the 'Point Density' tool was used to generate a density map of the colony showing density in flying-foxes per square metre. Mean flying-fox density (flying-foxes/m^2) was then calculated for each orthomosaic.

Next, to determine the extent of movement of the colonies across each roost over time, I calculated the geometric centre of the colony using the 'Zonal Geometry' tool, then the distance between each geometric centre was measured. Density and geometric centre data was then used to describe spatiotemporal changes in flying-fox distribution within the roosts.

3.3.4 Permits, regulations, training and logistics

All drone flights were performed by a Remote Pilot Licence (RePL) holder with approval from Remote operator's certificate (ReOC) holder and University chief pilot, Mitch Bannick of Overall Photography. All research protocols involving animals were approved by Western Sydney University, Animal Care and Ethics Committee (ACEC).

Fifteen flying-fox colonies throughout the Greater Sydney region were considered for inclusion in this study; however, due to proximity to roads, walkways or populous areas, and the possibility of the drone coming within 30 m of a person not involved in the study, a violation of CASR 101.245 (Australian Goverment Civil Aviation Safety Authority, 2019), eight of these colonies were excluded. For example, the colonies at Balgowlah (-33.789°, 151.26°) and Avalon (-33.6256°, 151.3251°) were excluded because they were too near main roads and housing to allow for safe and legal drone operation. In accordance with CASR 101.065 (Australian Goverment Civil Aviation Safety Authority, 2019), colonies located within restricted airspace were also excluded. For all colonies, landowner permission was obtained prior to drone flights.

3.3.5 Statistical analyses

All statistical analyses were two-tailed, employed an α value of 0.05 and were conducted in RStudio Desktop 1.2.5042 (R Core Team, 2018). Generalised linear mixed models (GLMMs) were constructed using the *nlme* package (Pinheiro et al., 2016). To analyse the relationship between thermal image point count and ground count for single trees, I constructed a GLMM with thermal image point count as the response variable, ground count as the fixed effect and roost ID as a random effect. Air temperature at the time of thermal image acquisition was excluded from the model due to collinearity with roost. The effect of the independent variable

was tested through a likelihood ratio test (ANOVA). The significance of the random effect was tested through parametric bootstrapping with one thousand iterations.

Using a GLMM, the effect of canopy closure on the difference between the ground and thermal image point counts for single trees was analysed, with the difference between counts as the response variable, canopy closure (%) as the fixed effect and roost ID as a random effect. The effect of the independent variable was tested through a likelihood ratio test (ANOVA). The significance of the random effect was tested through parametric bootstrapping with one thousand iterations. Post-hoc analysis was conducted using Tukey's test.

To compute the concordance between ground counts and thermal image point counts of a single tree, Lin's concordance correlation coefficient (ρc) (Lawrence & Lin, 1989) was computed for the relationship using the package *DescTools* (Signorell, 2016).

To determine the relationship between colony size estimates from drone-acquired orthomosaics to ground counts conducted by me, a GLMM was fit with the thermal image point count as the response variable, my ground count as a fixed effect and roost ID as a random effect. The effect of the independent variable was tested through a likelihood ratio test (ANOVA). The significance of the random effect was tested through parametric bootstrapping with one thousand iterations.

To determine the relationship between colony size estimates obtained from drone-acquired thermal orthomosaics to ground counts conducted by NFFMP counters, a GLMM was fit with the thermal image point count as the response variable, NFFMP ground count as a fixed effect and roost ID as a random effect. I excluded an extreme outlier, the Emu Plains counts, from 24/02/2020 for this analysis, as the NFFMP count was 1648% lower than the corresponding

count from drone-acquired thermal orthomosaic. The effect of the independent variable was tested through a likelihood ratio test (ANOVA). The significance of the random effect was tested through parametric bootstrapping with one thousand iterations.

A GLMM was constructed to investigate variables that may affect the difference between counts from drone-acquired thermal orthomosaics and my ground counts. For this GLMM, the response variable was the percentage difference between my ground count and counts from drone-acquired thermal orthomosaics, and fixed effects were count derived from drone-acquired thermal orthomosaic; orthomosaic resolution (cm^2/pixel); median air temperature at time of orthomosaic image acquisition (°C); spatial extent of the colony (m^2); and flying-fox density (flying-foxes/m^2); with roost ID as a random effect. The effects of the independent variables were tested through likelihood ratio tests (ANOVAs). The significance of the random effect was tested through parametric bootstrapping with one thousand iterations.

Another GLMM was constructed to investigate variables affecting the difference between counts from drone-acquired thermal orthomosaics and NFFMP ground counts. For this GLMM, the response variable was the percentage difference between NFFMP ground count and the drone-acquired thermal orthomosaic count, and fixed effects were count derived from drone-acquired thermal orthomosaic; orthomosaic resolution (cm^2/pixel); median air temperature at time of orthomosaic image acquisition (°C); spatial extent of the colony (m^2); and flying-fox density (flying-foxes/m^2); with roost and NFFMP counter ID as random effects. The effects of the independent variables were tested through likelihood ratio tests (ANOVAs). The significance of the random effects were tested through parametric bootstrapping with one thousand iterations.

Lastly, three GLMMs were run to evaluate the relationship between colony area (response variable) and flying-fox colony size estimates derived from (1) my ground counts, (2) NFFMP ground counts, and (3) counts derived from drone-acquired thermal orthomosaics (fixed effects), with roost ID as a random effect for each GLMM. The effects of the independent variables were tested through likelihood ratio tests (ANOVAs). The significance of random effects were tested through parametric bootstrapping with one thousand iterations.

3.4 RESULTS

3.4.1 Comparing drone and ground counts for a single tree

From point counts of drone-acquired thermal imagery, the number of flying-foxes roosting in a single tree and detected in thermal imagery ranged from 15 to 253 animals. For single trees, point counts derived from drone-acquired thermal images and ground counts conducted by me were positively related (GLMM: $F_{1,11} = 71.860$, $p < 0.001$, marginal $R^2 = 0.88$). Random effect, roost ID, had an effect on the number of flying-foxes observed in a single tree in drone-acquired thermal imagery ($p < 0.001$; Figure 3.3A). Furthermore, counts derived from thermal drone imagery had a high level of concordance with ground counts ($\rho c = 0.893$, 95% CI 0.731-0.960). Canopy cover was found to have no effect on the difference between counts derived from ground counts and drone-acquired thermal images (GLMM: $F_{1,11} = 0.222$, $p = 0.647$; Figure 3.3B).

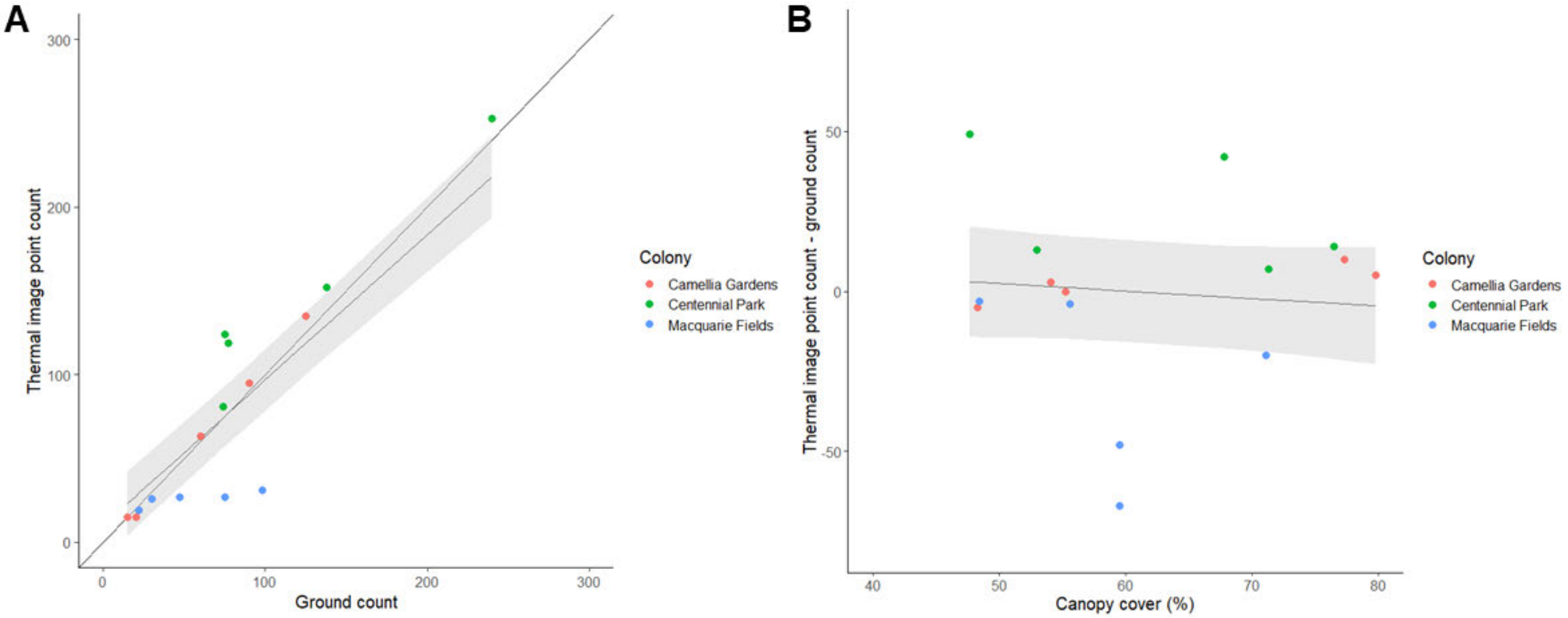

Figure 3.3. (A) There was a strong positive relationship between ground counts and point counts obtained from thermal images for a single tree. (B) There was no significant relationship for the difference between counts obtained from ground counts conducted by me and from thermal images for a single tree and canopy cover of the tree, as measured in GLAMA (Tichý, 2014). Grey shaded area indicates ± SE (standard error).

Random effect, roost ID, was found to have a significant effect on the difference between counts ($p < 0.001$). There was no significant difference between the accuracy of counts derived from thermal imagery for the Centennial Park and Camellia Gardens colonies ($p = 0.218$), or the Macquarie Fields and Camellia Gardens colonies ($p = 0.072$); however, the accuracy of counts derived from thermal imagery for Macquarie Fields and Centennial Park ($p = 0.003$; Figure 3.4).

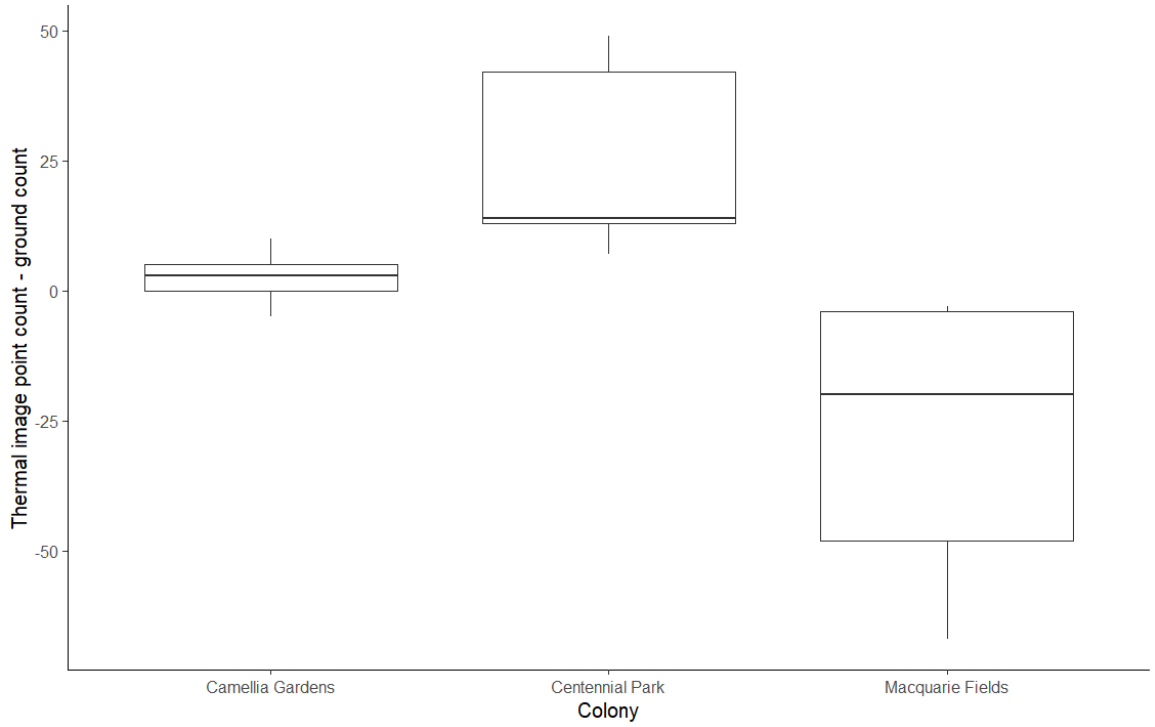

Figure 3.4. The difference between ground counts and point counts derived from drone-acquired thermal imagery for a single tree varied between the Centennial Park and Macquarie fields colonies.

3.4.2 Comparing whole colony ground counts to counts from drone-acquired thermal orthomosaics

The number of flying-foxes counted roosting in a colony ranged from 550-7290, from ground counts by me, 530-7670 from ground counts by NFFMP counters, and from 1115-12131 in counts from drone-acquired thermal orthomosaics (Appendix 10). Whole colony ground counts by me and from drone-acquired thermal orthomosaics were significantly related (GLMM: $F_{1,17}$ = 50.51, $p < 0.001$, marginal $R^2 = 0.83$; Figure 3.5A). However, counts from drone-acquired thermal orthomosaics were higher than ground counts conducted by me in 22 of 25 comparative counts and were on average 105% higher than ground counts conducted by me. The random effect, roost ID explained some variation in counts from drone-acquired thermal orthomosaics ($p < 0.001$).

NFFMP ground counts were significantly related to counts from drone-acquired thermal orthomosaics (GLMM: $F_{1,9} = 14.41$, $p = 0.004$, marginal $R^2 = 0.50$; Figure 3.5B). Counts from drone-acquired thermal orthomosaics were higher than NFFMP ground counts in 13 of 16 comparative counts and were on average 92% higher than NFFMP counts. The random effect, roost ID, did not explain significant variation in counts from drone-acquired thermal orthomosaics ($p > 0.05$).

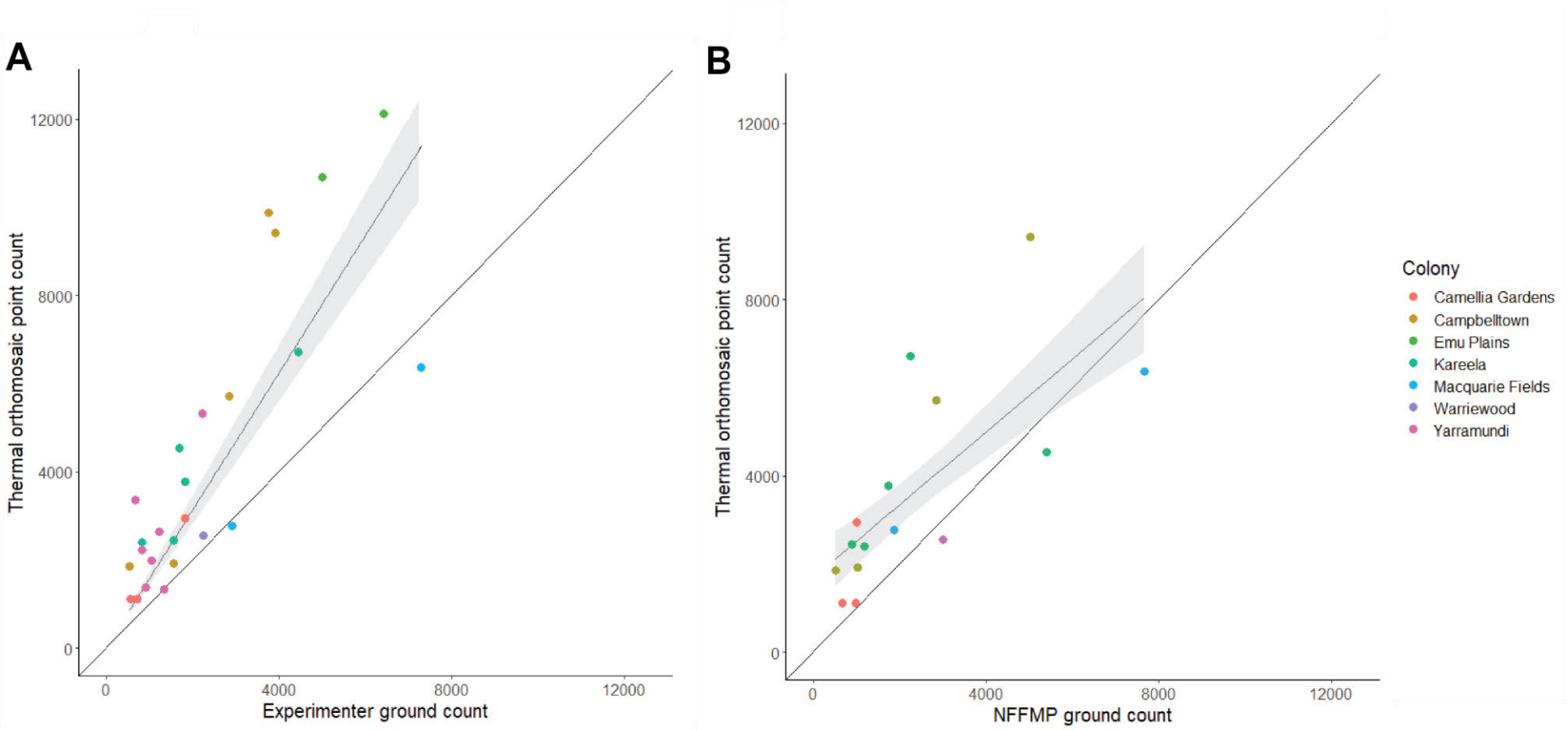

Figure 3.5. (A) Ground counts conducted by me and counts from drone-acquired thermal orthomosaics were positively related, however ground counts conducted by me were on average 105% lower than counts from drone-acquired thermal orthomosaics. (B) Ground counts conducted by NFFMP counters and counts from drone-acquired thermal orthomosaics were positively related, however ground counts conducted by NFFMP counters were on average 92% lower than counts from drone-acquired thermal orthomosaics.

3.4.3 Variables affecting the difference between ground counts and counts from drone-acquired thermal orthomosaics

The percentage difference between counts from drone-acquired thermal orthomosaics and ground counts conducted by me was positively related to flying-fox density (GLMM: $F_{1,13}$ = 6.78, p = 0.022; Table 3.1; Figure 3.6). Random effect, roost ID, did not have a significant effect on the percentage difference between counts from drone-acquired thermal orthomosaics and corresponding ground counts conducted by me or by NFFMP counters (|p| > 0.05). For the NFFMP counter analysis, random effect 'counter' had a significant effect on the percentage difference between counts from drone-acquired thermal orthomosaics and NFFMP counters (p < 0.001).

Table 3.1. GLMM results evaluating the effect of orthomosaic resolution, median air temperature at time of orthomosaic image acquisition, area of the colony, count from drone-acquired thermal orthomosaic and mean density of flying-foxes on the percentage difference between counts from drone-acquired thermal orthomosaics and ground counts.

Fixed effect	Results for ground counts by me	Results for ground counts by NFFMP counters
Resolution (cm^2/pixel)	$F_{1,13}$ = 4.15, p = 0.063	$F_{1,3}$ = 0.24, p = 0.660
Air temperature (°C)	$F_{1,13}$ = 0.10, p = 0.751	$F_{1,3}$ = 0.48, p = 0.540
Colony area (m^2)	$F_{1,13}$ = 2.32, p = 0.152	$F_{1,3}$ = 6.54, p = 0.083
Count from drone-acquired thermal orthomosaic	$F_{1,13}$ = 0.04, p = 0.841	$F_{1,3}$ = 3.83, p = 0.145
Mean density (flying-foxes/m^2)	**$F_{1,13}$ = 6.78, p = 0.022***	$F_{1,3}$ = 2.07, p = 0.246

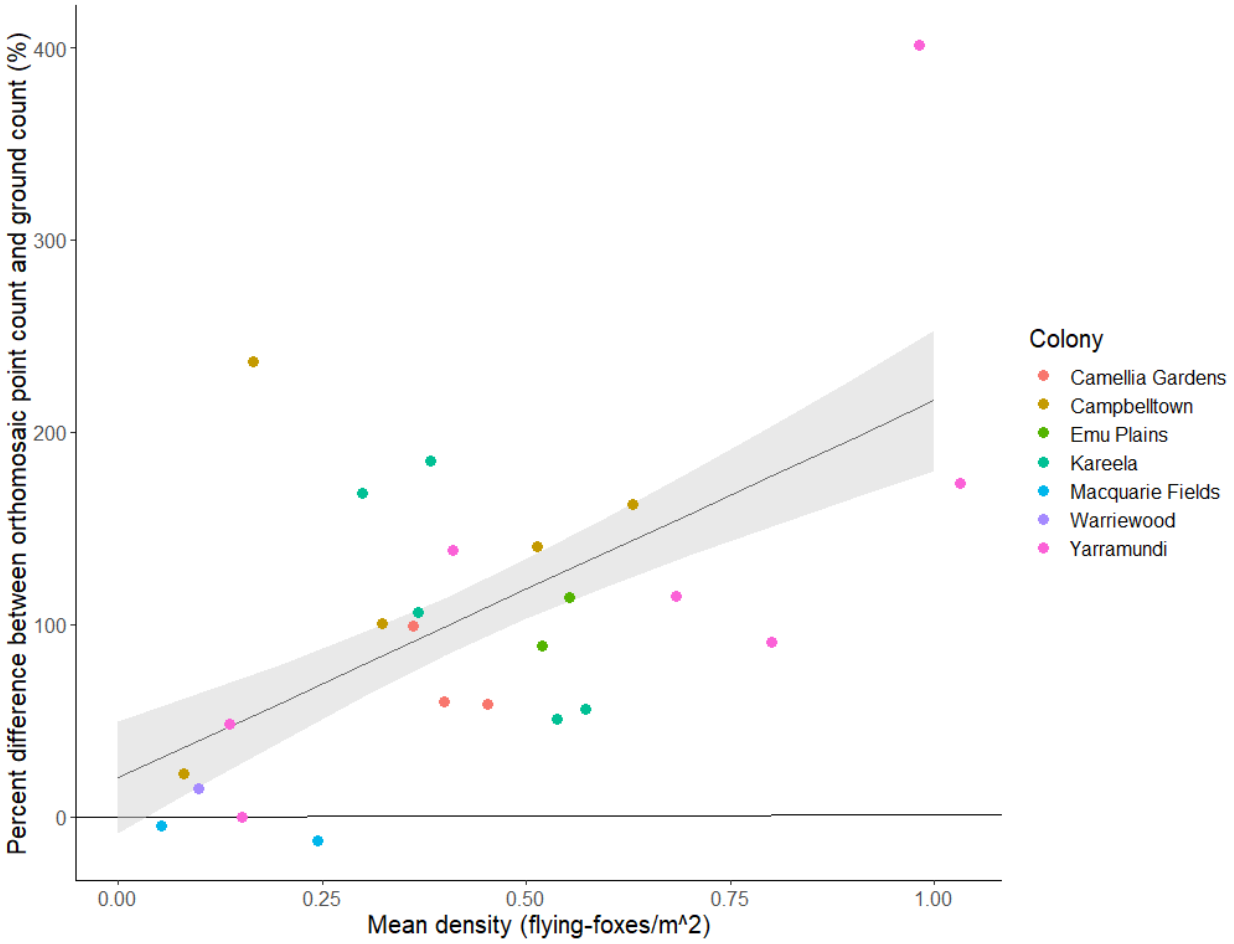

Figure 3.6. The percentage difference between colony size estimates obtained from counts from drone-acquired thermal orthomosaics and ground counts by me increased with increasing density of flying-foxes within the colony. Grey shaded area indicates ± SE.

There was a positive relationship between roost area occupied by the colony (m^2) and counts from drone-acquired thermal orthomosaics (GLMM: $F_{1,17} = 12.50$, $p = 0.0025$, marginal $R^2 = 0.39$), ground counts conducted by me (GLMM: $F_{1,17} = 19.83$, $p < 0.001$ marginal $R^2 = 0.50$), and by NFFMP counters (GLMM: $F_{1,9} = 8.36$, $p = 0.018$, marginal $R^2 = 0.38$). The random effect, roost ID, did not have a significant effect on colony area for any model ($p > 0.05$).

3.4.4 Spatiotemporal changes in flying-fox distribution within roosts

The Campbelltown colony had the highest number of flying-foxes present and highest average density in October 2019, then, number of individuals roosting, and average density decreased between October 2019 and August 2020 (Figure 3.7). For sampling periods in October and November 2019, and February, June and August 2020, the geometric centre of the Campbelltown colony moved 10, 9, 15 and 15 m between consecutive survey periods. The area occupied by the Campbelltown colony increased between October 2019 and February 2020, and then decreased between February and August 2020 (Appendix 10).

The Kareela colony had the highest colony size in February 2020, but the highest average density in October 2019, at this colony, the number of individuals roosting, and average density fluctuated throughout the survey period (Figure 3.8). The roost area occupied by the Kareela colony increased between October 2019 and February 2020, and then decreased between February and August 2020 (Appendix 10). For sampling periods in October and November 2019, and February, June and August 2020, the geometric centre of the colony moved 4, 18, 3 and 6 m between consecutive survey periods.

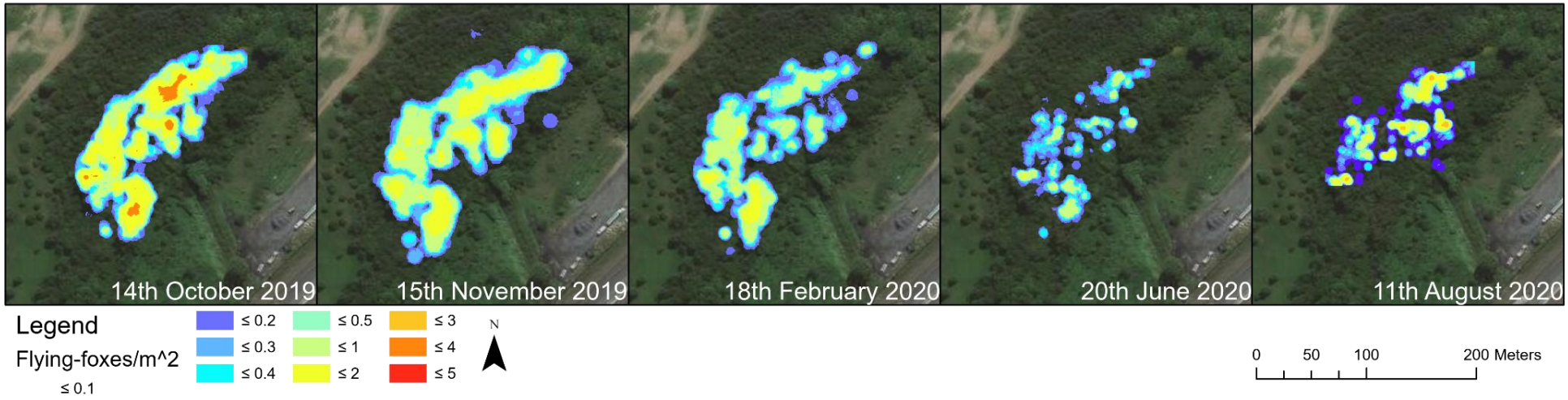

Figure 3.7. Flying-fox density decreased between October 2019 and August 2020 at the Campbelltown colony, roost area occupied by the colony increased between October 2019 and February 2020, and then decreased between February and August 2020. Density map has 0.5 m^2/pixel resolution (Background image source: Maxar).

Figure 3.8. Flying-fox density fluctuated between October 2019 and August 2020 at the Kareela colony, roost area occupied by the colony increased between October 2019 and February 2020, and then decreased between February and August 2020. Density map has 0.5 m^2/pixel resolution (Background image source: Maxar).

For the Yarramundi colony, the number of individuals in the colony and average roosting density fluctuated between September 2019 and March 2020 (Figure 3.9); the roost was then empty in the winter months, between June and August 2020. For sampling periods when the roost was occupied, the geometric centre of the colony moved 103 m between September and December, 107 m between December and January, and then 19, 16, 13 and 20 m between surveys in February and March. The roost area occupied by the colony decreased between September and December 2019, and then increased between January and the 6th of March 2020, decreasing again between the 6th and the 20th of March 2020 (Appendix 10).

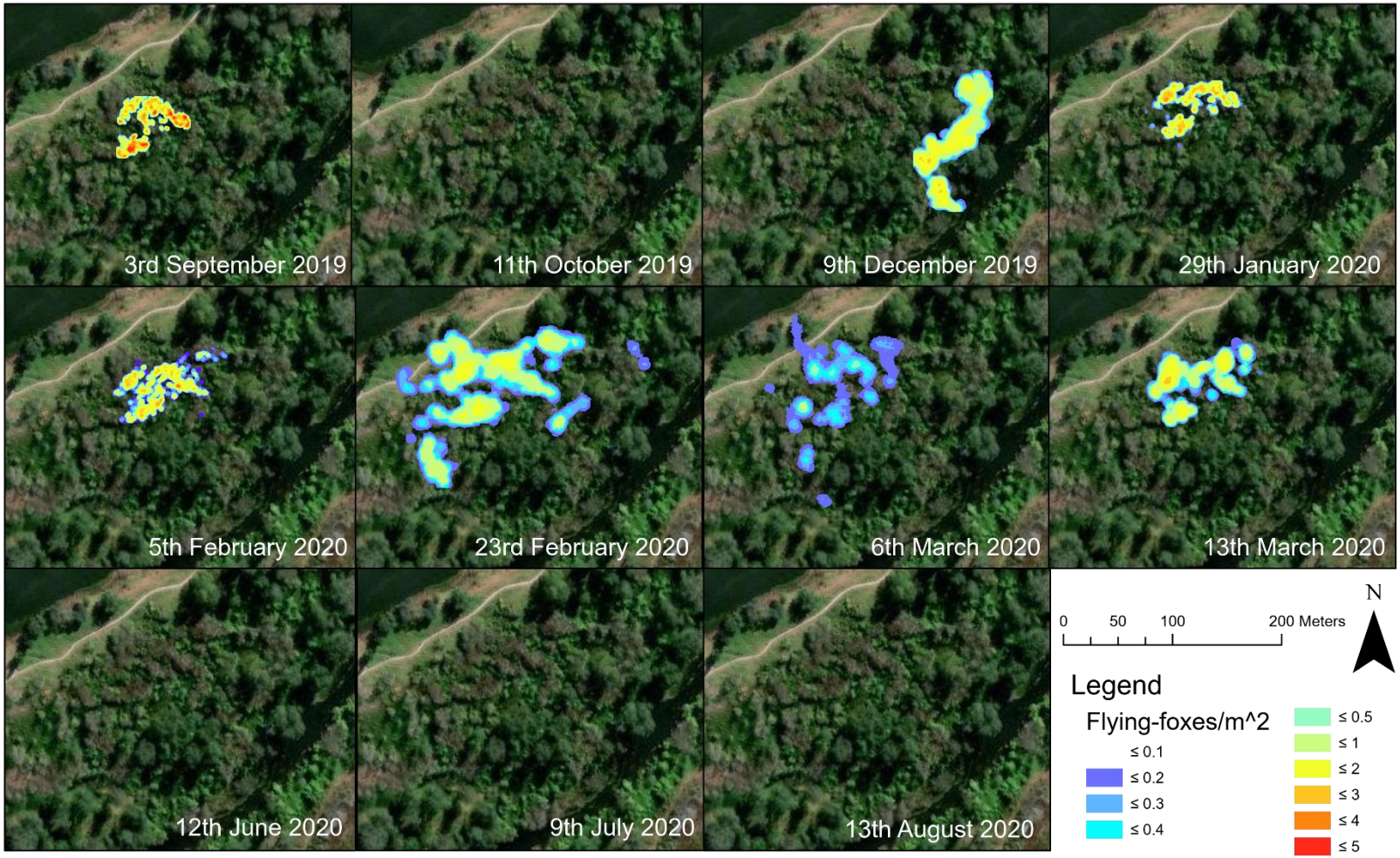

Figure 3.9. Yarramundi was opportunistically sampled between September 2019 and August 2020. Flying-fox colony density is shown for the surveys where the colony was occupied, for surveys in October 2019 and between July and August 2020 the roost was empty. Density map has 0.5 m^2/pixel resolution (Background image source: Maxar).

Trends in colony size and density did not appear to be consistent across the colonies (Figure 3.10). The Yarramundi colony was periodically empty throughout the survey period, whereas there is no data to suggest the Campbelltown and Kareela colonies were vacated during the survey period.

Average flying-fox density was shown to be significantly positively related with the number of individuals in the colony (from counts derived from drone-acquired thermal orthomosaics), at the three colonies (GLMM: $F_{1,17} = 7.67$, $p = 0.013$, marginal $R^2 = 0.29$). Random effect, roost ID, did not have a significant effect on density ($p > 0.05$).

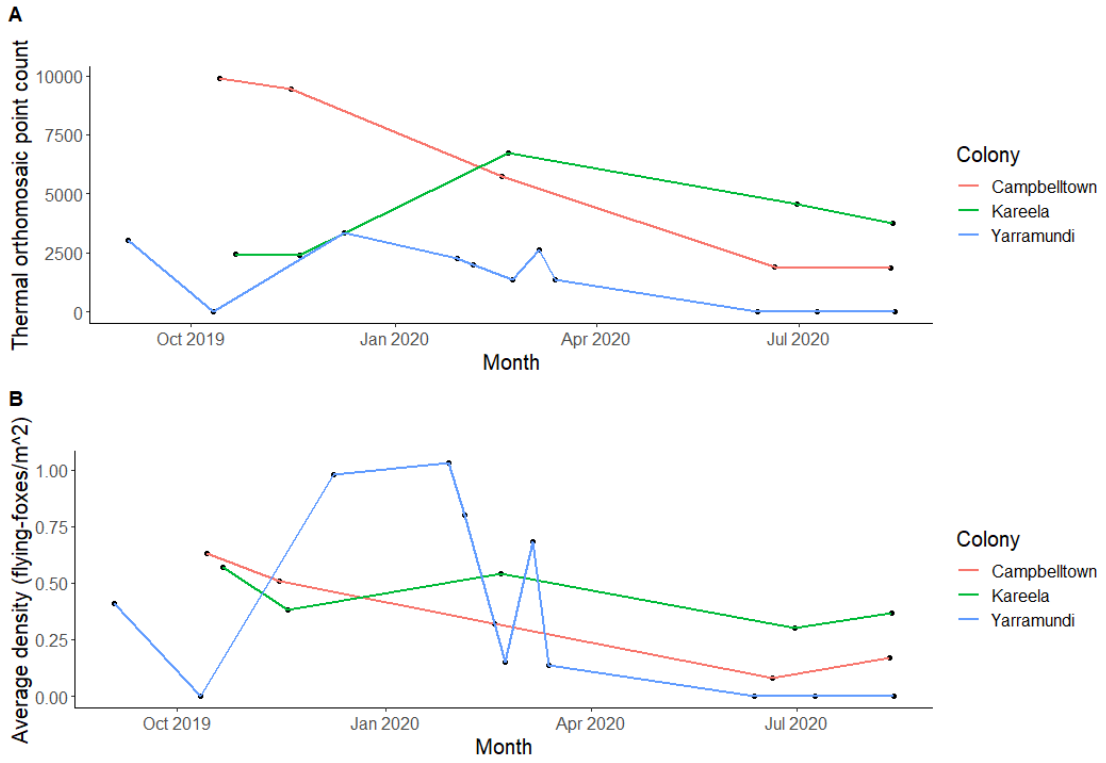

Figure 3.10. (A) Changes in the number of flying-foxes present in colonies between September 2019 and August 2020 at the Campbelltown, Kareela, and Yarramundi colonies. Here, counts are derived drone-acquired thermal orthomosaics. (B) Changes in roosting flying-fox density between September 2019 and August 2020 at the Campbelltown, Kareela, and Yarramundi colonies. Here, density data is extracted from point locations of flying-foxes in orthomosaics.

3.5 DISCUSSION

This study has demonstrated that drone-acquired thermal imagery can be used to accurately monitor the number of flying-foxes aggregated to form a colony at roost sites. For counts of the number of individuals in single trees, ground counts and thermal image point counts were highly concordant. Importantly, whole colony counts derived from drone-acquired thermal orthomosaics consistently identified larger numbers of flying-foxes roosting at colonies compared with ground counts conducted by me and NFFMP counters. Finally, the study showed that thermal orthomosaics of flying-fox colonies can be used to measure flying-fox roosting density and to track changes in the size and roost area occupied by the colony over time. This study shows that accurate flying-fox colony size estimates derived from drone-acquired thermal orthomosaics can be used to monitor and track changes in flying-fox colonies, informing evidence-based conservation and management for these species.

3.5.1 Exact ground counts and counts from drone-acquired thermal imagery were concordant for single trees

In this study, it was critical to assess the ability of users to detect roosting flying-foxes in drone-acquired thermal imagery captured at 50 m AGL. Accurately counting the exact number of roosting flying-foxes in a colony is difficult and likely to cause a high degree of disturbance even for the smallest, most accessible colonies (O'Shea & Bogan, 2003; Westcott et al., 2011). However, it is easier to count and monitor changes in the exact number of flying-foxes roosting in a single tree; therefore, I compared ground counts and counts from drone-acquired thermal imagery for 15 single trees across three flying-fox colonies. Counts of the number of flying-foxes in single trees derived from drone-acquired thermal imagery were concordant with

($\rho c = 0.893$) and strongly related to (marginal $R^2 = 0.88$) direct observer counts from the ground. This indicates that the proposed method for counting flying-foxes in drone-acquired thermal imagery at 50 m AGL is accurate. Furthermore, for trees in the Centennial Park and Camellia Gardens colonies, counts from thermal imagery tended to be similar, if not identical to ground counts. However, for the Macquarie Fields colony, some flying-foxes were not visible in thermal imagery, and consequently those counts were lower than ground counts (Figure 3.4). This may have been due to higher ambient temperature and higher sun elevation at Macquarie Fields, as it was later in the day, causing warming vegetation (see Burke et al., 2019a), and a flying-fox's thermal signature to be less distinguishable from the background environment. Ambient temperature is well understood to affect the visibility of animals in thermal imagery (Cilulko et al., 2013; Croon et al., 1968; Garner et al., 1995). This has been shown for thermal drone surveys of larger arboreal mammals in Panama, where detection was most successful when target animals' external body temperature was at least 3°C warmer than air temperature (Kays et al., 2019). Furthermore, spider monkeys (*A. geoffroyi*) have been successfully detected in low air temperatures, with high concordance between ground counts and counts derived from thermal ($\rho c = 0.90$) (Spaan et al., 2019). The results of this study indicate that counting flying-foxes in drone-acquired thermal imagery is accurate. However, in future studies, thermal imagery used to quantify the number of flying-foxes at colonies should be collected early in the day, when flying-foxes are more likely to be detectable, so as to avoid undercounting the number of individuals in colonies.

Unexpectedly, in this study I did not observe an effect of canopy cover on the similarity between ground counts and counts derived from thermal imagery (Figure 3.3B). Previously, background heat sources, such as vegetation, have been shown to obscure the line of sight

between animals surveyed and the sensor, which may lead to inaccurate temperature readings, misidentification, or failure to detect an animal (Burke et al., 2019a). For example, fewer fur-seals have been detected in coastal scrubland with areas of high canopy cover (>80%) compared to lower canopy cover areas (Gooday et al., 2018). In this study, I measured canopy cover readings at ground level, this may not have accurately represented canopy cover levels across the vertical canopy of the tree. In a future study, deriving canopy cover from the aerial LiDAR may provide different canopy cover estimates, that may be correlated with the thermal detectability of animals from the aerial perspective (advantages of LiDAR derived canopy cover metrics over ground-based estimates are discussed in Ma et al., 2017). Alternatively, canopy cover may not affect the detectability of flying-foxes in thermal imagery as they mostly roost towards the top of canopies of partially (or fully) denuded trees (e.g. Welbergen, 2005), where they are less likely to be obscured by foliage. This study indicates that for grey-headed flying-fox colonies, canopy cover does not affect the accuracy of counts of individuals derived from drone-acquired thermal imagery.

3.5.2 Colony size estimates derived from drone-acquired thermal orthomosaics tended to be higher than ground counts

Daytime ground counts are currently recommended for monitoring and quantifying flying-fox colony size in Australia (Westcott et al., 2015b) and were used to conduct 94% of NFFMP quarterly counts between February 2018 and February 2020 (A. McKeown, personal communication, August 20, 2020). In this study, we compared colony size estimates derived from drone-acquired thermal orthomosaics to results from ground counting methods, to assess the accuracy of ground counting methods. Ground counts of flying-fox colony size by both

myself and NFFMP counters were positively related with counts derived from drone-acquired thermal orthomosaics (Figures 3.5A & B). However, colony size estimates from thermal orthomosaics averaged 105% and 92% higher than ground counts conducted by me, and NFFMP counters, respectively. It should be noted that NFFMP ground counts were conducted up to seven days before or after corresponding drone surveys, so some variation may be attributed to temporal changes in colony size. However, we don't believe this is the source of consistent variation in colony estimates. Previously, ground counts have been thought to have an approximate accuracy of 70% with a coefficient of variation of 10% (Westcott et al., 2012); however, in this study, by comparing ground counts and more accurate counts from drone-acquired thermal orthomosaics, ground count accuracy was shown to be lower. Previously, ground counts for Weddell seals (*Leptonychotes weddellii*) have been shown to be strongly related with counts derived from high resolution optical satellite imagery (0.6 m resolution) (LaRue et al., 2011). However, in contrast to my study, seal counts from satellite imagery tended to be lower than concurrent ground counts. Seals are larger mammals viewable for ground counts during the day while they rested on sea ice so ground counting individuals may be simpler, whereas flying-foxes roost inconspicuously in vegetation; the high thermal contrast between flying-foxes and background enables the analyst to see the flying-fox more easily in thermal imagery (as described in Hamilton et al., 2020 and Beranek et al., 2020). By comparing ground counts to accurate counts derived from drone-acquired thermal imagery, this study suggests that ground counts underestimate true flying-fox colony size. Ground counts are widely used by the NFFMP to assess flying-fox species populations (Westcott et al., 2015b), and therefore, species estimates derived from NFFMP counts may underestimate the true number of flying-foxes in Australia.

For whole colony ground counts, vegetation density has been cited as a factor which may reduce a counter's ability to sight roosting animals, thus leading to an underestimation of total colony size (Eby et al., 1999). Previously, researchers have compared results of colony size estimates from traditional ground-based and fly-out counts, and found that in open canopy areas, both methods produced similar counts; however, in densely vegetated areas, ground counts were lower than fly-out counts (Eby et al., 1999). In this study, for the Macquarie Fields colony, counts from drone-acquired thermal orthomosaics, ground counts by me and NFFMP counters were consistently similar (Appendix 10); this may have been because of the long, narrow roost area, that allowed the ground counter was able to walk along the entire colony and sight most animals. Conversely, the Emu Plains colony featured dense, impenetrable vegetation, and counts from drone-acquired thermal orthomosaics were markedly higher than ground counts, with one NFFMP ground count being 1648% lower than the corresponding count from drone-acquired thermal orthomosaic. Additionally, I found that the difference between colony size estimates from drone-acquired thermal orthomosaic counts and ground counts conducted by me was positively related with flying-fox roosting density (Figure 3.6). Variable animal density and roosting patterns have previously been discussed as sources of error for surveying green sea turtles and Pacific Island flying-foxes (Dunstan et al., 2020; O'Shea & Bogan, 2003). Overall, dense vegetation; roost inaccessibility; flying-fox roosting density; and inconspicuousness, due to their small size and dark colour; may account for the outcome that ground counts tended to underestimate flying-fox colony size, compared to counts from drone-acquired thermal orthomosaics. In this study, the use of thermal drone imagery enabled higher contrast visualisation of these small arboreal mammals.

The relationship between NFFMP counts and counts from drone-acquired thermal orthomosaics had a lower coefficient of determination (R^2) than the relationship between the ground counts by me and counts from drone-acquired thermal orthomosaics (Figures 3.5 A & B). This indicates that the precision of ground counts is higher for counts conducted by a single observer. Furthermore, I found a significant effect of counter on the percentage difference between NFFMP counts and counts from drone-acquired thermal orthomosaics. Between-observer variability in animal counting is well documented (Elphick, 2008; Erwin, 1982; Forsyth et al., 2006; Hanger et al., 2017; Harris & Lloyd, 1977; Short & Bayliss, 1985), between-observer variability in flying-fox count methods has important implications for future flying-fox monitoring practices; for example, time-series analyses are a powerful tool for monitoring population fluctuations and measuring organism responses to environmental change (Frederick et al., 2003). However, if observers are using different techniques, have different levels of experience, or other counting biases, reported trends in colony size may be inaccurate and imprecise. For example, in this study, for colonies surveyed consistently throughout the survey period, observed temporal trends in flying-fox numbers were largely consistent between my ground counts, NFFMP ground counts, and counts from drone-acquired thermal orthomosaics for the Campbelltown colony (Appendix 11). However, for the Kareela colony, while ground counts by me and counts from drone-acquired thermal orthomosaics followed the same trend, NFFMP ground counts failed to detect an increase in flying-fox numbers in February 2020, and recorded an increase in numbers in June 2020, whereas the ground count by me and the count derived from thermal orthomosaic recorded a decrease (Appendix 11). It would be valuable to further investigate the effect of between-observer variability on ground counts across a wider

sample of colonies, which could inform best practices for counting, as well as the training and distribution of counters.

3.5.3 Flying-fox colony size, density and area occupied varied throughout the survey period

To demonstrate the effectiveness of drone-acquired thermal imagery for assessing spatiotemporal changes in flying-fox distribution within roosts, I assessed changes in flying-fox roosting density, colony size, colony area and geometric centre at three colonies between September 2019 and August 2020. Observed trends in the number of individuals in flying-fox colonies varied between the Campbelltown, Kareela and Yarramundi colonies. For the Campbelltown colony, the number of flying-foxes present in the colony was highest in October 2019 and appeared to decrease steadily until August 2020 (Figure 3.7). For Kareela, where fly-out counts have previously shown that colony numbers frequently fluctuate (Mo et al., 2020; Timmiss, 2017); the number of individuals roosting in the colony was lowest in October and November 2019, then peaked in February, then decreased in June, and then increased slightly again in August 2020 (Figure 3.8). At Yarramundi, a roost known to be intermittently occupied (Snoyman & Brown, 2011), colony numbers appeared to fluctuate more frequently than the other two colonies (Figure 3.9). However, Yarramundi was monitored more frequently than the other two colonies during the study, and so, increased monitoring may have allowed for transient fluctuations in colony numbers to be observed, which may have been missed at Kareela and Campbelltown. For all three colonies, geometric centres were temporally stable and did not move more than 20 m across the range of the roost throughout the survey period (with the exception of the 9th of December 2019 survey at Yarramundi, where the geometric centre of the colony was

approximately 100 m from all other geometric centres for that colony). High colony centre temporal stability has been described previously for two other permanently occupied grey-headed flying-fox colonies (Welbergen, 2005). During the survey period, whilst geometric centres of the colonies remained stable, flying-fox colony size, roosting density and roost area occupied fluctuated at the three colonies. Here I demonstrated that drone-acquired thermal imagery can be used to accurately assess the spatiotemporal dynamics of flying-fox distribution within colonies. This has important implications for better understanding species social organisation, as well as for managing human-wildlife conflicts (i.e. determining extent of vegetation buffers [Mo et al., 2020] and for preventing flying-foxes from roosting near private property).

The findings of this study, from drone-acquired thermal orthomosaics, supported previously described seasonal trends in colony size for flying-foxes in south-eastern Australia. The grey-headed flying-fox is an extremely mobile species, moving on average 1,554 km per year between roosts across its range (Welbergen et al., 2020). The number of individuals present in flying-fox colonies in New South Wales and Victoria is thought to decrease between summer and winter each year (Department of Environment, Land, Water and Planning, 2019; van der Ree et al., 2009; Westcott et al., 2015b). This decrease was observed for the Yarramundi and Campbelltown colonies, but not the Kareela colony (Figure 3.10). The number of individuals present in grey-headed flying-fox colonies has also been speculated to be associated with food supply abundance (Eby, 1991; Parry-Jones & Augee, 1992). Increases in the abundance of non-native food sources due to urbanisation may be facilitating changes in the distribution and migration patterns of grey-headed flying-foxes, and their occupation of urban colonies (e.g. the Gordon colony in Sydney, that has been shown to be continually occupied during the winter

[Parry-Jones & Augee, 2001; Williams et al., 2006]). It may be possible that the availability of food sources in the area surrounding the Kareela colony influenced the fluctuations in numbers for this colony (Figure 3.10). Accurate monitoring of the number of flying-foxes present in colonies from drone-acquired thermal orthomosaics can facilitate a greater understanding of the drivers of temporal changes in colony numbers if analysed alongside biotic and abiotic variables theorised to affect this (e.g. vegetation structure [Timmiss, 2017], food availability [Parry-Jones & Augee, 2001; Williams et al., 2006] and extreme temperature events [Welbergen et al., 2008]).

Previously, flying-fox roosting density data has been acquired through logistically complex ground based surveys that require hundreds of sampling points (Welbergen, 2005). Through using data from drone-acquired thermal orthomosaics, surveyors can gain unbiased and accurate insights into flying-fox roosting dynamics with minimal disturbance to the colony. Previously, the centre of the colony was thought to be the most densely populated; providing individuals with increased mating opportunities (Welbergen, 2005), whereas I found that patterns in roosting density varied between colonies. At the Kareela colony throughout the survey period, the consistently most densely occupied area was adjacent to a football field, along the southernmost perimeter of the colony. Here, flying-foxes roosted in a series of tall trees overlooking the rest of the colony in densities of up to 7.97 flying-foxes/m^2 (12^{th} of August 2020; Figure 3.8). For the Campbelltown and Yarramundi colonies, I found that flying-fox density tended to be lower around the perimeter of the colony and higher towards the centre, with densities of more than 4 flying-foxes/m^2, in line with the findings of Welbergen (2005). Overall, for these three colonies, data from drone-acquired thermal orthomosaics showed that high density areas were spread throughout the colony, where density was likely governed by the structure of roosting vegetation as well as social preferences.

Colonial roosting is theorised to aid in defence against predators (Jungwirth et al., 2015); foraging (Wilkinson, 1992; Wittenberger & Hunt, 1985); and reducing thermoregulation costs (Snoyman & Brown, 2011). In this study, I found that flying-fox average roosting density did not vary significantly between surveyed colonies; and that roosting density was positively related with, and followed roughly the same trend as the number of individuals present in each of the three colonies (Figure 3.10), confirming the pattern described in Welbergen (2005). However, trends in temporal changes in density differed between the colonies. When there are increased numbers of flying-foxes in a colony, denser roosting may offer advantages for sociality, including establishing and maintaining mating territories in the colony (Welbergen, 2005). Grey-headed flying-foxes may also roost more densely and occupy a larger roost area during the birthing season in August to October, and for the 4-5 months following, while pups are flightless (Eby, 1991; Martin et al., 1987), as was observed for Campbelltown and Yarramundi. This is also thought to be the case for Geoffroy's rousette fruit bat (*Rousettus amplexicaudatus*) maternity colonies (Carpenter et al., 2014). Longer-term density studies using thermal camera-equipped drones across a broader range of colonies can thus help elucidate how flying-fox biology and sociality influence roosting density for flying-foxes.

3.5.4 Conservation and management implications

Accurate methods for monitoring the number of individuals in flying-fox colonies enhances the evidence base for the conservation and management of these species. Between February 2018 and February 2020, 94% of the quarterly counts conducted by the NFFMP have used the ground count method (A. Mckeown, personal communication, August 20, 2020) and so, colony size estimates derived from ground counts at roosts across the species range may be underestimating the true species population. In future, colony size estimates from drone-acquired thermal

orthomosaics may be incorporated to periodically benchmark ground count accuracy. At present, it is not possible to survey all flying-fox roosts using drones, given the logistics of surveying hundreds of roosts within a meaningfully discrete time period. Through incorporating drone-acquired surveys traditional ground-based counting methods can incorporate a correction factor to predict the true number of flying-foxes at a roost. Conversion factors for flying-fox counts have been applied previously, despite their accuracy not being tested empirically (Stinson et al., 1992; Wiles, 1987; Worthington et al., 2001). Recently, evidence-based conversion factors have been used for green sea turtles (*Chelonia mydas*), when counts derived from drone-acquired imagery suggested there were more turtles than predicted by traditional capture-mark-recapture methods (Dunstan et al., 2020). Importantly for flying-foxes, drone-acquired thermal imagery does not allow the identification of flying-fox species, sex, or age, so visual censuses of roosts remain important.

More accurate estimates of flying-fox abundance at both the roost and population scales derived from drone-acquired thermal orthomosaics allows researchers to associate changes in flying-fox abundance with environmental and other influential factors. This can aid in determining factors influencing flying-fox abundance at a roost and contribute to evidence-based human-wildlife conflict mitigation (Kung et al., 2015). Land-managers dealing with human-wildlife conflict may use the thermal imaging method described here to precisely track changes in colony size, and roost area, shape, density, and positioning to better inform mitigation strategies and control measures at a roost (e.g. informing management actions aimed at alleviating conflict, such as the creation of cleared vegetation buffers [Mo et al., 2020]).

3.5.5 Conclusion

Drone-acquired thermal orthomosaics enabled the visualisation and accurate counting of colonies of flying-foxes at their roosts while causing minimal disturbance. Comparisons of colony size estimates derived from drone-acquired thermal orthomosaics and traditional ground counting methods indicated that ground counts underestimate the true number of individuals in roosts, with important implications for species-wide monitoring practices, and species conservation status assessments. Conservationists and land-managers may use the methods presented here to more accurately monitor colony spatiotemporal dynamics, informing studies on species sociality as well as human-wildlife conflict mitigation measures. The monitoring practices presented here will be valuable for informing evidence-based conservation and management of flying-foxes.

Chapter 4 - Conclusion

4.1 Main findings

I demonstrated that orthomosaics of whole colonies of roosting flying-foxes could be constructed from drone-acquired thermal imagery (Chapter 2). I showed that the number of flying-foxes in an orthomosaic could be counted either manually, or semi-automatically, using Computer Vision or object-based image analysis and machine learning methods. Testing these methods on 13 orthomosaics, I found that the Computer Vision method produced colony size estimates closest to manual counts of an orthomosaic. Then, I examined the variability between counts derived from orthomosaics generated from multiple surveys, conducted during the same day. I found that these surveys produced highly similar manual count results and were highly precise under ideal environmental conditions. Finally, I found that there was not significant variability between manual counts of the number of flying-foxes in drone-acquired orthomosaics conducted by five different counters, indicating that this new method was not affected by an observer bias.

I demonstrated that traditional ground count methods of colonial flying-foxes at a roost underestimate the colony size compared to counts derived from drone-acquired thermal orthomosaics (Chapter 3). Firstly, I showed that counts of flying-foxes from drone-acquired thermal images of single trees were highly related to exact ground counts, demonstrating the accuracy of monitoring colony size using drone-acquired thermal imagery. Then, I compared ground counts and counts derived from thermal orthomosaics for entire colonies, and found that while counts were positively related, thermal orthomosaic counts tended to be almost twice as high as ground counts. This indicates that ground counts underestimate the true number of flying-foxes in a colony. Finally, I demonstrated the successful use of drone-acquired

orthomosaics to monitor changes in colony size and roosting density at flying-fox colonies, and that temporal changes in these factors vary between colonies.

In sum, when acquired under favourable environmental conditions, drone-acquired thermal imagery of flying-fox roosts provides highly accurate and precise counts of the true number of animals present in colonies. Therefore, this provides a viable new means for monitoring flying-fox colonies for management and conservation. Researchers and land managers can reliably use the Computer Vision workflow to automatically generate colony size estimates, without the need for manually counting individuals in orthomosaics. Further, current roost and population estimates underestimate the true number of animals present in colonies, implying that currently species wide population estimates need to be revised and that future research should aim to establish correction factors that can be applied under different scenarios. Finally, longitudinal observations of flying-fox roosts with thermal drones enable the accurate assessment of the spatiotemporal dynamics of roosting and distribution within colonies. As such, this provides an exciting new methodology for understanding the species' social organisation and for monitoring flying-fox colonies in urban conflict settings.

4.2 Implications for flying-fox management and conservation

The colony monitoring method presented here will allow for more accurate, precise and unbiased monitoring of flying-fox colonies. More accurate and precise monitoring of the number of flying-foxes present in a colony enhances the evidence base for more effective conservation of this group of species. If this method were implemented on a large scale over a short time, for example, across the entire grey-headed flying-fox species range in a similar fashion to the National Flying-Fox Monitoring Program's (NFFMP) quarterly counts, researchers and policy

makers could generate more accurate and precise estimates of the entire species population to inform changes in species conservation status. The high precision of this method means that changes in population trends can be detected earlier and with defined confidence. However, wide use of this method is unlikely to be possible in the near future due to the prohibitive cost of equipment and training, and the hundreds of roosts that would require monitoring over several thousand kilometres of eastern Australia. Alternatively, the findings of this thesis may be used to periodically benchmark the accuracy of the existing monitoring methods and inform future ground counting practices. For example, with awareness that ground counts tend to underestimate the true number of individuals in a colony, conservation programs can incorporate correction factors into their colony size and species population estimates to account for this.

Opportunities for future research into the application of drones to inform the conservation and management of flying-foxes are plentiful. More accurate and precise colony size counts, such as those from thermal orthomosaics, substantially improve the statistical power of analyses examining changes in the number of individuals present in a colony (Westcott et al., 2012). In future studies, researchers may monitor temporal changes in colony size, to better understand how flying-foxes use the Australian landscape; the magnitude of their ecosystem services in an area; or to monitor the direct impacts of extreme weather events, such as extreme heat; on the number of individuals present in a colony. From these studies, researchers can continue to build the knowledge base on drivers of flying-fox redistributions for their proactive management and conservation.

At the local level, land managers can use aerial thermal imagery to monitor temporal changes in the number of individuals present in a colony, and the shape and extent of flying-fox colonies. Regular monitoring of number and distribution of flying-foxes in a roost can assist in

identifying factors leading to human-wildlife conflict, such as the extent and timing of flying-foxes roosting on private land. Combining more accurate flying-fox colony size estimates with data of mass flowering (Parry-Jones & Augee, 2001; Roberts et al., 2012), extreme weather (Shilton et al., 2008; Welbergen et al., 2008), and other biotic and abiotic determinants of flying-fox movement and migration can aid land managers to forecast future changes in the number of individuals in a colony.

4.3 Future research directions

4.3.1 Behavioural and foraging observations

Aerial thermal imagery also shows great promise for investigating flying-fox behaviours within roosts. Drones may also be used for recording activity budgets or the movement of individuals throughout the colony while they roost, as well as observing social interactions in specific areas, such as the centre of the colony, where male mating territories predominate and are actively defended (Welbergen, 2005). However, data collection with a drone may be limited by battery life. An unpowered aerial instrument, such as a helikite (a helium-filled kite-balloon), can be equipped with multiple sensors and would allow for longer surveys than a drone. Additionally, a helikite operator does not require a Remote Pilot License and the helikite can be used outside sunrise and sunset times, whereas nighttime drone use requires additional licensing (*Civil Aviation Safety Regulations 1998*, Austl.). A helikite has previously been used to launch acoustic detectors 100 m AGL (above ground level) to investigate land use patterns of the eastern bentwing-bat (*Miniopterus fuliginosus*) by their echolocation calls (Pennay & Mills, 2018). For flying-foxes, helikites equipped with thermal video could allow researchers to observe flying-fox social interactions at the roost over the course of the night, such as pups creching and females

returning to the roost to feed. During the sunrise fly-in, when the ambient temperature is likely to be coolest, a helikite may be used to film animals as they return to the roost, then, tracking software can be used to track and count the number of returning individuals, similar to methods for counting southern bent-wing bats (*M. schreibersii bassanii*) (Lumsden & Jemison, 2015). Aerial imagery collected from an unpowered aerial instrument would allow researchers to collect longer-term observational data, without the need for a Remote Pilot License.

4.3.2 Remote sensing flying-fox colonies in the landscape

There is scope to also use drones for the detection of previously unknown flying-fox colonies and roosts. With respect to counting the entire flying-fox population of Australia, modelling has identified that missing entire colonies during the NFFMP has a substantial effect on error (Westcott et al., 2012). Individual flying-foxes regularly move between colonies, as well as to formerly unoccupied areas, and have been shown to form colonies outside of their existing geographic ranges (Welbergen et al., 2020). Flying-foxes roosting away from known colonies likely results in an underestimate of approximately 11% of Australia's total flying-fox population (Westcott et al., 2015a). Therefore, it is essential that methods for locating newly formed colonies are developed. Previously, the hyperspectral signatures of large farm animals have been detected and categorised through stepwise discriminant analysis (Bortolot & Prater, 2009). With visual spectrum satellite imagery, deep learning has been used to detect albatrosses (Bowler et al., 2020) and supervised learning has been used to detect penguins (Fretwell et al., 2012). In a future study, very high-resolution visible spectrum or high-resolution hyperspectral imagery of known flying-fox colonies collected by a drone could be used to identify the unique spatial patterns and spectral signatures associated with flying-fox colonies (including the animals themselves, guano, and defoliated vegetation). Then, those same signatures could be detected in

large scale satellite or aerial imagery using machine learning or deep learning methods, to potentially detect formerly unknown flying-fox colonies in the landscape. This method is of particular interest across the remote north of Australia where we have a very limited understanding of flying-fox colony locations and occupation for three of the four Australian species (Fox et al., 2008; Westcott et al., 2012). Furthermore, during the wet season large parts of the north of Australia are difficult to access, enhancing the benefits of developing a remote monitoring method. The development of this method would enable researchers to detect and monitor previously unknown camps.

4.3.3 Assessing the response of flying-foxes to drone use

In my study drones were flown at least 30 m above roosting flying-foxes over a period of up to 2 hours without an observable response from the animals. Studies that require flying drones substantially closer to flying-foxes may nevertheless observe stress responses, and so a formal assessment of the potential welfare impacts of drones on these species would be informative. Previously, the immediate behavioural responses of an animal to the presence of a drone has been studied in mallards (*Anas platyrhynchos*), flamingos (*Phoenicopterus roseus*) and common greenshanks (*Tringa nebularia*) (Vas et al., 2015), and pinnipeds (Fritz, 2012). The physiological response of a species to drones has also been monitored for American black bears (*Ursus americanus*) (Ditmer et al., 2015). While it was found that mallards, flamingos and common greenshanks showed no visible response to drones approaching to within 4 m (Vas et al., 2015), in mammal species, dolphins have been observed flushing, a response to predators (Fritz, 2012), and American black bears exhibited a minor cardiac stress response (Ditmer et al., 2015). Studies assessing stress responses of flying-foxes to near-flying drones would inform future research methods.

4.3.4 Deep learning for automated counting of flying-foxes

The Computer Vision workflow I used to detect flying-foxes in thermal orthomosaics produced counts approximating corresponding manual count results ($\rho c = 0.83$), however semi-automated classification of drone-acquired thermal orthomosaic imagery through deep learning may further improve semi-automated classification accuracy. Recent studies have found that deep learning can be more accurate than shallow machine learning for classification of objects (Bycroft et al., 2019; Huang et al., 2020). In future studies, a custom-programmed deep learning algorithm for detecting flying-foxes in thermal imagery may produce more accurate classification and counting results (see Ridge et al., 2019).

4.3.5 Calibrating colony size estimates derived from weather radar

Recently, weather radar data were used to estimate the number of individuals present in the Yarra Bend flying-fox colony in Melbourne (Australia), as flying-foxes were detectable during the sunset fly-out (Meade et al., 2019). It was found that the slope expressing the relationship between radar-derived counts and ground-based counts was less than one; meaning that either ground-based counts overestimated, or radar-derived counts underestimated the true number of individuals present in the colony (Meade et al., 2019). The method developed in this thesis for estimating the number of individuals in a colony, using thermal orthomosaics, could be used synchronously with the radar count method to ensure the accuracy of the population count, allowing calibration of the radar count method. If successful, radar counts derived from weather stations could be used to estimate the true numbers of individuals present in a colony. As archival weather radar data are available from much of the southeast of Australia, and from up to two decades in the past, this means that weather radar data can be used to monitor true numbers

of flying-foxes (retrospectively) at the landscape scale, as well as to study spatiotemporal population dynamics over decadal and continental timescales. Thus, alleviating the reliance on the labour-intensive monitoring methods that are currently employed by the NFFMP.

APPENDICES

Appendix 1. Parameters used to generate thermal orthomosaics in Agisoft Metashape Professional Version 1.5 (LLC Agisoft, 2019).

Alignment parameters	
Accuracy	High
Generic preselection	Yes
Reference preselection	Yes
Key point limit	40000
Tie point limit	4000
Adaptive camera model fitting	Yes
Mesh	
Source data	Depth maps
Quality	High
Face count	High
Calculate vertex colours	Yes
Orthomosaic	
Projection	Geographic (WGS 84)
Surface	Mesh
Blending mode	Mosaic
Enable hole filling	Yes

Appendix 2. (A) Complete (not clipped to colony extent) thermal orthomosaic of the Yarramundi flying-fox colony on the 4th of September 2019, magnified section shows marking of individual flying-foxes; (B) The same thermal orthomosaic with marked points overlaid.

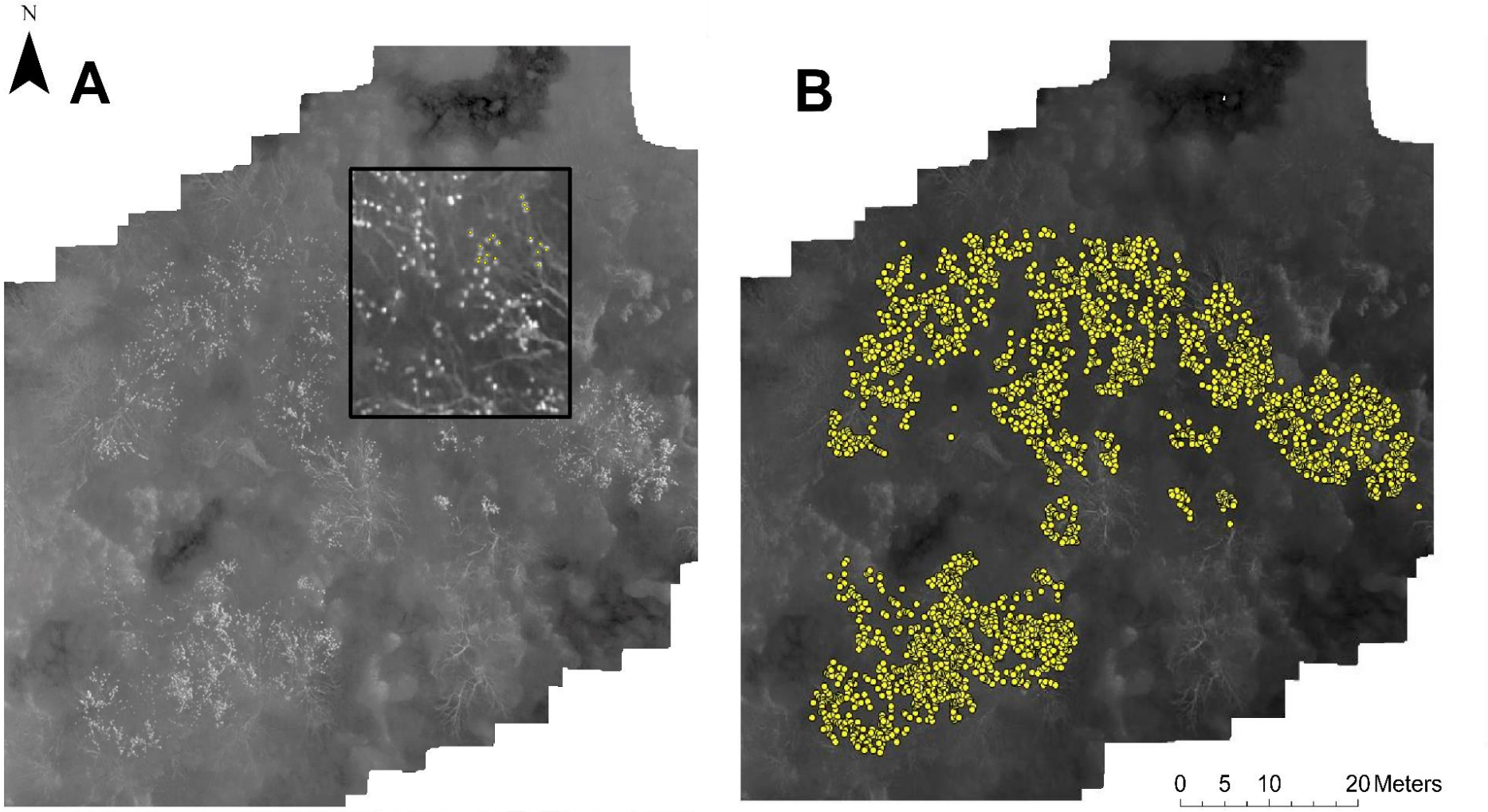

Appendix 3. Macro for implementing the Computer Vision classification workflow in Fiji 1.8.0_172 (Schindelin et al., 2012).

```
run("8-bit");

run("Smooth");

run("Subtract Background...", "rolling=50");

run("Find Edges");

setAutoThreshold("Default dark");

//run("Threshold...");

//setThreshold(x, y*);

setOption("BlackBackground", true);

run("Convert to Mask");

run("Despeckle");

run("Watershed");

run("Analyse Particles...", "size=10-300 pixel circularity=0.3-1.00 display clear include summarize add");
```

***Note:** The values for the '//setThreshold(x, y);' function should be manually adjusted until the user observes that the highest proportion of flying-foxes are visible in the thresholded image.

Appendix 4. Histograms displaying the pixel intensities of training samples representing background (A) and flying-foxes (B) for machine learning classification in ArcGIS Pro 2.5.0 (Environmental Systems Research Institute, 2020).

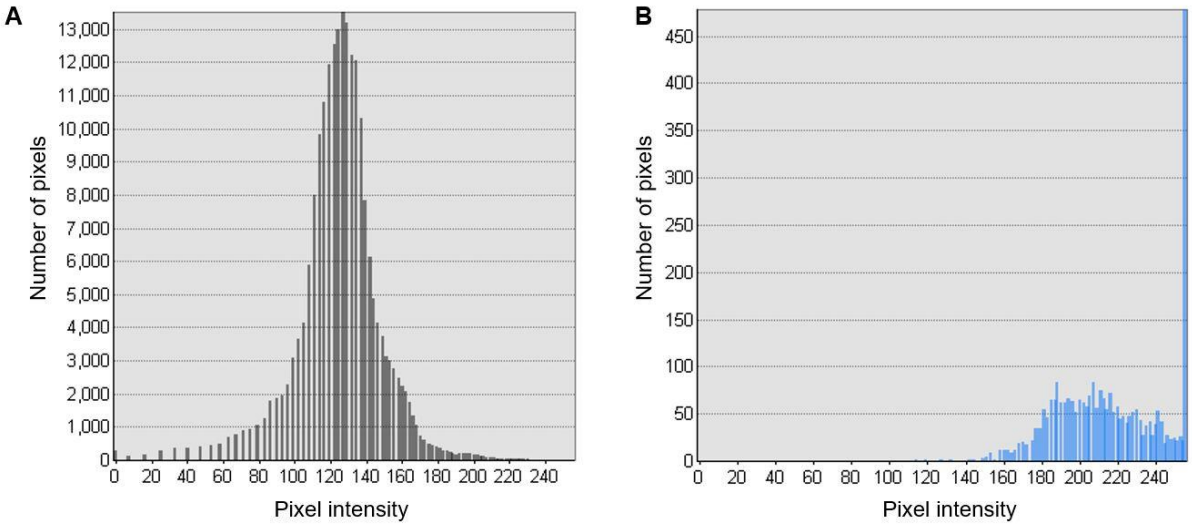

Appendix 5. Machine learning classifier specifications for object-based image classification in ArcGIS Pro 2.5.0 (Environmental Systems Research Institute, 2020).

Segment attributes for all classifiers		**Random Forest Classifier parameters**	
Active chromaticity colour	Yes	Maximum number of trees	50
Mean digital number (0-255)	Yes	Maximum tree depth	30
Standard deviation	Yes		
Count of pixels	Yes		
Compactness	Yes		
Rectangularity	Yes		

Appendix 6. Confusion matrix produced from an accuracy assessment of the Computer Vision classified drone-acquired thermal orthomosaic from the 3rd of September 2019 at the Yarramundi flying-fox colony. (i) indicates commission error, (ii) indicates omission error (iii) indicates probability of detection.

Class value	Background	Flying-fox	User accuracy	Kappa
Background	100	0(i)	1	0.56
Flying-fox	44(ii)	56(iii)	0.56	
Total	144	56	0	
Producer accuracy	0.69	1	**0.78**	

Appendix 7. Email sent out to the 4 participants in the study accessing between-counter variation in visual point counts of the number of flying-foxes in thermal orthomosaics.

Dear _____ ,

Thank you for agreeing to contribute to my Master of Research thesis. In this exercise, you will count the number of flying-foxes in three thermal images taken with a drone overhead a flying-fox colony located in NSW. Australian flying-foxes roost in groups of up to tens of thousands of individuals in urban and rural vegetated areas. Sometimes as many as a few hundred can be seen roosting in a single tree. Currently, methods used for estimating the number of flying-foxes in a colony have been shown to be inaccurate and imprecise. My project involves developing and testing more accurate and precise methods for quantifying flying-fox colony sizes from drone-acquired thermal imagery. In this imagery, flying-foxes, because they are warm compared to vegetation, appear as very bright circular objects.

The three thermal images you will be counting from were taken at one location. We are interested to know if and how the number of flying-foxes counted varies between counters. If this method turns out to be precise between counters it can be used more widely as a reliable indicator for the number of flying-foxes in a roost.

This entire exercise should not take more than four hours to complete. Instructions for completing the exercise as well as the three thermal images you will be counting can be downloaded at the following link: (a link to a Dropbox folder containing a .pdf file detailing instructions, as well as .tiff image files of the three orthomosaics was provided here, this is now viewable through the link provided in Appendix 8).

Please read through the instructions before commencing the exercise. This exercise will require you to download a program called Fiji[1]. You may already be familiar with ImageJ, Fiji is a very similar software made by the same developers as ImageJ, with all ImageJ's plugins preinstalled. The software is free and safe for your computer.

Your help with my project is greatly appreciated!

Kind regards,

Eliane McCarthy

Appendix 8. Web links to Figshare repositories containing orthomosaics used in Chapters 2 and 3 of this thesis.

Orthomosaics and classified image products used in **Chapter 2** are downloadable:

https://figshare.com/s/ac14e845bb9ab8cdfca0

Orthomosaics used in **Chapter 3** are downloadable:

https://figshare.com/s/907b40b746e880535789

Appendix 9. Location, date of image acquisition, median air temperature at time of survey, average resolution, colony area, and number of flying-foxes manually counted for each orthomosaic used to evaluate the accuracy of the semi-automated counting methods when compared with manual point counts of orthomosaics. Counts were conducted between September 2019 and March 2020. Air temperature data was downloaded from the Australian Bureau of Meteorology from the nearest weather station to each colony within two days of conclusion of each drone survey (Bureau of Meteorology, 2020).

Location	Date	Median air temperature (°C)	Resolution (cm^2/pixel)	Colony area (m^2)	Visual point count of flying-foxes
Camellia Gardens	22/10/2019	16.9	3.55	1450.90	1126
Camellia Gardens	20/02/2020	20.0	4.21	4074.55	2945
Campbelltown	14/10/2019	13.3	4.8	7634.24	9888
Campbelltown	18/02/2020	21.8	2.71	10438.64	5723
Centennial Park	18/03/2020	18.1	6.50	21112.07	7933
Emu Plains	24/02/2020	19.9	4.27	14823.92	10698
Emu Plains (partial*)	19/10/2019	21.6	2.53	10192.06	12131
Kareela	21/10/2019	16.3	3.45	2654.15	2452
Kareela	21/02/2020	20.4	5.08	6253.08	6723
Macquarie Fields	27/02/2020	19.4	4.66	10983.01	6384

Warriewood	25/02/2020	22.6	8.24	12745.79	2566
Yarramundi	03/09/2019	5.0	2.55	1909.24	3042
Yarramundi	09/12/2019	22.0	2.61	2149.38	3358

*approximately 50% of area captured.

Appendix 10. Flying-fox colony size estimates derived from visual point counts of thermal orthomosaics, ground counts conducted by myself and National Flying-Fox Monitoring Program (NFFMP) participants, as well as median air temperature, colony area, orthomosaic resolution and mean density of flying-foxes for seven flying-fox roosts across the Greater Sydney region. Counts were conducted between October 2019 and August 2020. Air temperature data was downloaded from the Australian Bureau of Meteorology (Bureau of Meteorology, 2020) from the nearest weather station to each colony within two days of conclusion of each drone survey.

Roost	**Date of thermal orthomosaic survey**	**Count from drone-acquired thermal orthomosaic**	**Ground count by experimenter**	**Ground count by NFFMP participant**	**Median air temperature (°C)**	**Colony area (m^2)**	**Orthomosaic resolution (cm^2/pixel)**	**Mean density of flying-foxes (flying-foxes/m^2)**
Campbelltown	14/10/2019	9888	3770	-	11.2	7634	3.55	0.63
	15/11/2019	9417	3920	5027	20.2	9386	2.21	0.51
	18/02/2020	5723	2850	2860	21.8	10438	2.71	0.32
	20/06/2020	1917	1570	1034	10.3	6339	3.17	0.08
	11/08/2020	1851	550	530	10.9	5164	2.38	0.17
Camellia Gardens	22/10/2019	1126	710	675	17.0	1451	3.55	0.45
	19/11/2019	1115	560	994	16.2	2296	2.2	0.36
	20/02/2020	2945	1840	1001	20.0	4075	4.21	0.40
Emu Plains	19/10/2019	12131	6420	-	21.6	10192	2.53	0.52
	24/02/2020	10698	5000	612	19.9	14824	4.27	0.55
Kareela	21/10/2019	2452	1570	900	16.6	2654	3.45	0.57
	19/11/2019	2396	840	1190	22.7	3927	2.01	0.38
	21/02/2020	6723	4450	2260	20.4	6253	5.08	0.54

	30/06/2020	4545	1695	5400	12.0	4476	2.16	0.30
	12/08/2020	3773	1830	1750	10.6	4424	2.52	0.37
Macquarie Fields	27/02/2020	6384	7290	7670	19.4	10983	4.66	0.24
	18/06/2020	2783	2920	1870	14.5	6217	2.44	0.05
Warriewood	25/02/2020	2566	2240	3000	22.6	12746	8.24	0.10
Yarramundi	09/12/2019	3358	670	-	19.8	2149	2.61	0.98
	29/01/2020	2240	820	-	22.7	1268	3.07	1.03
	05/02/2020	2003	1050	-	21.4	1640	2.54	0.80
	23/02/2020	5321	2230	-	20.4	6133	7.36	0.41
	06/03/2020	1347	1350	-	22.5	6183	9.68	0.15
	13/03/2020	2638	1230	-	17.5	2065	4.74	0.68
	20/03/2020	1381	930	-	22.7	2489	10.8	0.14

Appendix 11. Trends in the number of flying-foxes present in the Campbelltown (top) and Kareela colonies (bottom) between October 2019 and August 2020. Thermal drone surveys and ground counts by me were conducted on the same day, ground counts by NFFMP counters were conducted within seven days of drone surveys for each survey period.

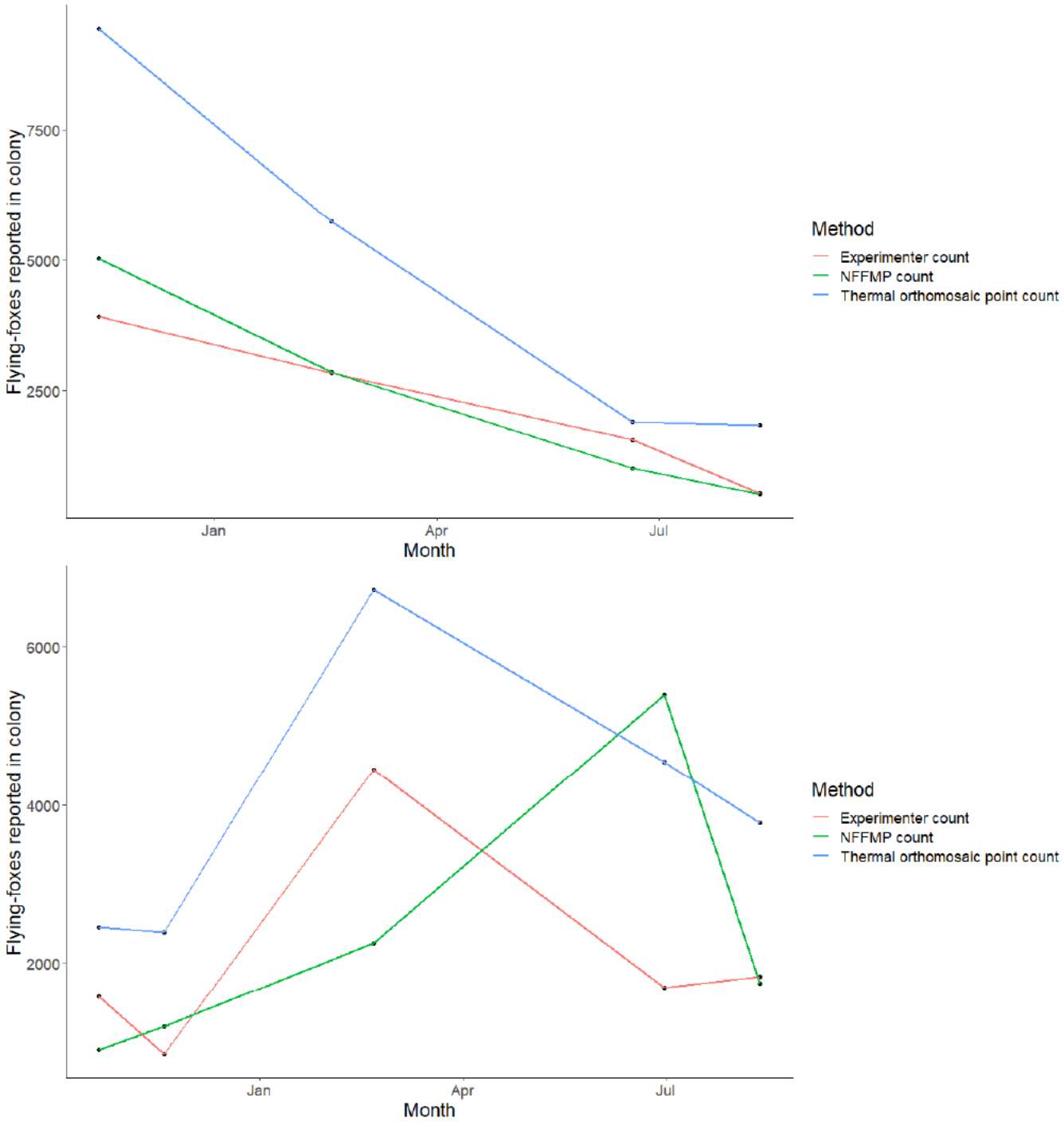

REFERENCES

Adão, T., Hruška, J., Pádua, L., Bessa, J., Peres, E., Morais, R., & Sousa, J. (2017). Hyperspectral imaging: A review on UAV-based sensors, data processing and applications for agriculture and forestry. *Remote Sensing*, *9*(11), 1110. https://doi.org/10.3390/rs9111110

Afán, I., Máñez, M., & Díaz-Delgado, R. (2018). Drone monitoring of breeding waterbird populations: The case of the glossy ibis. *Drones*, *2*(4), 42. https://doi.org/10.3390/drones2040042

Alldredge, M. W., Pacifici, K., Simons, T. R., & Pollock, K. H. (2008). A novel field evaluation of the effectiveness of distance and independent observer sampling to estimate aural avian detection probabilities. *Journal of Applied Ecology*, *45*(5), 1349-1356. https://doi.org/10.1111/j.1365-2664.2008.01517.x

Anderson, K., & Gaston, K. J. (2013). Lightweight unmanned aerial vehicles will revolutionize spatial ecology. *Frontiers in Ecology and the Environment*, *11*(3), 138-146. https://doi.org/10.1890/120150

Aplin, P. (2005). Remote sensing: ecology. *Progress in Physical Geography*, *29*(1), 104-113. https://doi.org/10.1191/030913305pp437pr

Archer, C. R., Pirk, C. W. W., Carvalheiro, L. G., & Nicolson, S. W. (2014). Economic and ecological implications of geographic bias in pollinator ecology in the light of pollinator declines. *Oikos*, *123*(4), 401-407. https://doi.org/10.1111/j.1600-0706.2013.00949.x

Augee, M. L., & Ford, D. (1999). Radio-tracking studies of grey-headed flying-foxes, *Pteropus poliocephalus*, from the Gordon colony, Sydney. *Proceedings of the Linnean Society of New South Wales*, *121*, 61-70.

Australian Goverment Civil Aviation Safety Authority. (2019). *Advisory circular AC 101-01v3.0 - remotely piloted aircraft systems - licensing and operations*. https://www.casa.gov.au/sites/default/files/101c01.pdf

Aziz, S. A., Clements, G. R., Giam, X., Forget, P.-M., & Campos-Arceiz, A. (2017). Coexistence and conflict between the island flying fox (*Pteropus hypomelanus*) and humans on Tioman Island, Peninsular Malaysia. *Human Ecology*, *45*(3), 377-389. https://doi.org/10.1007/s10745-017-9905-6

Baena, S., Moat, J., Whaley, O., & Boyd, D. S. (2017). Identifying species from the air: UAVs and the very high resolution challenge for plant conservation. *PLoS ONE*, *12*(11), e0188714. https://doi.org/10.1371/journal.pone.0188714

Barbedo, J. G. A., Koenigkan, L. V., Santos, T. T., & Santos, P. M. (2019). A study on the detection of cattle in UAV images using deep learning. *Sensors*, *19*(24), 5436. https://doi.org/10.3390/s19245436

Beranek, C. T., Roff, A. M., Denholm, B., Howell, L. G., & Witt, R. R. (2020). Trialling a real-time drone detection and validation protocol for the koala (*Phascolarctos cinereus*). *Australian Mammalogy*. Advance online publication. https://doi.org/10.1071/AM20043

Betke, M., Hirsh, D. E., Makris, N. C., McCracken, G. F., Procopio, M., Hristov, N. I., Tang, S., Bagchi, A., Reichard, J. D., & Horn, J. W. (2008). Thermal imaging reveals significantly smaller Brazilian free-tailed bat colonies than previously estimated. *Journal of Mammalogy*, *89*(1), 18-24. https://doi.org/10.1644/07-MAMM-A-011.1

Blackwell, B. F., Seamans, T. W., Washburn, B. E., & Cepek, J. D. (2006). Use of infrared technology in wildlife surveys. *Proceedings of the 22nd Vertebrate Pest Conference*, *22*, 467-472. https://doi.org/10.5070/V422110116

Blaschke, T. (2010). Object based image analysis for remote sensing. *ISPRS Journal of Photogrammetry and Remote Sensing*, *65*(1), 2-16. https://doi.org/10.1016/j.isprsjprs.2009.06.004

Bortolot, Z. J., & Prater, P. E. (2009). A first assessment of the use of high spatial resolution hyperspectral imagery in discriminating among animal species, and between animals and their surroundings. *Biosystems Engineering*, *102*(4), 379-384. https://doi.org/10.1016/j.biosystemseng.2009.01.005

Bowler, E., Fretwell, P. T., French, G., & Mackiewicz, M. (2020). Using deep learning to count albatrosses from space: assessing results in light of ground truth uncertainty. *Remote Sensing*, *12*(12), 2026. https://doi.org/10.3390/rs12122026

Breiman, L. (2001). Random forests. *Machine Learning*, *45*(1), 5-32. https://doi.org/10.1023/A:1010933404324

Brooke, A. P. (2001). Population status and behaviours of the Samoan flying fox (*Pteropus samoensis*) on Tutuila Island, American Samoa. *Journal of Zoology*, *254*(3), 309-319. https://doi.org/10.1017/S0952836901000814

Brooke, A. P., Solek, C., & Tualaulelei, A. (2000). Roosting behavior of colonial and solitary flying foxes in American Samoa (Chiroptera: Pteropodidae). *Biotropica*, *32*(2), 338-350. https://doi.org/10.1111/j.1744-7429.2000.tb00477.x

Brooke, A. P., & Tschapka, M. (2002). Threats from overhunting to the flying fox, *Pteropus tonganus*, (Chiroptera: Pteropodidae) on Niue Island, South Pacific Ocean. *Biological Conservation*, *103*(3), 343-348. https://doi.org/10.1016/S0006-3207(01)00145-8

Brown, G. W., Scroggie, M. P., & Choquenot, D. (2008). Precision and accuracy of flyout counts of the common bent-wing bat (*Miniopterus schreibersii*). *Acta Chiropterologica*, *10*(1), 145-151. https://doi.org/10.3161/150811008X331162

Brunton, E. A., Leon, J. X., & Burnett, S. E. (2020). Evaluating the efficacy and optimal deployment of thermal infrared and true-colour imaging when using drones for monitoring kangaroos. *Drones*, *4*(2), 20. https://doi.org/10.3390/drones4020020

Buckland, S. T., Rexstad, E. A., Marques, T. A., & Oedekoven, C. S. (2015). *Distance sampling: methods and applications*. Springer.

Bureau of Meteorology. (2020). *Latest weather observations for the Sydney area*. http://www.bom.gov.au/nsw/observations/sydney.shtml?ref=hdr

Burke, C., Rashman, M., Wich, S., Symons, A., Theron, C., & Longmore, S. (2019a). Optimizing observing strategies for monitoring animals using drone-mounted thermal infrared cameras. *International Journal of Remote Sensing*, *40*(2), 439-467. https://doi.org/10.1080/01431161.2018.1558372

Burke, C., Rashman, M. F., Longmore, S. N., McAree, O., Glover-Kapfer, P., Ancrenaz, M., & Wich, S. (2019b). Successful observation of orangutans in the wild with thermal-equipped drones. *Journal of Unmanned Vehicle Systems*, *7*(3), 235-257. https://doi.org/10.1139/juvs-2018-0035

Burn, D. M., Webber, M. A., & Udevitz, M. S. (2006). Application of airborne thermal imagery to surveys of pacific walrus. *Wildlife Society Bulletin*, *34*(1), 51-58. https://doi.org/10.2193/0091-7648(2006)34[51:AOATIT]2.0.CO;2

Bycroft, R., Leon, J. X., & Schoeman, D. (2019). Comparing random forests and convoluted neural networks for mapping ghost crab burrows using imagery from an unmanned aerial

vehicle. *Estuarine Coastal and Shelf Science*, *224*, 84-93. https://doi.org/10.1016/j.ecss.2019.04.050

Carpenter, E., Gomez, R., Waldien, D. L., & Sherwin, R. E. (2014). Photographic estimation of roosting density of geoffroys rousette fruit bat *Rousettus amplexicaudatus* (Chiroptera: Pteropodidae) at Monfort bat cave, Philippines. *Journal of Threatened Taxa*, *6*(6), 5838-5844. https://doi.org/10.11609/JoTT.o3522.5838-44

Carrivick, J. L., Smith, M. W., Quincey, D. J., & Carver, S. J. (2013). Developments in budget remote sensing for the geosciences. *Geology Today*, *29*(4), 138-143. https://doi.org/10.1111/gto.12015

Chabot, D., & Bird, D. M. (2015). Wildlife research and management methods in the 21st century: where do unmanned aircraft fit in? *Journal of Unmanned Vehicle Systems*, *3*(4), 137-155. https://doi.org/10.1139/juvs-2015-0021

Chen, C.-H., & Liu, K.-H. (2017). Stingray detection of aerial images with region-based convolution neural network. Consumer Electronics-Taiwan (ICCE-TW), 2017 IEEE International Conference, Taipei, Taiwan.

Christie, K. S., Gilbert, S. L., Brown, C. L., Hatfield, M., & Hanson, L. (2016). Unmanned aircraft systems in wildlife research: current and future applications of a transformative technology. *Frontiers in Ecology and the Environment*, *14*(5), 241-251. https://doi.org/10.1002/fee.1281

Cilulko, J., Janiszewski, P., Bogdaszewski, M., & Szczygielska, E. (2013). Infrared thermal imaging in studies of wild animals. *European Journal of Wildlife Research*, *59*(1), 17-23. https://doi.org/10.1007/s10344-012-0688-1

Civil Aviation Safety Regulations 1998. (Austl.). https://www.legislation.gov.au/Details/F2020C00596

Collier, B. A., Ditchkoff, S. S., Raglin, J. B., & Smith, J. M. (2007). Detection probability and sources of variation in white-tailed deer spotlight surveys. *The Journal of Wildlife Management*, *71*(1), 277-281. https://doi.org/10.2193/2005-728

Comaniciu, D., & Meer, P. (2002). Mean shift: A robust approach toward feature space analysis. *IEEE Transactions on Pattern Analysis and Machine Intelligence*, *24*(5), 603-619. https://doi.org/10.1109/34.1000236

Commonwealth of Australia Department of Environment and Energy. (2019a). *Flying-foxes and national environment law*. http://www.environment.gov.au/biodiversity/threatened/species/flying-fox-law

Commonwealth of Australia Department of Environment and Energy. (2019b). *National flying-fox monitoring viewer*. http://www.environment.gov.au/webgis-framework/apps/ffc-wide/ffc-wide.jsf

Commonwealth Scientific and Industrial Research Organisation. (2019). *The national flying-fox monitoring program - report on the May 2019 survey*. http://www.environment.gov.au/system/files/pages/391f5fed-e287-4dd3-85ac-640037926ef5/files/flying-fox-may2019-count-report.pdf

Congalton, R. G. (1988). Using spatial autocorrelation analysis to explore the errors in maps generated from remotely sensed data. *Photogrammetric Engineering and Remote Sensing*, *54*(5), 587-592.

Corcoran, E., Denman, S., Hanger, J., Wilson, B., & Hamilton, G. (2019). Automated detection of koalas using low-level aerial surveillance and machine learning. *Scientific Reports*, *9*(1), 3208. https://doi.org/10.1038/s41598-019-39917-5

Cortes, C., & Vapnik, V. (1995). Support-vector networks. *Machine Learning*, *20*(3), 273-297. https://doi.org/10.1007/BF00994018

Courts, S. E. (1998). Dietary strategies of Old World fruit bats (Megachiroptera, Pteropodidae): how do they obtain sufficient protein? *Mammal Review*, *28*(4), 185-194. https://doi.org/10.1046/j.1365-2907.1998.00033.x

Cracknell, A. P. (2007). *Introduction to remote sensing*. CRC press.

Croon, G. W., McCullough, D. R., Olson Jr, C. E., & Queal, L. M. (1968). Infrared scanning techniques for big game censusing. *The Journal of Wildlife Management*, *32*(4), 751-759. https://doi.org/10.2307/3799549

Currey, K., Kendal, D., van der Ree, R., & Lentini, P. E. (2018). Land manager perspectives on conflict mitigation strategies for urban flying-fox camps. *Diversity*, *10*(2), 39. https://doi.org/10.3390/d10020039

de Arruda, M. D. S., Spadon, G., Rodrigues, J. F., Gonçalves, W. N., & Machado, B. B. (2018). Recognition of endangered Pantanal animal species using deep learning methods. 2018 International Joint Conference on Neural Networks (IJCNN), Rio, Brazil.

DeGroote, L. W., & Rodewald, P. G. (2008). An improved method for quantifying hematozoa by digital microscopy. *Journal of Wildlife Diseases*, *44*(2), 446-450. https://doi.org/10.7589/0090-3558-44.2.446

Dell, A. I., Bender, J. A., Branson, K., Couzin, I. D., de Polavieja, G. G., Noldus, L. P. J. J., Pérez-Escudero, A., Perona, P., Straw, A. D., Wikelski, M., & Brose, U. (2014).

Automated image-based tracking and its application in ecology. *Trends in Ecology & Evolution*, *29*(7), 417-428. https://doi.org/10.1016/j.tree.2014.05.004

Department of Environment, Land, Water and Planning. (2019). *Victoria's flying fox colonies*. https://www.wildlife.vic.gov.au/our-wildlife/flying-foxes/victorias-flying-fox-colonies

Díaz-Delgado, R., Mañez, M., Martínez, A., Canal, D., Ferrer, M., & Aragonés, D. (2017). Using UAVs to map aquatic bird colonies. In R. Díaz-Delgado, R. Lucas, & C. Hurford (Eds.), *The roles of remote sensing in nature conservation* (pp. 277-291). Springer.

Ditmer, M. A., Vincent, J. B., Werden, L. K., Tanner, J. C., Laske, T. G., Iaizzo, P. A., Garshelis, D. L., & Fieberg, J. R. (2015). Bears show a physiological but limited behavioral response to unmanned aerial vehicles. *Current Biology*, *25*(17), 2278-2283. https://doi.org/10.1016/j.cub.2015.07.024

Dobbertin, M., & Brang, P. (2001). Crown defoliation improves tree mortality models. *Forest Ecology and Management*, *141*(3), 271-284. https://doi.org/10.1016/S0378-1127(00)00335-2

Downey, P. O., Scanlon, T. J., & Hosking, J. R. (2010). Prioritizing weed species based on their threat and ability to impact on biodiversity: a case study from New South Wales. *Plant Protection Quarterly*, *25*(3), 111-126.

Dronova, I., Gong, P., Clinton, N. E., Wang, L., Fu, W., Qi, S., & Liu, Y. (2012). Landscape analysis of wetland plant functional types: The effects of image segmentation scale, vegetation classes and classification methods. *Remote Sensing of Environment*, *127*, 357-369. https://doi.org/10.1016/j.rse.2012.09.018

Drury, J. A., Nik, H., van Oppenraaij, R. H. F., Tang, A.-W., Turner, M. A., & Quenby, S. (2011). Endometrial cell counts in recurrent miscarriage: a comparison of counting

methods. *Histopathology*, *59*(6), 1156-1162. https://doi.org/10.1111/j.1365-2559.2011.04046.x

Duffy, J. P., Cunliffe, A. M., DeBell, L., Sandbrook, C., Wich, S. A., Shutler, J. D., Myers-Smith, I. H., Varela, M. R., & Anderson, K. (2018). Location, location, location: considerations when using lightweight drones in challenging environments. *Remote Sensing in Ecology and Conservation*, *4*(1), 7-19. https://doi.org/10.1002/rse2.58

Dunn, W. C., Donnelly, J. P., & Krausmann, W. J. (2002). Using thermal infrared sensing to count elk in the southwestern United States. *Wildlife Society Bulletin*, *30*(3), 963-967.

Dunstan, A., Robertson, K., Fitzpatrick, R., Pickford, J., & Meager, J. (2020). Use of unmanned aerial vehicles (UAVs) for mark-resight nesting population estimation of adult female green sea turtles at Raine Island. *PLoS ONE*, *15*(6), e0228524. https://doi.org/10.1371/journal.pone.0228524

Eberhardt, L. L. (1978). Transect methods for population studies. *The Journal of Wildlife Management*, *42*(1), 1-31. https://doi.org/10.2307/3800685

Eberhardt, L. L., & Thomas, J. M. (1991). Designing environmental field studies. *Ecological Monographs*, *61*(1), 53-73. https://doi.org/10.2307/1942999

Eby, P. (1991). Seasonal movements of grey-headed flying-foxes, *Pteropus poliocephalus* (Chiroptera: Pteropodidae), from two maternity camps in northern New South Wales. *Wildlife Research*, *18*(5), 547-559. https://doi.org/10.1071/WR9910547

Eby, P., Richards, G., Collins, L., & Parry-Jones, K. A. (1999). The distribution, abundance and vulnerability to population reduction of a nomadic nectarivore, the grey-headed flying-fox *Pteropus poliocephalus* in New South Wales, during a period of resource concentration. *Australian Zoologist*, *31*(1), 240-253. https://doi.org/10.7882/az.1999.024

Edson, D., Field, H., McMichael, L., Jordan, D., Kung, N., Mayer, D., & Smith, C. (2015). Flying-fox roost disturbance and Hendra virus spillover risk. *PLoS ONE*, *10*(5), e0125881. https://doi.org/10.1371/journal.pone.0125881

Eisenbeiss, H., & Sauerbier, M. (2011). Investigation of uav systems and flight modes for photogrammetric applications. *The Photogrammetric Record*, *26*(136), 400-421. https://doi.org/10.1111/j.1477-9730.2011.00657.x

Elphick, C. S. (2008). How you count counts: the importance of methods research in applied ecology. *Journal of Applied Ecology*, *45*(5), 1313-1320. https://doi.org/10.1111/j.1365-2664.2008.01545.x

Environmental Systems Research Institute. (2020). *ArcGIS Pro release 2.5.0*.

Erwin, R. M. (1982). Observer variability in estimating numbers: an experiment. *Journal of Field Ornithology*, *53*(2), 159-167.

Falk, T., Mai, D., Bensch, R., Çiçek, Ö., Abdulkadir, A., Marrakchi, Y., Böhm, A., Deubner, J., Jäckel, Z., & Seiwald, K. (2019). U-Net: deep learning for cell counting, detection, and morphometry. *Nature Methods*, *16*(1), 67-70. https://doi.org/10.1038/s41592-018-0261-2

Florens, F. B. V., Baider, C., Marday, V., Martin, G. M. N., Zmanay, Z., Oleksy, R., Krivek, G., Vincenot, C. E., Strasberg, D., & Kingston, T. (2017). Disproportionately large ecological role of a recently mass-culled flying fox in native forests of an oceanic island. *Journal for Nature Conservation*, *40*, 85-93. https://doi.org/10.1016/j.jnc.2017.10.002

Fonstad, M. A., Dietrich, J. T., Courville, B. C., Jensen, J. L., & Carbonneau, P. E. (2013). Topographic structure from motion: a new development in photogrammetric measurement. *Earth Surface Processes and Landforms*, *38*(4), 421-430. https://doi.org/10.1002/esp.3366

Forsyth, D. M., Scroggie, M. P., & McDonald-Madden, E. (2006). Accuracy and precision of grey-headed flying-fox (*Pteropus poliocephalus*) flyout counts. *Wildlife Research*, *33*(1), 57-65. https://doi.org/10.1071/WR05029

Fox, J., & Weisberg, S. (2018). *An R companion to applied regression* (3rd ed.). Sage Publications.

Fox, S., Luly, J., Mitchell, C., Maclean, J., & Westcott, D. A. (2008). Demographic indications of decline in the spectacled flying fox (*Pteropus conspicillatus*) on the Atherton Tablelands of northern Queensland. *Wildlife Research*, *35*(5), 417-424. https://doi.org/10.1071/WR07127

Francis, R. J., Lyons, M. B., Kingsford, R. T., & Brandis, K. J. (2020). Counting mixed breeding aggregations of animal species using drones: lessons from waterbirds on semi-automation. *Remote Sensing*, *12*(7), 1185. https://doi.org/10.3390/rs12071185

Frederick, P. C., Becky, H., Julie, H. A., & Martin, R. (2003). Accuracy and variation in estimates of large numbers of birds by individual observers using an aerial survey simulator. *Journal of Field Ornithology*, *74*(3), 281-287. https://doi.org/10.1648/0273-8570-74.3.281

Fretwell, P. T., LaRue, M. A., Morin, P., Kooyman, G. L., Wienecke, B., Ratcliffe, N., Fox, A. J., Fleming, A. H., Porter, C., & Trathan, P. N. (2012). An emperor penguin population estimate: the first global, synoptic survey of a species from space. *PLoS ONE*, *7*(4), e33751. https://doi.org/10.1371/journal.pone.0033751

Fritz, L. (2012). *By land, sea, and air: a collaborative steller sea lion research cruise in the Aleutian Islands*. NOAA Fisheries Alaska Fisheries Science Center quarterly report, January-March 2012. http://www.afsc.noaa.gov/Quarterly/jfm2012/divrptsNMML1.htm

Fujita, M. S., & Tuttle, M. D. (1991). Flying foxes (Chiroptera: Pteropodidae): threatened animals of key ecological and economic importance. *Conservation Biology*, *5*(4), 455-463. https://doi.org/10.1111/j.1523-1739.1991.tb00352.x

Garner, D. L., Underwood, H. B., & Porter, W. F. (1995). Use of modern infrared thermography for wildlife population surveys. *Environmental Management*, *19*(2), 233-238. https://doi.org/10.1007/BF02471993

Garnett, S., Whybird, O., & Spencer, H. (1999). The conservation status of the spectacled flying fox *Pteropus conspicillatus* in Australia. *Australian Zoologist*, *31*(1), 38-54. https://doi.org/10.7882/AZ.1999.006

Geoscience Australia. (2001). *Geoscience Australia GEODATA TOPO series - 1:1 million to 1:10 million scale. bioregional assessment source dataset.* Retrieved 23 April 2020 from http://data.bioregionalassessments.gov.au/dataset/310c5d07-5a56-4cf7-a5c8-63bdb001cd1a

Gibbs, J. P. (2000). Monitoring populations. In L. Boitani & T. K. Fuller (Eds.), *Research techniques in animal ecology: controversies and consequences* (pp. 213-252). Columbia University.

Goldsmith, B. (1991). *Monitoring for conservation and ecology*. Chapman & Hall.

Gonzalez, L., Montes, G., Puig, E., Johnson, S., Mengersen, K., & Gaston, K. (2016). Unmanned aerial vehicles (UAVs) and artificial intelligence revolutionizing wildlife monitoring and conservation. *Sensors*, *16*(1), 97. https://doi.org/10.3390/s16010097

Gooday, O. J., Key, N., Goldstien, S., & Zawar-Reza, P. (2018). An assessment of thermal-image acquisition with an unmanned aerial vehicle (UAV) for direct counts of coastal

marine mammals ashore. *Journal of Unmanned Vehicle Systems*, *6*(2), 100-108. https://doi.org/10.1139/juvs-2016-0029

Graves, H. B., Bellis, E. D., & Knuth, W. M. (1972). Censusing white-tailed deer by airborne thermal infrared imagery. *The Journal of Wildlife Management*, *36*(3), 875-884. https://doi.org/10.2307/3799443

Grémillet, D., Puech, W., Garçon, V., Boulinier, T., & Le Maho, Y. (2012). Robots in ecology: welcome to the machine. *Open Journal of Ecology*, *2*(2), 49-57. https://doi.org/10.4236/oje.2012.22006

Grenzdörffer, G. J., Engel, A., & Teichert, B. (2008). The photogrammetric potential of low-cost UAVs in forestry and agriculture. *The International Archives of the Photogrammetry, Remote Sensing and Spatial Information Sciences*, *31*, 1207-1214.

Grishagin, I. V. (2015). Automatic cell counting with ImageJ. *Analytical Biochemistry*, *473*, 63-65. https://doi.org/10.1016/j.ab.2014.12.007

Groom, G., Stjernholm, M., Nielsen, R. D., Fleetwood, A., & Petersen, I. K. (2013). Remote sensing image data and automated analysis to describe marine bird distributions and abundances. *Ecological Informatics*, *14*, 2-8. https://doi.org/10.1016/j.ecoinf.2012.12.001

Guilherme, P. D. B., Borzone, C. A., Padial, A. A., & Harris, L. R. (2018). A semi-automated approach to classify and map ecological zones across the dune-beach interface. *Estuarine, Coastal and Shelf Science*, *208*, 61-69. https://doi.org/10.1016/j.ecss.2018.04.030

Guisan, A., & Thuiller, W. (2005). Predicting species distribution: offering more than simple habitat models. *Ecology Letters*, *8*(9), 993-1009. https://doi.org/10.1111/j.1461-0248.2005.00792.x

Guschanski, K., Vigilant, L., McNeilage, A., Gray, M., Kagoda, E., & Robbins, M. M. (2009). Counting elusive animals: comparing field and genetic census of the entire mountain gorilla population of Bwindi Impenetrable National Park, Uganda. *Biological Conservation*, *142*(2), 290-300. https://doi.org/10.1016/j.biocon.2008.10.024

Hall, L. S., & Richards, G. (2000). *Flying foxes: fruit and blossom bats of Australia*. UNSW Press.

Halpin, K., Young, P. L., Field, H., & Mackenzie, J. S. (1999). Newly discovered viruses of flying foxes. *Veterinary Microbiology*, *68*(1), 83-87. https://doi.org/10.1016/S0378-1135(99)00063-2

Hamilton, G., Corcoran, E., Denman, S., Hennekam, M. E., & Koh, L. P. (2020). When you can't see the koalas for the trees: using drones and machine learning in complex environments. *Biological Conservation*, *247*, 108598. https://doi.org/10.1016/j.biocon.2020.108598

Hanger, J., de Villiers, D., Forbes, N., Nottidge, B., Beyer, H., Loader, J., & Timms, P. (2017). Moreton Bay rail koala management program: final technical report for Queensland Department of Transport and Main Roads. *Endeavour Veterinary Ecology, Toorbul*.

Harris, J. W., & Stocker, H. (1998). *Maximum likelihood method*. Springer-Verlag.

Harris, M. P., & Lloyd, C. S. (1977). Variations in counts of seabirds from photographs. *British Birds*, *70*(5), 200-205.

Hassell, J. M., Begon, M., Ward, M. J., & Fèvre, E. M. (2017). Urbanization and disease emergence: dynamics at the wildlife–livestock–human interface. *Trends in Ecology & Evolution*, *32*(1), 55-67. https://doi.org/10.1016/j.tree.2016.09.012

Havens, K. J., & Sharp, E. (1996). The use of thermal imagery in the aerial survey of panthers (and other animals) in the Florida Panther National Wildlife Refuge and the Big Cypress

National Preserve. *Final report to the U.S. Fish and Wildlife Service*. https://doi.org/10.25773/3sk2-7w97

Hill, J. E., & Smith, J. D. (1984). *Bats: A natural history*. University of Texas Press.

Hodgson, J. C., & Koh, L. P. (2016). Best practice for minimising unmanned aerial vehicle disturbance to wildlife in biological field research. *Current Biology*, *26*(10), R404-R405. https://doi.org/10.1016/j.cub.2016.04.001

Hodgson, J. C., Mott, R., Baylis, S. M., Pham, T. T., Wotherspoon, S., Kilpatrick, A. D., Raja Segaran, R., Reid, I., Terauds, A., & Koh, L. P. (2018). Drones count wildlife more accurately and precisely than humans. *Methods in Ecology and Evolution*, *9*(5), 1160-1167. https://doi.org/10.1111/2041-210x.12974

Höfener, H., Homeyer, A., Weiss, N., Molin, J., Lundström, C. F., & Hahn, H. K. (2018). Deep learning nuclei detection: a simple approach can deliver state-of-the-art results. *Computerized Medical Imaging and Graphics*, *70*, 43-52. https://doi.org/10.1016/j.compmedimag.2018.08.010

Horning, N., Robinson, J. A., Sterling, E. J., Turner, W., & Spector, S. (2010). *Remote sensing for ecology and conservation: a handbook of techniques*. Oxford University Press.

Huang, H., Lan, Y., Yang, A., Zhang, Y., Wen, S., & Deng, J. (2020). Deep learning versus object-based Image Analysis (OBIA) in weed mapping of UAV imagery. *International Journal of Remote Sensing*, *41*(9), 3446-3479. https://doi.org/10.1080/01431161.2019.1706112

Hung, I., Unger, D., Kulhavy, D., & Zhang, Y. (2019). Positional precision analysis of orthomosaics derived from drone captured aerial imagery. *Drones*, *3*(2), 46. https://doi.org/10.3390/drones3020046

International Union for Conservation of Nature and Natural Resources. (2020). *The IUCN Red List of Threatened Species*. http://www.iucnredlist.org/

Jiménez López, J., & Mulero-Pázmány, M. (2019). Drones for conservation in protected areas: present and future. *Drones*, *3*(1), 10. https://doi.org/10.3390/drones3010010

Jungwirth, A., Josi, D., Walker, J., & Taborsky, M. (2015). Benefits of coloniality: communal defence saves anti-predator effort in cooperative breeders. *Functional Ecology*, *29*(9), 1218-1224. https://doi.org/10.1111/1365-2435.12430

Kays, R., Sheppard, J., Mclean, K., Welch, C., Paunescu, C., Wang, V., Kravit, G., & Crofoot, M. (2019). Hot monkey, cold reality: surveying rainforest canopy mammals using drone-mounted thermal infrared sensors. *International Journal of Remote Sensing*, *40*(2), 407-419. https://doi.org/10.1080/01431161.2018.1523580

Keeping, D., & Pelletier, R. (2014). Animal density and track counts: understanding the nature of observations based on animal movements. *PLoS ONE*, *9*(5), e96598. https://doi.org/10.1371/journal.pone.0096598

Kelly, M., Blanchard, S. D., Kersten, E., & Koy, K. (2011). Terrestrial remotely sensed imagery in support of public health: New avenues of research using object-based image analysis. *Remote Sensing*, *3*(11), 2321-2345. https://doi.org/10.3390/rs3112321

Kotsiantis, S. B., Zaharakis, I., & Pintelas, P. (2007). Supervised machine learning: A review of classification techniques. In I. G. Maglogiannis (Ed.), *Emerging artificial intelligence applications in computer engineering* (Vol. 160, pp. 3-24). IOS Press.

Kung, N. Y., Field, H. E., McLaughlin, A., Edson, D., & Taylor, M. (2015). Flying-foxes in the Australian urban environment—community attitudes and opinions. *One Health*, *1*, 24-30. https://doi.org/10.1016/j.onehlt.2015.07.002

Laliberte, A. S., & Ripple, W. J. (2003). Automated wildlife counts from remotely sensed imagery. *Wildlife Society Bulletin*, *31*(2), 362-371.

LaRue, M. A., Rotella, J. J., Garrott, R. A., Siniff, D. B., Ainley, D. G., Stauffer, G. E., Porter, C. C., & Morin, P. J. (2011). Satellite imagery can be used to detect variation in abundance of Weddell seals (*Leptonychotes weddellii*) in Erebus Bay, Antarctica. *Polar Biology*, *34*(11), 1727. https://doi.org/10.1007/s00300-011-1023-0

Lawrence, I., & Lin, K. (1989). A concordance correlation coefficient to evaluate reproducibility. *Biometrics*, *45*(1), 255-268. https://doi.org/10.2307/2532051

LeCun, Y., Bengio, Y., & Hinton, G. (2015). Deep learning. *Nature*, *521*(7553), 436-444. https://doi.org/10.1038/nature14539

Lentini, P. E., & Welbergen, J. A. (2019). Managing tensions around urban flying-fox roosts. *Austral Ecology*, *44*(2), 380-385. https://doi.org/10.1111/aec.12738

Lewis, J. C. (1970). Wildlife census methods: a resume. *Journal of Wildlife Diseases*, *6*(4), 356-364.

Lewis, S. E. (1995). Roost fidelity of bats: a review. *Journal of Mammalogy*, *76*(2), 481-496. https://doi.org/10.2307/1382357

Lhoest, S., Linchant, J., Quevauvillers, S., Vermeulen, C., & Lejeune, P. (2015). How many hippos (HOMHIP): algorithm for automatic counts of animals with infra-red thermal imagery from UAV. *The International Archives of the Photogrammetry, Remote Sensing and Spatial Information Sciences*, *XL-3/W3*, 355-362. https://doi.org/10.5194/isprsarchives-XL-3-W3-355-2015

Linchant, J., Lisein, J., Semeki, J., Lejeune, P., & Vermeulen, C. (2015). Are unmanned aircraft systems (UASs) the future of wildlife monitoring? A review of accomplishments and challenges. *Mammal Review*, *45*(4), 239-252. https://doi.org/10.1111/mam.12046

Linkert, M., Rueden, C. T., Allan, C., Burel, J.-M., Moore, W., Patterson, A., Loranger, B., Moore, J., Neves, C., MacDonald, D., Tarkowska, A., Sticco, C., Hill, E., Rossner, M., Eliceiri, K. W., & Swedlow, J. R. (2010). Metadata matters: access to image data in the real world. *The Journal of Cell Biology*, *189*(5), 777-782. https://doi.org/10.1083/jcb.201004104

LLC Agisoft. (2019). Agisoft Metashape user manual: professional edition, version 1.5. *St. Petersburg*.

Lowman, M., & Heatwole, H. (1992). Spatial and temporal variability in defoliation of Australian eucalypts. *Ecology*, *73*(1), 129-142. https://doi.org/10.2307/1938726

Lumsden, L. F., & Jemison, M. L. (2015). *National recovery plan for the southern bent-wing bat Miniopterus schreibersii bassanii*. Heidelberg, Australia: Department of Environment, Land, Water and Planning.

Ma, Q., Su, Y., & Guo, Q. (2017). Comparison of canopy cover estimations from airborne LiDAR, aerial imagery, and satellite imagery. *IEEE Journal of Selected Topics in Applied Earth Observations and Remote Sensing*, *10*(9), 4225-4236. https://doi.org/10.1109/JSTARS.2017.2711482

Manning, T., Edge, W. D., & Wolff, J. O. (1995). Evaluating population-size estimators: an empirical approach. *Journal of Mammalogy*, *76*(4), 1149-1158. https://doi.org/10.2307/1382606

Mao, F. (2019). *How one heatwave killed 'a third' of a bat species in Australia*. BBC News. https://www.bbc.com/news/world-australia-46859000

Margalida, A., Oro, D., Cortés-Avizanda, A., Heredia, R., & Donázar, J. A. (2011). Misleading population estimates: biases and consistency of visual surveys and matrix modelling in the endangered bearded vulture. *PLoS ONE, 6*(10), e26784. https://doi.org/10.1371/journal.pone.0026784

Marsh, D. M., & Trenham, P. C. (2008). Current trends in plant and animal population monitoring. *Conservation Biology*, *22*(3), 647-655. https://doi.org/10.1111/j.1523-1739.2008.00927.x

Martin, L., Towers, P. A., McGuckin, M. A., Little, L., Luckhoff, H., & Blackshaw, A. W. (1987). Reproductive biology of flying-foxes (Chiroptera: Pteropodidae). *Australian Mammalogy*, *10*(2), 115-118.

McEvoy, J. F., Hall, G. P., & McDonald, P. G. (2016). Evaluation of unmanned aerial vehicle shape, flight path and camera type for waterfowl surveys: disturbance effects and species recognition. *PeerJ, 4*, e1831. https://doi.org/10.7717/peerj.1831

McIntosh, R., Burlton, F. W. E., & McReddie, G. (1995). Monitoring the density of a roe deer *Capreolus capreolus* population subjected to heavy hunting pressure. *Forest Ecology and Management, 79*(1), 99-106. https://doi.org/10.1016/0378-1127(95)03623-7

McKelvey, K. S., Aubry, K. B., & Schwartz, M. K. (2008). Using anecdotal occurrence data for rare or elusive species: the illusion of reality and a call for evidentiary standards. *BioScience, 58*(6), 549-555. https://doi.org/10.1641/B580611

Meade, J., van der Ree, R., Stepanian, P. M., Westcott, D. A., & Welbergen, J. A. (2019). Using weather radar to monitor the number, timing and directions of flying-foxes emerging

from their roosts. *Scientific Reports*, *9*(1), 10222. https://doi.org/10.1038/s41598-019-46549-2

Mo, M., Roache, M., Williams, R., Drinnan, I. N., & Noël, B. (2020). From cleared buffers to camp dispersal: mitigating impacts of the Kareela flying-fox camp on adjacent residents and schools. *Australian Zoologist*, *25*(4), 387-397. https://doi.org/10.7882/AZ.2020.002

Mohd-Azlan, J., Zubaid, A., & Kunz, T. H. (2001). Distribution, relative abundance, and conservation status of the large flying fox, *Pteropus vampyrus*, in peninsular Malaysia: a preliminary assessment. *Acta Chiropterologica*, *3*(2), 149-162.

Moorthy, S. M. K., Bao, Y., Calders, K., Schnitzer, S. A., & Verbeeck, H. (2019). Semi-automatic extraction of liana stems from terrestrial LiDAR point clouds of tropical rainforests. *ISPRS Journal of Photogrammetry and Remote Sensing*, *154*, 114-126. https://doi.org/10.1016/j.isprsjprs.2019.05.011

Mulero-Pázmány, M., Jenni-Eiermann, S., Strebel, N., Sattler, T., Negro, J. J., & Tablado, Z. (2017). Unmanned aircraft systems as a new source of disturbance for wildlife: A systematic review. *PLoS ONE*, *12*(6), e0178448. https://doi.org/10.1371/journal.pone.0178448

Naugle, D. E., Jenks, J. A., & Kernohan, B. J. (1996). Use of thermal infrared sensing to estimate density of white-tailed deer. *Wildlife Society Bulletin*, *24*(1), 37-43.

Neff, D. J. (1968). The pellet-group count technique for big game trend, census, and distribution: a review. *The Journal of Wildlife Management*, *32*(3), 597-614. https://doi.org/10.2307/3798941

Nichols, J. D. (1992). Capture-recapture models. *BioScience*, *42*(2), 94-102. https://doi.org/10.2307/1311650

O'Shea, T. J., & Bogan, M. A. (2003). *Monitoring trends in bat populations of the United States and territories: problems and prospects*. U.S. Geological Survey, Biological Resources Discipline. https://pubs.usgs.gov/itr/2003/0003/report.pdf

Old, J. M., Lin, S. H., & Franklin, M. J. M. (2019). Mapping out bare-nosed wombat (*Vombatus ursinus*) burrows with the use of a drone. *BMC Ecology*, *19*(1), 39. https://doi.org/10.1186/s12898-019-0257-5

Otto, M. C., & Pollock, K. H. (1990). Size bias in line transect sampling: a field test. *Biometrics*, *46*(1), 239-245. https://doi.org/10.2307/2531648

Pal, M. (2005). Random forest classifier for remote sensing classification. *International Journal of Remote Sensing*, *26*(1), 217-222. https://doi.org/10.1080/01431160412331269698

Palmer, C., & Woinarski, J. (1999). Seasonal roosts and foraging movements of the black flying fox (*Pteropus alecto*) in the Northern Territory: resource tracking in a landscape mosaic. *Wildlife Research*, *26*(6), 823-838. https://doi.org/10.1071/WR97106

Papadopulos, F., Spinelli, M., Valente, S., Foroni, L., Orrico, C., Alviano, F., & Pasquinelli, G. (2007). Common tasks in microscopic and ultrastructural image analysis using ImageJ. *Ultrastructural Pathology*, *31*(6), 401-407. https://doi.org/10.1080/01913120701719189

Parry-Jones, K. A., & Augee, M. L. (1992). Movements of grey-headed flying foxes (*Pteropus poliocephalus*) to and from colony site on the central coast of New South Wales. *Wildlife Research*, *19*(3), 331-339. https://doi.org/10.1071/WR9920331

Parry-Jones, K. A., & Augee, M. L. (2001). Factors affecting the occupation of a colony site in Sydney, New South Wales by the grey-headed flying-fox *Pteropus poliocephalus* (Pteropodidae). *Austral Ecology*, *26*(1), 47-55. https://doi.org/10.1111/j.1442-9993.2001.01072.pp.x

Pennay, M., & Mills, D. (2018). *Measuring bat activity in the landscape and at 100m altitude; a pilot study using ground and balloon mounted acoustic detectors to determine windfarm development risk.* 18th Australasian Bat Society conference, Sydney, Australia.

Pennekamp, F., & Schtickzelle, N. (2013). Implementing image analysis in laboratory-based experimental systems for ecology and evolution: a hands-on guide. *Methods in Ecology and Evolution*, *4*(5), 483-492. https://doi.org/10.1111/2041-210X.12036

Phinn, S. R., Roelfsema, C. M., & Mumby, P. J. (2012). Multi-scale, object-based image analysis for mapping geomorphic and ecological zones on coral reefs. *International Journal of Remote Sensing*, *33*(12), 3768-3797. https://doi.org/10.1080/01431161.2011.633122

Pimm, S. L., Alibhai, S., Bergl, R., Dehgan, A., Giri, C., Jewell, Z., Joppa, L., Kays, R., & Loarie, S. (2015). Emerging technologies to conserve biodiversity. *Trends in Ecology & Evolution*, *30*(11), 685-696. https://doi.org/10.1016/j.tree.2015.08.008

Pinheiro, J., Bates, D., DebRoy, S., Sarkar, D., Heisterkamp, S., Van Willigen, B., & Maintainer, R. (2016). *Package 'nlme'*. https://cran.r-project.org/web/packages/nlme/nlme.pdf

Pix4D, S. (2017). Pix4Dmapper 4.1 user manual. *Pix4D SA: Lausanne, Switzerland*.

Plowright, R. K., Foley, P., Field, H. E., Dobson, A. P., Foley, J. E., Eby, P., & Daszak, P. (2011). Urban habituation, ecological connectivity and epidemic dampening: the emergence of Hendra virus from flying foxes (*Pteropus* spp.). *Proceedings of the Royal Society B: Biological Sciences*, *278*(1725), 3703-3712. https://doi.org/10.1098/rspb.2011.0522

R Core Team. (2018). *R: A language and environment for statistical computing. R Foundation for Statistical Computing, Vienna, Austria*. https://www.R-project.org/

Ratcliffe, F. N. (1931). *The flying fox (Pteropus) in Australia*. Melbourne, Australia: Council for Scientific and Industrial Research. http://nla.gov.au/nla.obj-52860992

Ratcliffe, N., Guihen, D., Robst, J., Crofts, S., Stanworth, A., & Enderlein, P. (2015). A protocol for the aerial survey of penguin colonies using UAVs. *Journal of Unmanned Vehicle Systems*, *3*(3), 95-101. https://doi.org/10.1139/juvs-2015-0006

Reby, D., Hewison, M. A. J., Cargnelutti, B., Angibault, J.-M., & Vincent, J.-P. (1998). Use of vocalizations to estimate population size of roe deer. *The Journal of Wildlife Management*, *62*(4), 1342-1348. https://doi.org/10.2307/3802000

Reddiex, B., Forsyth, D. M., McDonald-Madden, E., Einoder, L. D., Griffioen, P. A., Chick, R. R., & Robley, A. J. (2006). Control of pest mammals for biodiversity protection in Australia. I. Patterns of control and monitoring. *Wildlife Research*, *33*(8), 691-709. https://doi.org/10.1071/WR05102

Reddy, S., & Dávalos, L. M. (2003). Geographical sampling bias and its implications for conservation priorities in Africa. *Journal of Biogeography*, *30*(11), 1719-1727. https://doi.org/10.1046/j.1365-2699.2003.00946.x

Ribeiro-Gomes, K., Hernández-López, D., Ortega, J., Ballesteros, R., Poblete, T., & Moreno, M. (2017). Uncooled thermal camera calibration and optimization of the photogrammetry process for UAV applications in agriculture. *Sensors*, *17*(10), 2173. https://doi.org/10.3390/s17102173

Ridge, J. T., Gray, P. C., Windle, A. E., & Johnston, D. W. (2019). Deep learning for coastal resource conservation: automating detection of shellfish reefs. *Remote Sensing in Ecology and Conservation*. Advance online publication. https://doi.org/10.1002/rse2.134

Rieucau, G., Kiszka, J. J., Castillo, J. C., Mourier, J., Boswell, K. M., & Heithaus, M. R. (2018). Using unmanned aerial vehicle (UAV) surveys and image analysis in the study of large surface-associated marine species: a case study on reef sharks *Carcharhinus melanopterus* shoaling behaviour. *Journal of Fish Biology*, *93*(1), 119-127. https://doi.org/10.1111/jfb.13645

Roberts, B. J., Catterall, C. P., Eby, P., & Kanowski, J. (2012). Long-distance and frequent movements of the flying-fox *Pteropus poliocephalus*: implications for management. *PLoS ONE, 7*(8), e42532. https://doi.org/10.1371/journal.pone.0042532

Schindelin, J., Arganda-Carreras, I., Frise, E., Kaynig, V., Longair, M., Pietzsch, T., Preibisch, S., Rueden, C., Saalfeld, S., & Schmid, B. (2012). Fiji: an open-source platform for biological-image analysis. *Nature Methods*, *9*(7), 676-682. https://doi.org/10.1038/nmeth.2019

Seber, G. A. F. (1986). A review of estimating animal abundance. *Biometrics*, *42*(2), 267-292. https://doi.org/10.2307/2531049

Seymour, A. C., Dale, J., Hammill, M., Halpin, P. N., & Johnston, D. W. (2017). Automated detection and enumeration of marine wildlife using unmanned aircraft systems (UAS) and thermal imagery. *Scientific Reports*, *7*, 45127. https://doi.org/10.1038/srep45127

Shilton, L. A., Latch, P. J., Mckeown, A., Pert, P., & Westcott, D. A. (2008). Landscape-scale redistribution of a highly mobile threatened species, *Pteropus conspicillatus* (Chiroptera, Pteropodidae), in response to tropical cyclone Larry. *Austral Ecology*, *33*(4), 549-561. https://doi.org/10.1111/j.1442-9993.2008.01910.x

Short, J., & Bayliss, P. (1985). Bias in aerial survey estimates of kangaroo density. *Journal of Applied Ecology*, *22*(2), 415-422. https://doi.org/10.2307/2403174

Signorell, A. (2016). *DescTools: tools for descriptive statistics.* https://cran.r-project.org/web/packages/DescTools/index.html

Silveira, L., Jácomo, A. T. A., & Diniz-Filho, J. A. F. (2003). Camera trap, line transect census and track surveys: a comparative evaluation. *Biological Conservation*, *114*(3), 351-355. https://doi.org/10.1016/S0006-3207(03)00063-6

Simmons, N. B. (2005). order Chiroptera. In D. E. Wilson & D. M. Reeder (Eds.), *Mammal species of the world: a taxonomic and geographic reference* (Vol. 3, pp. 312-529). The Johns Hopkins University Press.

Smith, M. W., Carrivick, J. L., & Quincey, D. J. (2015). Structure from motion photogrammetry in physical geography. *Progress in Physical Geography: Earth and Environment*, *40*(2), 247-275. https://doi.org/10.1177/0309133315615805

Snoyman, S., & Brown, C. (2011). Microclimate preferences of the grey-headed flying fox (*Pteropus poliocephalus*) in the Sydney region. *Australian Journal of Zoology*, *58*(6), 376-383. https://doi.org/10.1071/ZO10062

Spaan, D., Burke, C., McAree, O., Aureli, F., Rangel-Rivera, C. E., Hutschenreiter, A., Longmore, S. N., McWhirter, P. R., & Wich, S. A. (2019). Thermal infrared imaging from drones offers a major advance for spider monkey surveys. *Drones*, *3*(2), 34. https://doi.org/10.3390/drones3020034

Stapleton, S., LaRue, M., Lecomte, N., Atkinson, S., Garshelis, D., Porter, C., & Atwood, T. (2014). Polar bears from space: assessing satellite imagery as a tool to track Arctic wildlife. *PLoS ONE*, *9*(7), e101513. https://doi.org/10.1371/journal.pone.0101513

Stinson, D. W., Glass, P. O., & Taisacan, E. M. (1992). Declines and trade in fruit bats on Saipan, Tinian, Aguijan, and Rota. Pacific flying foxes – Proceedings of an international conservation conference, Washington DC, United States.

Sutherland, W. J. (2006). Predicting the ecological consequences of environmental change: a review of the methods. *Journal of Applied Ecology*, *43*(4), 599-616.

Tabak, M. A., Norouzzadeh, M. S., Wolfson, D. W., Sweeney, S. J., VerCauteren, K. C., Snow, N. P., Halseth, J. M., Di Salvo, P. A., Lewis, J. S., & White, M. D. (2019). Machine learning to classify animal species in camera trap images: applications in ecology. *Methods in Ecology and Evolution*, *10*(4), 585-590. https://doi.org/10.1111/2041-210X.13120

Tait, J., Perotto-Baldivieso, H. L., McKeown, A., & Westcott, D. A. (2014). Are flying-foxes coming to town? Urbanisation of the spectacled flying-fox (*Pteropus conspicillatus*) in Australia. *PLoS ONE*, *9*(10), e109810. https://doi.org/10.1371/journal.pone.0109810

Taylor, M. (2019). *Bats: an illustrated guide to all species*. Ivy Press.

Terletzky, P. A., & Ramsey, R. D. (2016). Comparison of three techniques to identify and count individual animals in aerial imagery. *Journal of Signal and Information Processing*, *7*(3), 123-135. https://doi.org/10.4236/jsip.2016.73013

Thenkabail, P. S. (2016). *Remote sensing handbook; volume 1: remotely sensed data characterization, classification, and accuracies*. Taylor & Francis.

Thiele, S. T., Varley, N., & James, M. R. (2017). Thermal photogrammetric imaging: a new technique for monitoring dome eruptions. *Journal of Volcanology and Geothermal Research*, *337*, 140-145. https://doi.org/10.1016/j.jvolgeores.2017.03.022

Tichý, L. (2014). *GLAMA-gap light analysis mobile application*. https://www.sci.muni.cz/botany/glama/

Tichý, L. (2016). Field test of canopy cover estimation by hemispherical photographs taken with a smartphone. *Journal of Vegetation Science, 27*(2), 427-435. https://doi.org/10.1111/jvs.12350

Tidemann, C. R., & Nelson, J. E. (2004). Long-distance movements of the grey-headed flying fox (*Pteropus poliocephalus*). *Journal of Zoology*, *263*(2), 141-146. https://doi.org/10.1017/S0952836904004960

Timmiss, E. (2017). *Spatial factors influencing the establishment and occupancy of camps of the four mainland Australian flying-fox species (Pteropus spp.)* [Unpublished honours thesis, The University of New South Wales]. Sydney, Australia.

Tomaštík, J., Mokroš, M., Saloň, Š., Chudý, F., & Tunák, D. (2017). Accuracy of photogrammetric UAV-based point clouds under conditions of partially-open forest canopy. *Forests*, *8*(5), 151. https://doi.org/10.3390/f8050151

Townshend, J. R. G., Huang, C., Kalluri, S. N. V., Defries, R. S., Liang, S., & Yang, K. (2000). Beware of per-pixel characterization of land cover. *International Journal of Remote Sensing*, *21*(4), 839-843. https://doi.org/10.1080/014311600210641

Valletta, J. J., Torney, C., Kings, M., Thornton, A., & Madden, J. (2017). Applications of machine learning in animal behaviour studies. *Animal Behaviour*, *124*, 203-220. https://doi.org/10.1016/j.anbehav.2016.12.005

van der Ree, R., Wilson, C., & Yazgin, V. (2009). *Yarra Bend Park flying-fox campsite: review of the scientific research*. Department of Sustainability and Environment, Victorian Government. https://catalogue.nla.gov.au/Record/4833968

Van Dyck, S., & Strahan, R. (2008). *The mammals of Australia*. New Holland Publishers

van Toor, M. L., O'Mara, M. T., Abedi-Lartey, M., Wikelski, M., Fahr, J., & Dechmann, D. K. N. (2019). Linking colony size with quantitative estimates of ecosystem services of African fruit bats. *Current Biology*, *29*(7), R237-R238. https://doi.org/10.1016/j.cub.2019.02.033

van Wynsberghe, A., & Donhauser, J. (2018). The dawning of the ethics of environmental robots. *Science and Engineering Ethics*, *24*(6), 1777-1800. https://doi.org/10.1007/s11948-017-9990-3

Vapnik, V. N. (1999). An overview of statistical learning theory. *IEEE transactions on Neural Networks*, *10*(5), 988-999. https://doi.org/10.1109/72.788640

Vardon, M. J., & Tidemann, C. R. (1999). Flying-foxes (*Pteropus alecto* and *P. scapulatus*) in the Darwin region, north Australia: patterns in camp size and structure. *Australian Journal of Zoology*, *47*(4), 411-423. https://doi.org/10.1071/ZO99022

Vas, E., Lescroël, A., Duriez, O., Boguszewski, G., & Grémillet, D. (2015). Approaching birds with drones: first experiments and ethical guidelines. *Biology Letters*, *11*(2), 20140754. https://doi.org/10.1098/rsbl.2014.0754

Vinson, S. G., Johnson, A. P., & Mikac, K. M. (2020). Thermal cameras as a survey method for Australian arboreal mammals: a focus on the greater glider. *Australian Mammalogy*. Advance online publication. https://doi.org/10.1071/AM19051

Wagner, J. L. (1981). Visibility and bias in avian foraging data. *The Condor*, *83*(3), 263-264. https://doi.org/10.2307/1367320

Walsh, M. G., Wiethoelter, A., & Haseeb, M. A. (2017). The impact of human population pressure on flying fox niches and the potential consequences for Hendra virus spillover. *Scientific Reports*, *7*(1), 8226. https://doi.org/10.1038/s41598-017-08065-z

Wang, K., Franklin, S. E., Guo, X., & Cattet, M. (2010). Remote sensing of ecology, biodiversity and conservation: a review from the perspective of remote sensing specialists. *Sensors*, *10*(11), 9647-9667. https://doi.org/10.3390/s101109647

Weih, R. C., & Riggan, N. D. (2010). Object-based classification vs. pixel-based classification: comparative importance of multi-resolution imagery. *The International Archives of the Photogrammetry, Remote Sensing and Spatial Information Sciences*, *38*(4/C7).

Weinstein, B. G. (2018). A computer vision for animal ecology. *Journal of Animal Ecology*, *87*(3), 533-545. https://doi.org/10.1111/1365-2656.12780

Welbergen, J. A. (2005). *The social organisation of the grey-headed flying-fox, Pteropus poliocephalus* [Unpublished doctoral dissertation, University of Cambridge]. Cambridge, UK.

Welbergen, J. A., Klose, S. M., Markus, N., & Eby, P. (2008). Climate change and the effects of temperature extremes on Australian flying-foxes. *Proceedings of the Royal Society B: Biological Sciences*, *275*(1633), 419-425. https://doi.org/10.1098/rspb.2007.1385

Welbergen, J. A., Meade, J., Field, H. E., Edson, D., McMichael, L., Shoo, L. P., Praszczalek, J., Smith, C., & Martin, J. M. (2020). Extreme mobility of the world's largest flying mammals creates key challenges for management and conservation. *BMC biology*, *18*(1), 101. https://doi.org/10.1186/s12915-020-00829-w

West, C. (2002). Contemporary issues in managing flying-fox camps: a publicly-documented conflict from Maclean on the north coast of NSW. In P. Eby & D. Lunney (Eds.),

Managing the grey-headed flying-fox Pteropus poliocephalus as a threatened species in New South Wales (pp. 202-214). Royal Zoological Society of New South Wales.

Westcott, D. A., Caley, P., Heersink, D. K., & McKeown, A. (2018). A state-space modelling approach to wildlife monitoring with application to flying-fox abundance. *Scientific Reports*, *8*(1), 4038. https://doi.org/10.1038/s41598-018-22294-w

Westcott, D. A., Dennis, A. J., McKeown, A., Bradford, M. G., & Margules, C. R. (2001). *The spectacled flying fox, Pteropus conspicillatus, in the context of the world heritage values of the wet tropics world heritage area: a report for Environment Australia*. CSIRO Sustainable Ecosystems and the Rainforest Cooperative Research Centre. https://doi.org/10.25919/5ecc15be10924

Westcott, D. A., Fletcher, C. S., McKeown, A., & Murphy, H. T. (2012). Assessment of monitoring power for highly mobile vertebrates. *Ecological Applications*, *22*(1), 374-383. https://doi.org/10.1890/11-0132.1

Westcott, D. A., Heersink, D. K., McKeown, A., & Caley, P. (2015a). *The status and trends of Australia's EPBC-listed flying-foxes*. CSIRO Land and Water Flagship. https://www.environment.gov.au/system/files/resources/9799051f-e0a2-4617-ba0d-8e2be2a364df/files/status-trends-australias-epbc-listed-flying-foxes.pdf

Westcott, D. A., & McKeown, A. (2004). Observer error in exit counts of flying-foxes (*Pteropus* spp.). *Wildlife Research*, *31*(5), 551-558. https://doi.org/10.1071/WR03091

Westcott, D. A., McKeown, A., Murphy, H. T., & Fletcher, C. S. (2011). *A monitoring method for the grey-headed flying-fox, Pteropus poliocephalus*. Commonwealth Scientific and Industrial Research Organisation.

http://www.environment.gov.au/biodiversity/threatened/species/pubs/310112-monitoring-methodology.pdf

Westcott, D. A., McKeown, A., Parry, H., Parsons, J., Jurdak, R., Kusy, B., & Caley, P. (2015b). *Implementation of the national flying-fox monitoring program*. https://publications.csiro.au/rpr/pub?pid=csiro:EP156844

Westoby, M. J., Brasington, J., Glasser, N. F., Hambrey, M. J., & Reynolds, J. M. (2012). 'Structure-from-motion' photogrammetry: a low-cost, effective tool for geoscience applications. *Geomorphology*, *179*, 300-314. https://doi.org/10.1016/j.geomorph.2012.08.021

Wich, S. A., & Koh, L. P. (2018). *Conservation drones: mapping and monitoring biodiversity*. Oxford University Press. https://doi.org/10.1093/oso/9780198787617.001.0001

Wiles, G. J. (1987). The status of fruit bats on Guam. *Pacific Science*, *41*, 148-157.

Wilkinson, G. S. (1992). Information transfer at evening bat colonies. *Animal Behaviour*, *44*(3), 501-518. https://doi.org/10.1016/0003-3472(92)90059-I

Williams, N. S. G., McDonnell, M. J., Phelan, G. K., Keim, L. D., & van der Ree, R. (2006). Range expansion due to urbanization: Increased food resources attract grey-headed flying-foxes (*Pteropus poliocephalus*) to Melbourne. *Austral Ecology*, *31*(2), 190-198. https://doi.org/10.1111/j.1442-9993.2006.01590.x

Wittenberger, J. F., & Hunt, G. L. (1985). The adaptive significance of coloniality in birds. *Avian Biology*, *8*, 1-78. https://doi.org/10.1016/b978-0-12-249408-6.50010-8

Woinarski, J. (2018). *A bat's end: the Christmas Island pipistrelle and extinction in Australia*. CSIRO Publishing.

Worthington, D. J., Marshall, A. P., Wiles, G. J., & Kessler, C. C. (2001). Abundance and management of Mariana fruit bats and feral ungulates on Anatahan, Mariana Islands. *Pacific Conservation Biology*, *7*(2), 134-142. https://doi.org/10.1071/PC010134

Xue, Y., & Ray, N. (2017). *Cell detection in microscopy images with deep convolutional neural network and compressed sensing*. Unpublished manuscript. https://arxiv.org/abs/1708.03307

Yang, Y., & Lee, X. (2019). Four-band thermal mosaicking: a new method to process infrared thermal imagery of urban landscapes from UAV flights. *Remote Sensing*, *11*(11), 1365. https://doi.org/10.3390/rs11111365

Yang, Z., Wang, T., Skidmore, A. K., de Leeuw, J., Said, M. Y., & Freer, J. (2015). Spotting east African mammals in open savannah from space. *PLoS ONE*, *9*(12), e115989. https://doi.org/10.1371/journal.pone.0115989